AD-A149 557 MIXING CHARACTERISTICS OF AN UNDEREXPANDED MULTIPLE JET EJECTOR..(U) STANFORD UNIV CA DEPT OF AERONAUTICS AND ASTRONAUTICS M S CHANDRASEKHARA ET AL. JUN 84 1/1

UNCLASSIFIED JIAA-TR-55 AFOSR-TR-84-1195 F/G 20/4 NL

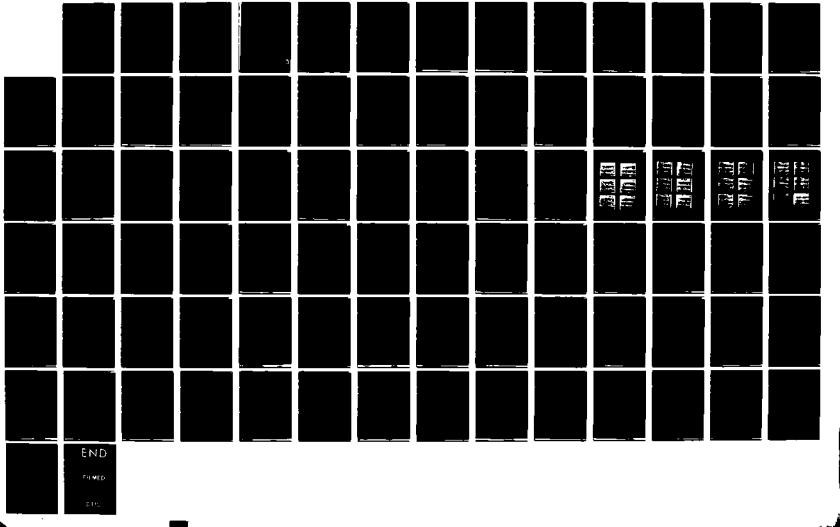

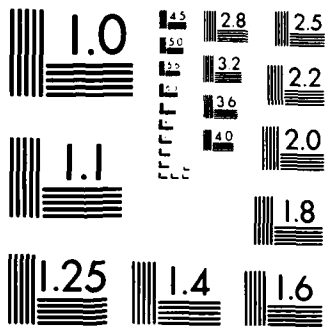

UNCLASSIFIED
SECURITY CLASSIFICATION OF THIS PAGE

REPORT DOCUMENTATION PAGE

1a REPORT SECURITY CLASSIFICATION **AD-A149 557**	1b RESTRICTIVE MARKINGS
2	3 DISTRIBUTION/AVAILABILITY OF REPORT APPROVED FOR PUBLIC RELEASE: DISTRIBUTION UNLIMITED
4 REPORT NUMBER(S)	5 MONITORING ORGANIZATION REPORT NUMBER(S) AFOSR-TR- 84-1195
6a NAME OF PERFORMING ORGANIZATION STANFORD UNIVERSITY 6b OFFICE SYMBOL (If applicable)	7a NAME OF MONITORING ORGANIZATION AFOSR/NA
6c ADDRESS (City, State, and ZIP Code) Dept. of Aeronautics and Astronautics Stanford, California 94305	7b ADDRESS (City, State, and ZIP Code) Building 410 Bolling AFB, DC 20332
8a NAME OF FUNDING/SPONSORING ORGANIZATION AFOSR 8b OFFICE SYMBOL (If applicable) NA	9 PROCUREMENT INSTRUMENT IDENTIFICATION NUMBER F49620-79-C-0189
8c ADDRESS (City, State, and ZIP Code) Building 410 Bolling AFB, DC	10 SOURCE OF FUNDING NUMBERS PROGRAM ELEMENT NO. 61102F; PROJECT NO. 2307; TASK NO. A1; WORK UNIT ACCESSION NO.

11 TITLE (Include Security Classification)
MIXING CHARACTERISTICS OF AN UNDEREXPANDED MULTIPLE JET EJECTOR

12 PERSONAL AUTHOR(S)
M.S. CHANDRASEKHARA, A. Krothapalli D. Baganoff

13a TYPE OF REPORT	13b TIME COVERED	14 DATE OF REPORT (Year, Month, Day)	15 PAGE COUNT
INTERIM	FROM _____ TO _____	JUNE 1984	81

16 SUPPLEMENTARY NOTATION

17 COSATI CODES			18 SUBJECT TERMS (Continue on reverse if necessary and identify by block number)
FIELD	GROUP	SUB-GROUP	

19 ABSTRACT (Continue on reverse if necessary and identify by block number)

(ATTACHED)

20 DISTRIBUTION/AVAILABILITY OF ABSTRACT	21 ABSTRACT SECURITY CLASSIFICATION
☐ UNCLASSIFIED/UNLIMITED ☐ SAME AS RPT. ☐ DTIC USERS	
22a NAME OF RESPONSIBLE INDIVIDUAL	22b TELEPHONE (Include Area Code) / 22c OFFICE SYMBOL

DD FORM 1473, 84 MAR — 83 APR edition may be used until exhausted. All other editions are obsolete.

SECURITY CLASSIFICATION OF THIS PAGE

TK-84-1195

ABSTRACT

A study of the mixing characteristics of an underexpanded multiple jet ejector is presented. Results obtained using schlieren flow visualization pitot tube and hot wires are discussed. The parameters varied were: nozzle pressure ratio, ejector area ratio, ejector throat to nozzle exit plane distance, and the number and spacing of the jets. Performance characteristics derived from ejector exit plane velocity distributions have been drawn for two area ratios. In addition, a fair reference base for conparison of results has been established, by conducting identical tests on an equivalent single jet ejector. Results show that there is little difference between the two ejectors at subsonic conditions of operation. However, at underexpanded discharge conditions, a compact multiple jet ejector is distinctly superior. Mixing characteristics are better in such an ejector, even though the acoustic effects responsible for mixing in a single jet are almost insignificant. The location of the ejector throat has a strong effect on the ability of the ejector to entrain the ambient fluid. The best performance is obtained for the location closest to the nozzle exit. The number and spacing of the jets do not have a significant effect for the range of values studied.

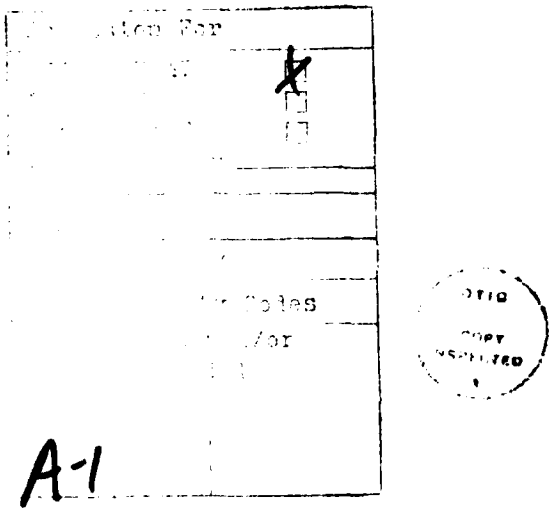

JOINT INSTITUTE FOR AERONAUTICS AND ACOUSTICS

National Aeronautics and
Space Administration

Ames Research Center

Stanford University

JIAA TR - 55

MIXING CHARACTERISTICS OF AN UNDEREXPANDED MULTIPLE JET EJECTOR

M.S. Chandrasekhara, A. Krothapalli and D. Baganoff

STANFORD UNIVERSITY
Department of Aeronautics and Astronautics
Stanford, California 94305

JUNE 1984

JIAA TR - 55

MIXING CHARACTERISTICS OF AN UNDEREXPANDED MULTIPLE JET EJECTOR

M. S. Chandrasekhara, A. Krothapalli and D. Baganoff

The work here presented has been supported by the U.S. Air Force under grant F49620-79-C-0189.

JUNE 1984

ABSTRACT

A study of the mixing characteristics of an underexpanded multiple jet ejector is presented. Results obtained using schlieren flow visualization pitot tube and hot wires are discussed. The parameters varied were: nozzle pressure ratio, ejector area ratio, ejector throat to nozzle exit plane distance, and the number and spacing of the jets. Performance characteristics derived from ejector exit plane velocity distributions have been drawn for two area ratios. In addition, a fair reference base for comparison of results has been established, by conducting identical tests on an equivalent single jet ejector. Results show that there is little difference between the two ejectors at subsonic conditions of operation. However, at underexpanded discharge conditions, a compact multiple jet ejector is distinctly superior. Mixing characteristics are better in such an ejector, even though the acoustic effects responsible for mixing in a single jet are almost insignificant. The location of the ejector throat has a strong effect on the ability of the ejector to entrain the ambient fluid. The best performance is obtained for the location closest to the nozzle exit. The number and spacing of the jets do not have a significant effect for the range of values studied.

ACKNOWLEDGEMENTS

This work was supported by the Air Force Office of Scientific Reseach under contract F49620-79-0189.

Special thanks go to Mr. Aldo Rossi for his help in model fabrication.

TABLE OF CONTENTS

LIST OF SYMBOLS

AR	Area ratio
$\bar{C}_{p_t}$	Average throat static pressure coefficient
D	Nozzle width
ESJ	Equivalent single jet
M	Mach number
MJ	Multiple jets
N-T	Nozzle-throat distance
P_o	Nozzle pressure
P_a	Atmospheric pressure
p_{o_2}	Total pressure on the axis
$\bar{p}$	Average wall static pressure
$\bar{p}_t$	Average throat static pressure
R	Nozzle pressure ratio
$\bar{U}$	Longitudinal mean velocity
X, Y, Z	Carterisian coordinate system
X	Distance from ejector throat
X_o	Distance from nozzle exit
ϕ	Thrust augmentation ratio
ψ	Mass augmentation ratio
ρ	Density

LIST OF FIGURES

1. INTRODUCTION

Several experimental studies have been reported in the past on thrust augmenting ejectors using a single jet; Hsia (1984), Quinn (1977), Viets (1975), Skoblenick and Hill (1977), Bernal and Sarohia (1983) to name a few. The necessary theoretical framework for this work was provided by Von Karman (1949). This theory has been extended to the compressible flow range by Keenan et al. (1950), Nagaraja et al. (1973). The conclusion from the work reported so far is that the performance of the ejector can be greatly improved if the primary and secondary flows mix completely. One of the methods attempted to obtain better mixing is the use of hyper-mixing nozzles (Bevilaqua, 1974) in which the nozzle exit plane is segmented alternately to produce vortices that enhance mixing. Krothapalli et al. (1982), Hsia (1984), Quinn (1977) have all shown that effective and enhanced mixing can be obtained by generating screech tones in the natural instability range of the jet. The resulting interaction causes rapid spreading of the jet and increased entrainment - an effect that translates to an improvement in the augmentation characteristics of the ejector. The flow visualization pictures of Hsia (1984) document this interaction vividly.

The above mentioned studies are all on an ejector using a single jet. In real life application - as in an augmentor wing for V/STOL aircraft - it is common to use an array of nozzles. These multiple jets are, generally, believed to have superior mixing characteristics. Hence a multiple jet ejector is expected to deliver a better performance. In addition, the multiple jet flow is quieter than a single jet - even under supersonic conditions - making a multiple jet ejector an attractive alternative to a long slot jet ejector. Aiken (1973) measured the overall aerodynamic effects of slot type and lobe type nozzles and found that the latter show a better performance. These results are, however, limited to a plenum pressure ratio of 1.53. The available data on a multiple jet ejector over the operating range encountered in the present day application is scant, at best. The present study is aimed at providing this vital information.

In order to be able to compare the performance of a multiple jet ejector, it is necessary to obtain results on an 'equivalent' single jet. This is because of the fact that the entrainment characteristics in the near-field would be vastly different for the two cases. A complete definition of the equivalent jet is not possible because such a jet should be able to generate all the effects of the multiple jet. This means that the pressure field set up by the merging jets, the appropriate length scale for this flow, the effect of spacing, etc. should all be reproduced by this equivalent jet. With these limitations in mind, the equivalent single jet is defined as a jet having the same total area and aspect ratio as that of the multiple nozzle tested. Identical tests were carried out on this jet under identical conditions to establish the reference.

The performance characteristics of an ejector are a function of the following parameters:

1. nozzle pressure ratio
2. ejector/jet area ratio
3. ejector length
4. distance from the nozzle exit plane to the throat of the ejector shroud
5. the number of jets
6. the spacing between the jets

In the experiment, the nozzle pressure was varied over a range starting from 1 psig to 38 psig. The area ratio was varied from 14:1 to 33:1. The shroud length was kept fixed. The nozzle-throat distance was varied from 1.1cm to 5.2cm. The number and spacing between the jets were also varied.

Detailed velocity traverses were taken at the ejector exit plane for 4 specific pressure ratios. The wall static pressure distributions were obtained over the entire range of nozzle pressures. However, results for only those pressures at which the velocity data were obtained will be presented and discussed. Schlieren flow visualization pictures of the jet interaction taken with and without the ejector will also be discussed.

2. EXPERIMENTAL APPARATUS AND PROCEDURE

2.1 The Facility

The Joint Institute's high pressure blow down type air facility was used for the experiment. This consists of a high pressure air compressor, which pumps a 104 ft.^{3} storage tank to 2400 psig in 16 hours. This HP air was used as the air supply. The details of the facility have been described elsewhere (Krothapalli et al. 1979). The original arrangement included heaters in the system for studying heated jets. However, owing to the need to maintain steady operating conditions while passing the larger mass flow required for the multiple jet system, these were bypassed. The resulting reduction in pressure drop was sufficient to achieve this goal.

2.2 The Models

Two nozzle assemblies were used in the experiment. The multilobe nozzle was the same as that used by Krothapalli et al. (1979). This is shown in figure 1. It consists of 5 rectangular slots each 0.3cm wide and 5cm long placed on a wedge of 70° included angle. The lobes are placed 2.4cm (8 slotwidths) apart. It is possible to block any of these lobes to get a different arrangement of the multiple jet flow. Most of the experiments were performed by blocking the outer most slots, on either side of the central slot, thus resulting in 3 jets spaced 2.4cm apart. Since it was felt worthwhile to study the effect of the number of jets and spacing, some tests were done on the 5 jet configuration also. To obtain the operating pressure ratios, however, it was necessary to reduce the exit area of these slots. This was accomplished by attaching a shim of aluminum onto one of the inner walls of the slot for all the slots. The combined thickness of the insert was 1 mm. The shims were of the same height as the slots. The settling chamber end of these were chamfered so as to guide the flow properly into the slot. The resulting slot dimension was 0.2cm × 5cm, with the slots now placed 2.5cm (12.5 slot widths) apart. The total flow area was only about 10% greater than that of the three jets. Thus, fair comparison of the performance under

identical operating conditions was possible.

Data on the equivalent single jet was obtained using the nozzle shown in figure 2. As stated earlier, the exit dimensions of this nozzle were arrived at by stipulating that the aspect ratio and the total flow area are the same for this jet as the multiple jet. The dimensions of such a slot are 0.52cm × 8.66cm. This nozzle has the same included angle (70°) as the multilobe array. However, its longer dimension is along the wedge so that the same settling chamber and ejector shroud could be used for the test.

The contraction leading upto the nozzle is two-dimensional in both the models. Sufficient care was exercised during model fabrication to ensure smooth flow passages.

2.3 The Ejector Shroud

Figure 3 presents the details of the ejector shroud along with the pressure tap locations. This consisted of a duct made out of 4 plexiglas walls with rounded, bell mouth inlets to permit gradual acceleration of the entrained air. The inside (flow) area can be varied by moving these four walls continuously in the X-Y plane and discretely (by inserting spacers) in the X-Z plane. The four corners of intersection of these walls were taped to prevent leakage of air, lest the ejector action is lost. The length of the shroud (mixing duct) is kept fixed at 50cm. It is possible to move the ejector relative to the nozzle exit plane. Accordingly, the throat position (defined to be the plane at which the inlet bell-mouth meets the straight walls) can also be varied.

2.4 Instrumentation and Techniques

Flow visualization pictures were taken using the schlieren method. The system used is of the conventional single pass type, with the optical axis folded twice, using two spherical mirrors. The collimating mirror has a focal length of 306cm and diameter of 25cm. The focussing mirror has a focal length of 200cm with a diameter of 32cm. A stroboscopic flash, whose duration could be varied from 1.3 to 7 μ sec at five discrete values, served as the light source.

Photographs of the flowfield were obtained by displaying the image on a ground glass screen and on a polaroid film. Single flash pictures were taken on 3000 ASA film with a flash duration of 1.5 μ sec. Further details of this can be found in Hsia (1984).

The wall static pressure measurements were obtained using a four barrel, 24 port scanivalve. Figure 3 shows the location of the taps along the walls and also on the lip. The static presure in any Y-Z (horizontal) plane was determined by averaging the measured static pressure on three of the ejector walls. The 4 barrels of the scanivalve were connected to 4 pressure transducers ($\pm$ 2.5 psig). The transducer voltages were suitably amplified and fed to the Analog-Digital Convector of a PDP-11/23 system. The digitized voltages were stored on a disk and processed in real-time. The average of 100 samples obtained over 500 millisec was taken to be the static pressure.

Axial total pressure data were obtained using a pitot tube. This was suspended from the top and positioned in the mixing duct from a traverse. In order to prevent its vibration and movement in the high velocity flow in which it was used, the tube was anchored by a 4mm rod introduced through a side wall. The point of anchoring was placed sufficiently downstream (> 100d, where d is the pitot tube diameter) of the measurement point so that the disturbances due to it could to be ignored. The total pressure was read on an averaging digital voltmeter, using a 3 sec (sometimes 10 sec.) averaging time. The DVM was driven by signal from a $\pm$ 25psig transducer, connected to the pitot tube.

The velocity data were obtained by using a DISA 55P11 single normal hot wire probe in conjunction with a 55M10 system. The bridge voltage was linearized through a DISA 55M25 linearizer. The linearized voltage was averaged on a DISA voltmeter and a RMS meter for 3sec to get the mean velocity and turbulence intensity.

The hot wire was calibrated using the DISA calibration equipment for a velocity range from 10 m/s to 250 m/s. By fine adjustments of the linearizer settings, it was possible to get a calibration curve linear to 1% or better for a velocity range up to 200 m/s. The

calibration was repeated frequently.

Velocity profiles in the X-Y and X-Z planes were obtained by traversing the hot wire normal to the flow by a stepper motor controlled traverse. A maximum of 8 profiles at the exit plane of the duct were taken. Usually 5 of these were in the X-Z plane and 3 in the X-Y plane. Velocities at points of intersection of these profiles were used as a check on the accuracy of the data.

Since the high pressure air was throttled and the jet coming out of the nozzle went through a series of shock cells, there was a need to ensure that these effects did not cause a significant change in the air temperature at the measurement plane. Hence, temperature surveys were taken using a thermistor at this plane. It was found that the measured non-uniformities were less than 10%. This is because of the entrainment of the ambient (room) air in large quantities. The resulting air temperature at the exit was about 15 to 18°C. The air temperature during calibration was also $\simeq$ 18°C. This fortunate coincidence meant that errors introduced due to temperature effects on velocity measurements were relatively small. Hence, no corrections were applied to the data.

The highest velocities measured were in the vicinity of $M \simeq 0.6$. Studies by Hsia et al. (1982) have shown that there is no qualitative difference caused by the introduction of a hot-wire probe at $M \simeq 0.8$. This being the case, the quantitative effects, if any, at $M \simeq 0.6$ could be ignored. Hence, no corrections for transonic effects were applied. It should be noted further that the calibration equipment provides for some compressibility corrections, and hence, additional corrections appear unnecessary.

Inspite of all this, the uncertainty of velocity measurement is estimated to be between 5-10%. This is because the turbulent intensities encountered in the flow are fairly high (10-15%) and the use of hot wire anemometry in highly turbulent flows has its own limitations.

On the contrary, the uncertainty of the static pressure data is believed to be less than 2% because static pressure can be determined far more reliably.

2.5 The Experiment

The experiment itself consisted of taking velocity profiles and pressure distributions for various conditions. Velocities were measured for stagnation pressures of 7.7, 15, 25, and 35 psig (corresponding to pressure ratios of 1.52, 2.02, 2.7 and 3.38) for the multiple jet and equivalent single jet at the exit plane. Two area ratios, 20:1 and 26:1, were considered for both the jets.

The wall static pressure distribution was obtained for stagnation pressures ranging from 1 psig to 38 psig and for nozzle-throat distances of 1.1cm, 2.6cm and 5.2cm. The exercise was repeated for both the jets at area ratios of 26:1 and 33:1.

Axial total pressure distributions were measured for P_o = 7.7, 15, 25 and 35 psig starting from the jet exit (except for P_o = 35psig, for which the measurements were started slightly downstream) and for area ratios of 20:1, 26:1, and 33:1.

In addition, single flash schlieren pictures were taken for the free multiple jets and the confined jets (ejector) for an area ratios of 14:1 and 20:1, at various pressure ratios.

Also, throat static pressure were obtained mannually for a multiple jet ejector with 5 primary jets and with an area ratio of 20:1.

The results from the experiments will be discussed in the next section.

RESULTS AND DISCUSSION

3.1 Flow Visualization Studies

Single exposure schlieren pictures taken on 3000 ASA polariod film of the multiple free jet are presented in figure 4a. The field of view extends upto X/D $\simeq$ 35. These show that merger of the jets occurs increasingly closer to the jet origin as the pressure ratio R, is increased from 1.52 to 3.59. Note that at $R = 1.52$, merger occurs at X/D $\simeq$ 20, whereas for $R = 3.04$ or 3.59, it is at X/D $\simeq 10 - 12$. The strong acoustic wave structure and interaction that exist in the case of a single free jet (Krothapalli, et al. 1982 or Hsia, 1984) is not so evident for highly underexpanded flow condition. Yet, some acoustic waves emanating outwards from the third shock cell are faintly visible near the outer jets. This suggests that the middle (inside) jet actually cancels the acoustic waves of the outer jets - an effect that should reduce the noise levels preceived by an observer. This has been observed by Parthasarathy et al. (1980). No discrete sounds like the screech tone were detectable from the multiple jet flow, unlike that in a single underexpanded jet. Yet, the spreading of the jets is quite rapid for $R = 3.59$ and the jets appear to have mixed considerably by X/D $\simeq$ 30. It is believed that the pressure field set up by the jets is mainly responsible for this, because the screech tone effect is absent.

Also of interest is the long series of tiny, weak shock cells for the sonic discharge conditions. As many as 8 shock cells can be seen for the outer jets.

Figure 4b shows the flow inside an ejector having an area ratio (AR) of 20:1 and figure 4c that in an ejector with an area ratio 14:1. The presence of the shroud in the case of AR=20:1 delays the merger of the jets. This is because of the confining effects of the secondary flow which limits the jet spreading. Even for $R = 3.59$, merging occurs at X/D $\simeq$ 20. On the other hand, the flow nearly fills the passage in the 14:1 ejector. The jets spread much more than in the 20:1 ejector indicating that the wall proximity has a favorable effect on the intermixing of the jets. Also, a comparison of the three figures 4a,

4b and 4c reveals the strongly vortical nature of the flow in figure 4c, for a compact ejector, which is a desirable outcome. This, it appears, is actually responsible for the better mixing seen. In both the ejectors, no discrete acoustic wave pattern is discernible.

Figure 4d provides a picture of the flow inside the 5 jet, 20:1 area ratio ejector. The central three jets can be clearly seen and the outer jets are only partially visible. Eventhough the jets are issuing out of smaller nozzles (2mm wide), they appear to have spread well in the nearfield. However, because of their separation (12.5 slot widths), the internal interaction is not sufficiently strong as to generate good mixing inside the duct, although these jets are operating under the same conditions as those considered previously.

These pictures suggest that a compact ejector is good from mixing considerations. Acoustic interactions are not a strong feature of multiple jet flow, as opposed to that of a single jet flow.

3.2 Throat Static Pressure

Figures 5a and 5b are plots of the average throat static pressures $\bar{C}_{p_t}$ with increasing pressure ratio R. This pressure is an indication of the ability of the ejector to entrain the ambient fluid. The average was computed from the pressures measured at 7 points in the throat plane on 3 walls of the mixing duct. The ordinate has been normalized by the atmospheric pressure. In both the figures, data for three area ratios 20:1, 26:1 and 33:1 are given, for different nozzle exit plane to ejector throat (N-T) distances. The following can be said of multiple jet ejector behavior from figure 5a.

1) The magnitude of the throat pressure coefficient increases quite drastically as the shroud (and hence the throat) is moved away from the nozzle. For example at $R = 3.38$, $\bar{C}_{p_t} = -0.122$ at 1.1cm and -0.065 at 5.2 cm for the 20:1 ejector. This behavior is true for all the area ratios tested.

2) The throat pressure coefficient increases significantly as the duct area is increased. Again at $R = 3.38$, for AR=20:1, we have $\bar{C}_{p_t} = -0.122$ and for AR=33:1, $\bar{C}_{p_t} = -0.065$.

3) The magnitude of the increase in both of the above cases increases with R.

This means that the entrainment rate of the primary jets is decreased substantially if the area ratio is increased. However, this decrease is offset somewhat by the increase in the secondary flow area, so that the quantity of fluid entrained could still be large.

Similar results were obtained for the equivalent single jet (ESJ) ejector as can be seen from figure 5b. But this system is not as sensitive to the N-T distance as the multiple jet system even at high pressure ratios (upto R=2- 2.5), especially when operating at area ratios of 26:1 and 33:1. Typical throat pressures in the ESJ ejector are noticeably lower than that in the multiple jet ejector as figures 6a, 6b and 6c show. The irregular variation of $\bar{C}_{p_t}$ at high pressure ratios is a feature of the confined underexpanded single jet (see Hsia, 1984). These are simply cross plots of figures 5a and 5b. The effectiveness of a multiple jet ejector, particularly at small area ratios and short N-T distances, is very clear from figure 6a. For AR=20:1, where the multiple jet system yields a $\bar{C}_{p_t} \simeq -0.122$ at R=3.38, the ESJ system only yields a $\bar{C}_{p_t} \simeq -0.075$, despite the fact that in the latter strong acoustic effects are present that actually enhance the mixing capacity of the ejector. Differences at low pressure ratios are marginal, and at times, even insignificant. At N-T=5.2 cm, an ESJ system appears to be slightly better. Since the suction levels are so small at this distance for either of the jets, it is recommended that this distance be not considered for application. Qualitatively similar results were obtained for AR=26:1 (figure 6b) and AR=33:1 (figure 6c). For the largest area ratio tested no apparent differences can be seen in the entrainment characteristics. As before, it is felt that this is not a worthwhile configuration for the ejector from consideration of flow mixing and performance.

A comparison of the 3 and 5 jet ejector characteristics is made in figure 7. For the range of pressure ratios tested, there appears to be no appreciable difference between the two jets. Since the secondary flow area available for the 5 jets is the same as that for the 3 jets, the performance delivered by the 5 jet configuration is not expected to be any better

than the 3 jet system.

3.3 Wall Static Pressure Distrubution

Figures 8 through 12 show the distribution of the average wall static pressure along the shroud walls. The pressures plotted are the average pressures (measured in the same axial plane) on three sides of the shroud downstream of the throat. Upstream of the throat, the pressures were measured at 6 locations on three walls in the same plane. The pressure coefficient was computed as follows:

$$\bar{C}_p = \frac{\bar{p} - p_a}{p_t}$$

where $\bar{p}$ is the average static pressure, $\bar{p}_a$ is the atmospheric pressure, and $\bar{p}_t$ is the average throat static pressure. This particular way of normalization was chosen because it reveals some interesting features.

From Figures 8a for a multiple jet ejector at nozzle-throat distance of 1.1cm, and an AR of 20:1 the distributions for all operating pressure ratios show self- similarity. Considering the fact that both subsonic and underexpanded discharge conditions were tested, this shows that the basic phenomenon of acoustic interaction is absent in high speed flows in a multiple jet ejector. This is a significant result and it can also be seen from the schlieren pictures (Fig. 4b). As the shroud is drawn away from the nozzle (figures 8b and 8c) some differences begin to appear and at a distance of 5.2 cm (X/D = 17.3, figure 8c), the similarity breaks down. However, the two highly underexpanded cases of $R = 3.38$ and $R = 2.7$ show the same behavior. Also the distributions for cases of $R = 2.02$ and $R = 1.52$ are nearly identical in the region $0 \leq$ X/D ≤ 120. Beyond this point, the profiles merge again. At this nozzle-throat distance, the jets initially expand like free jets and it is possible that there is mild acoustic interaction (figure 4a) present. The pressure on the shroud lip increases with increasing distance from the nozzle ($\bar{C}_{p_t}$ = -0.068, -0.065, and -0.6 for N-T = 1.1, 2.6 and 5.2 cm). Since this is actually the thrust augmentation

obtainable with the decreases, with increasing static pressure on the lip, it is clear that the best performance can be obtained only at the closest spacing.

Figures 9a, 9b and 9c are the distribitions for the equivalent single jet. No self similarity can be observed. This is because acoustic interactions are significant for a single jet. Also, a very distinct change of slope can be observed in the profiles at $X/D \simeq 40$. It is believed that the flow meets the duct walls around this point. This point moves slightly upstream as the shroud is raised above the nozzle. In figure 9c the flow touches the walls between X/D = 25-35 for all pressure ratios.

The distribution for area ratios of 26:1 and 33:1 for the multiple jet ejector are depicted in figures 10a and 10b. Once again they are both self similar. However, comparison of figures 8a, 10a, and 10b shows that as the area ratio is increased, the profile gets flatter in the region $50 \simeq X/D \simeq 100$. In this region, a constant pressure mixing takes place. However, to satisfy the condition at the duct exit, the pressure rapidly increases to the atmospheric value.

Data for the equivalent single jet shows the same behavior. As can be deduced from figure 11a and 11b, for area ratios of 26:1 and 33:1 respectively, there is a constant (or slowly increasing) pressure region between X/D = 20-45, after which the wall pressure rapidly approaches the ambient value at the exit. In fact, the two distributions are very nearly identical, demonstrating the negligible effect of increasing the area ratio beyond 26:1. A hint of this result is present in figure 5b.

Figures 12a and 12b are drawn for a compact ejector with area ratio of 14:1. Figure 12a is vastly different from those discussed above. A striking feature of this is that the pressure completely raises to the atmospheric value by $X/D \simeq 80-90$ and remains constant from there on. This suggest that all the mixing has taken place by this distance and the flow has filled the channel completely. If this is so, then the velocity profiles should be nearly flat at the duct exit (see figures 4c and 16a). It then appears that for a compact

ejector, a multiple jet array provides desirable exit velocity profiles, for short nozzle - throat distances. It can be seen from figure 12b that the behavior for $R = 1.52$ and $R = 2.02$ are very similar to that seen in figure 8a. However, for higher pressure ratios of $R = 2.7$ and $R = 3.38$, the distribution shows a distinct change of slope at $X/D \simeq 60$, the point of flow attachment to walls.

3.4 Axial Total Pressure Measurements

Figures 13a, 13b and 13c show the axial total pressure distributions in the duct - i.e., the behavior of the central jet as affected by mixing with the outer jets and the secondary stream. It is well known that ejector flows have a tendency to lean toward one wall (Rajaratnam, 1976). However, the measured total presures still represent the axial distribution. This is because, data taken randomly at slightly displaced locations from the axis showed that the total pressures are within 10% of the axial values in the region $20 \leq X/D \leq 60$ and 5% beyond X/D=60.

Some measurements through the shock cells are seen in figure 13a for an area ratio of 20:1. By $X/D \simeq 8$ the velocity has decayed to subsonic values, and beyond $X/D \simeq 20$ the decay rate has reduced significantly. The flow is mixing in the regions $20 \simeq X/D \simeq 160$ and the decay is only gradual here for the underexpanded cases. For $R = 1.52$, ($P_o = 7.7$ psig) i.e. the subsonic discharge condition, the total pressure is nearly constant till $X/D \simeq 6$ (end of potential core) i.e. the jet is expanding like a free jet. Overlaying figures 13b and 13c for AR=26:1 and 33:1, respectively, reveals that the jets show almost identical decay for all pressure ratios. However, a flatter region can be seen for $40 \simeq X/D \simeq 80$ for AR=33:1 in figure 13c. Interestingly, the pressures for the subsonic discharge condition are identical beyond $X/D \simeq 20$ for all three cases, showing that after merging the confining walls have no effect on the jet decay. But for R=3.38, the pressures for AR=26:1 and 33:1 are higher than those for AR=20:1, indicating that the interaction between the jets is not very strong beyond a certain area ratio.

It would be necessary to make detailed measurements inside the duct before extending the above results to predict the duct exit flow profiles.

3.5 Velocity Measurements

The velocity data obtained using a hot wire is presented in figures 14 through 16 for the multiple jet ejector and in figures 17 and 18 for the equivalent single jet ejector. These were taken at about 5mm downstream of the duct exit plane. The plots on the left side are measurements in the X-Y plane (containing the long dimension of the duct) and those on the right in the X-Z plane (with the short dimension of the duct).

For an area ratio of 20:1 (figures 14a -14d), the multiple jet flow in the X-Y plane has a fairly uniform exit velocity profile, for all pressure ratios at the center line, and they exhibit a saddle shape in planes away from the central plane. The variation seen at any location is within 30% for $P_o = 7.7$ psig in figure 14a and less than 20% at $P_o = 38$ psig in figure 14d. In the X-Z plane, data obtained at 5 different Y-planes are presented. First of all, the variation seen from plane to plane is about 15-10%. Also, the profiles are relatively flat. In addition, a tendency for the flow to lean towards one (right) wall can be seen too. Whereas the flow has not mixed completely within the duct, a fair degree of mixing has taken place in this ejector configuration. Even though the data shows scatter, it should be noted that a check on the measured velocity values at the intersecting grid points of X-Y and X-Z plane certifies the quality of the data. The values are within a maximum of 10% at most nodes, even though obtained, at times, by different probes and on different days. Considering the limitations of hot wire anemometry in high speed, high turbulent intensity flows, this should be considered as good.

Data for $AR = 26 : 1$ at the same pressure ratios (1.52, 2.02, 2.7 and 3.8 psig) are plotted in figures 15a-15d. Figure 15a is qualitatively similar to figure 14a. But, the effects of the increased duct width are clear. Data for P_o = 15psig (figure 15b) shows peaky profiles in the X-Z plane. Figures 15c and 15d show a tendency of the velocity

profiles towards flatness. In fact, in the central X-Y plane, the profile is very flat for both the cases. Variations seen within the duct can be expected, because the ratio of the duct length to its equivalent diameter is about $\simeq 4.6$ and this is not sufficient to ensure proper mixing.

Figure 16a and 16b show the velocity profiles for an area ratio of 14:1 for $P_o = 7.7$ psig and 30 psig respectively. That complete mixing has taken place for the subsonic case is clear from figure 16a. The velocity is constant across the duct in different planes and the variation is $\leq 10\%$ over most of the exit plane. Results for $P_o = 30$ psig (figure 16b) show nearly flat profiles in the X-Z plane, although varying between different planes by 20%. The saddle shape is distinct at all Z locations in the X-Y plane. This shape, incidentally, is a consequence of incomplete mixing of the resultant multiple jet flow with the secondary (entrained) flow.

The three figures 14, 15 and 16 point out that best mixing occurs only for the smallest area ratio. Thus, a compact ejector is the one that has the necessary mixing properties.

In figure 17 and 18, the velocity profiles for an equivalent single jet are displayed. The profiles in the X-Y plane (note that the long dimension of the nozzle is in the X-Y plane now) for AR=20:1 and 26:1 (figures 17a and 18a respectively) are reasonably uniform and similar to that of a multiple jet for R=1.52. The same can be said of the X-Z plane data also for R=2.20. Figures 17b and 18b show that, whereas the X-Y plane data has similar behavior, presence of the peaks is clear in the X-Z plane profiles, with the maximum velocity being in the central plane in both the cases. But, the variation in any given Y plane is not much. As the pressure ratio is increased to 2.7, figures 17c and 18c show extremely peakly profiles in both the planes, i.e. there is a wide variation in the velocity across the duct cross section. Similar, but even more pronounced, variations show up in figures 17d and 18d for R=3.38. Interestingly, the flow has a tendency to be symmetric in the X-Y plane. It is very clear that mixing is not complete, even though at these pressure

ratios, strong acoustic interactions are present.

This result brings out a very interesting point. It shows that it is not sufficient to make measurements just in the central plane alone (as is most often done!) for one would measure extermely high velocities in this plane and any estimates of the ejector performance based on this would be inaccurate and unrealistic.

Comparison of figures 14 through 18 reveals that a multiple jet array is far superior in producing better mixing, expecially in compact congurations.

3.6 Performance Characteristics

The performance characteristics of an ejector are measured in terms of the mass augmentation ratio ψ and thrust augmentation ratio ϕ. These are defined here as

$$\psi = \frac{\text{total mass flow at the duct exit (primary + secondary)}}{\text{primary jet mass flow}} = \frac{\dot{m}_t}{\dot{m}_p}$$

$$\phi = \frac{\text{actual thrust produced by the ejector}}{\text{thrust produced by isentropically expanding the primary jet}} = \frac{\dot{m}_t \bar{U}_t}{\dot{m}_p V_{isen}}$$

where,

$\bar{U}_t$ = mass averaged duct velocity

V_{isen} = isentropic velocity of the primary jet

The actual thrust produced was not directly measured. It was estimated by integrating the measured exit velocity profiles and obtaining a mass averaged velocity $\bar{U}_t$, which was obtained from the equation:

$$\dot{m}_t = \rho A \bar{U}_t = \left\{ \frac{\Sigma \rho d \int_{-\frac{b}{2}}^{\frac{b}{2}} U dy}{n_z} + \frac{\Sigma \rho b \int_{-\frac{d}{2}}^{\frac{d}{2}} U dz}{n_y} \right\}$$

where, b and d are the breadth and depth of the mixing duct respectively, n_y and n_z are the number of velocity profiles taken in the $X-Y$ and $X-Z$ planes and A is the duct cross sectional area.

This method of performance computation depends on the accuracy of the hot wire data and the distribution of data points across a profile. However, ϕ and ψ computed for the two jets studied suffer from the same uncertainties and so the comparison is still valid.

The mass augmentation characteristics of the ejectors are presented in figures 19a and 20a, for AR = 20:1 and 26:1 respectively. These show that, under identical subsonic conditions of operation, the equivalent single jet ejector entrains about 5% more ambient air than a multiple jet ejector. But, this trend reverses under underexpanded conditions of operation. The percentage difference noticeable is slightly higher for AR = 20:1.

The thrust augmentation characteristics show similar trends, except that at an AR of 20:1, (figure 19b) the multiple jet ejector can provide more than 10% additional augmentation over the equivalent single jet ejector for R = 2.7. In general, the improvements seen are better for AR = 20:1. Figure 20b also shows the augmentation values obtained by Quinn (1977) in an axisymmetric, ejector with AR = 25.8 and with a comparable duct length/diameter ratio. He made direct measurement of thrust and obtained slightly higher (0-15%) values.

Note that the maximum ϕ levels are about 1.15-1.2, and ψ drops from 5.5 for the subsonic case to 3.5-4 for R=3.38. This means, at best, about 20% more thrust is the maximum realized. However, a multiple jet system is preferable in view of the fact that the exit velocity is more uniform and it is quieter. It is also definitely superior for AR=20:1.

Also plotted in figures 19 and 20 are the estimated values of ϕ and ψ computed through the throat static pressure, $\bar{p}_t$. These were obtained as follows. The secondary flow velocity was calculated from $\bar{p}_t$ using isentropic flow relations. The secondary mass flow was computed using one-dimensional theory. The total mass flow was used to determine the exit velocity, assuming perfect i.e. complete and lossless mixing. The estimated ϕ and ψ values are significantly higher. This simply sets the upper bound of performance obtainable. One should not be misled by the very high performance indicated, because it cannot be attained in reality. Because, the secondary flow will not (and need not) be constant across the duct inlet and all real physical flows have losses. It is also difficult to achieve perfect mixing.

4. CONCLUSIONS

This work was undertaken with the view of determining the performance characteristics of a multiple jet ejector. In so doing, it was realized that a proper base for comparison of the results was not available. The study was slightly redirected to establishing this base - by defining an equivalent single nozzle and conducting identical tests on an ejector using such a nozzle.

The following major conclusions can be drawn from the study.

1. Acoustic interaction is not a significant feature of the multiple jet flow and ejector-screech tones, so distinctly heard in single jets are not evident in the multiple jets. The flow mixing that occurs should then be mainly due to the interaction of the jets. The mixing properties of the flow inside the duct depend on the area ratio, with better mixing found in a compact ejector.

2. The location of the throat relative to the nozzle exit plane has a large effect on the ability of the ejector to entrain the ambient fluid and also deliver a better performance. The performance deteriorates monotonically as the throat moves farther, in the range of distances tested, in contrast to the behavior of a two-dimensional incompresible ejector.

3. The wall static pressure distribution shows self-similarity in a multiple jet ejector, when normalized by the throat pressure, for the closest nozzle-throat spacing. At longer distances, a slight break down in self similarity can be seen.

4. A multiple jet ejector is distinctly superior to a single jet ejector from a performance point of view, especially at low area ratios and highly underexpanded exit conditions.

5. Increasing the number of jets may not result in a better ejector for jet spacing of upto $\simeq$ 15 jet widths.

6. In a multiple jet system, the velocity profiles at the duct exit are fairly uniform and

thus the flow quality in it is better. However, in a single jet ejector, the velocity variations could be as much as 100% and this is highly undesirable.

7. The gross variation in velocity at the exit from the shroud of a single jet ejector establishes the need to perform detailed measurements in several planes during bench tests before the results can be extended to flight conditions.

REFERENCES

1. Aiken, T. N., "Aerodynamic and Noise Measurements on a Quasi- Two Dimensional Augmentor Wing Model with Lobe-Type Nozzles", NASA TMX-62,237, September 1973.

2. Bernal, L. and Sarohia, V. K., "Entrainment and Mixing in Thrust Augmenting Ejectors", Jet Propulsion Laboratory, Cal tech, Report D-66, February 1982.

3. Bevilaqua, P. M., "Evaluation of Hyper-mixing for Thrust Augmenting Ejectors", Journal of Aircraft, Vol 11, No. 6, 348-354.

4. Hsia, Y. C., "An Experimental Investigation of an Underexpanded Rectangular Jet Ejector", Ph.D. Thesis, Stanford University, March 1984.

5. Hsia, Y; Krothapalli, A.; Baganoff, D. and Karamcheti, K., "The Structure of a Subsonic Compressible Rectangular Jet", JIAA TR-43, Stanford University, January 1982.

6. Hsia, Y. C., "An Experimental Investigation of an Underexpanded Rectangular Jet Ejector", Ph.D. Thesis, Stanford University, March 1984.

7. Hsia, Y. C.; Krothapalli, A. and Baganoff, D., "Some observations on the Mixing of an Underexpanded Rectangular Jet Ejector", AIAA-84-0280; 1984.

7. Keenan, J. H.; Neumann, E. P. and Lustwerk, F., "An Investigation of Ejector Design by Analysis and Experiment", Journal of Applied Mechanics, Vol 17, No. 3, pp 299-309, 1950.

8. Krothapalli, A.; Baganoff, D. and Karamcheti, K., "An Experimental Study of Multiple Jet Mixing", JIAA TR-23, Stanford University, June 1979.

9. Krothapalli, A.; Hsia, Y.; Baganoff, D. and Karamcheti, K., "On the Structure of an Underexpanded Rectangular Jet", JIAA TR-47, Stanford University, July 1982.

10. Nagaraja, K.S.; Hammond, D.L. and Graetch, J. E., "One Dimensional Compressible

Ejector Flows", AIAA-73-1184, 1973.

11. Parthasarathy, S. P.; Cuffel, R. F. and Massier, P. F., "Twin-Jet Shielding", Journal of Aircraft, Vol 17, No. 9, 618-626, 1980.

12. Quinn, B., "Interaction Between Screech Tones and Ejector Performance", Journal of Aircraft, Vol. 14, No. 5, 467-473, 1977.

13. Rajaratnam, N., "Turbulent Jets", Elsevier, New York, 1976.

14. Skoblenick, H. R. and Hill, P.G., "Experimental and Analytical Study of an Axisymmetric Thrust Augmentor", Journal of Aircraft, Vol. 14, No. 5, 474-480, 1977.

15. Viets, H., "Thrust Augmenting Ejectors, ARL Report No. 75-0224, Wright Patterson Air Force Base, Ohio 1975.

16. Von Karman, T., "Theoretical Remarks on Thrust Augmentation", Reissner Anniversary Volume, Contributions to Applied Mechanics, 1949.

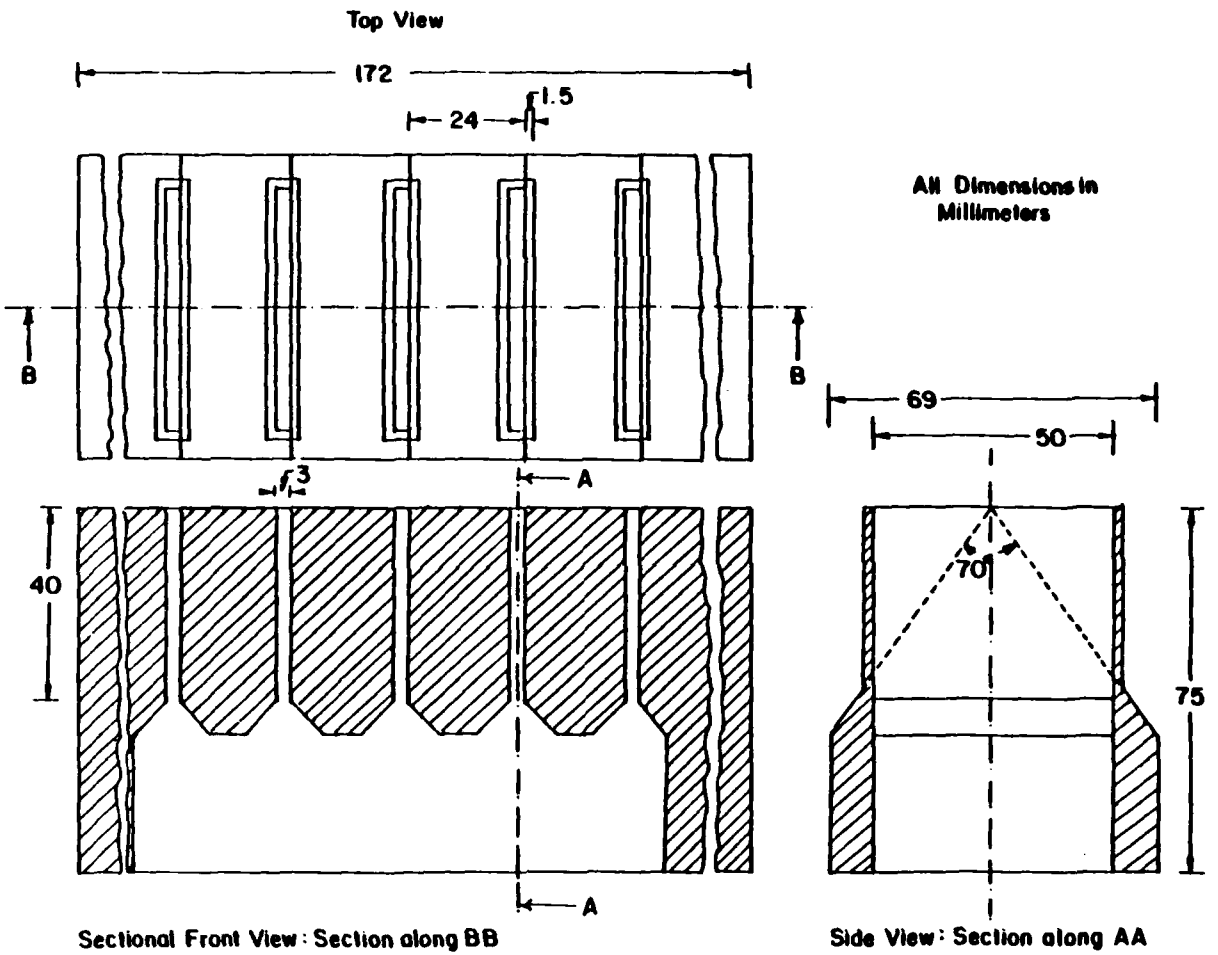

Figure 1. Details of the multiple jet assembly.

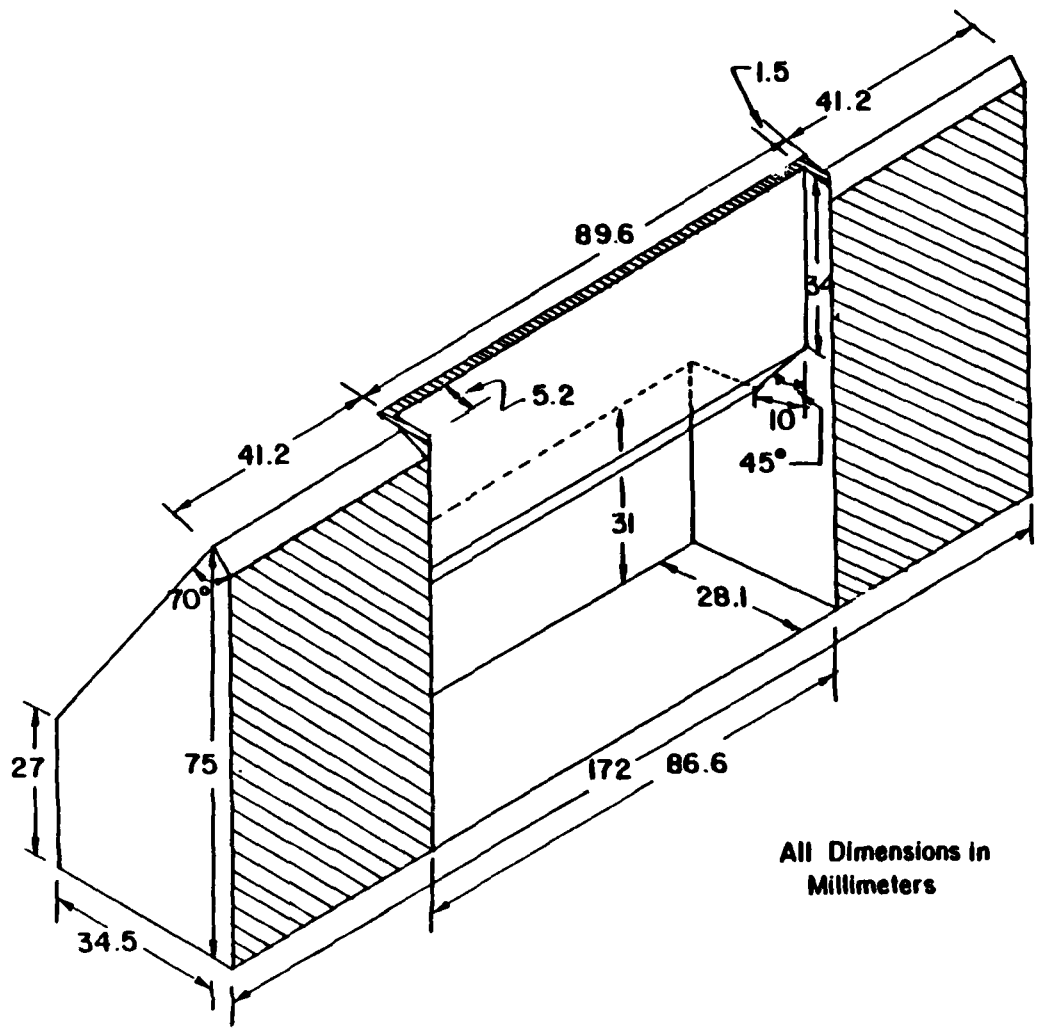

Figure 2. Details of the equivalent single jet.

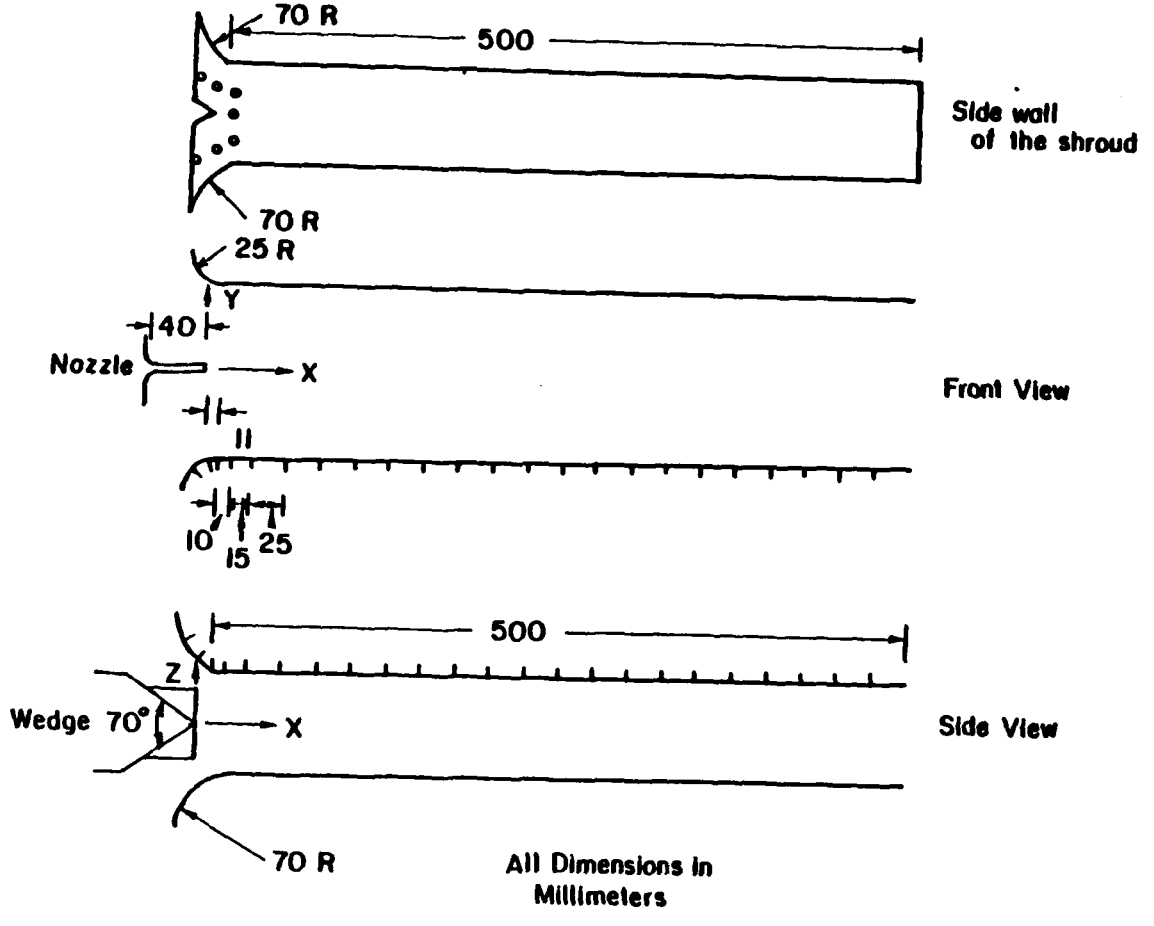

Figure 3. Schematic of the ejector shroud and details of pressure taps.

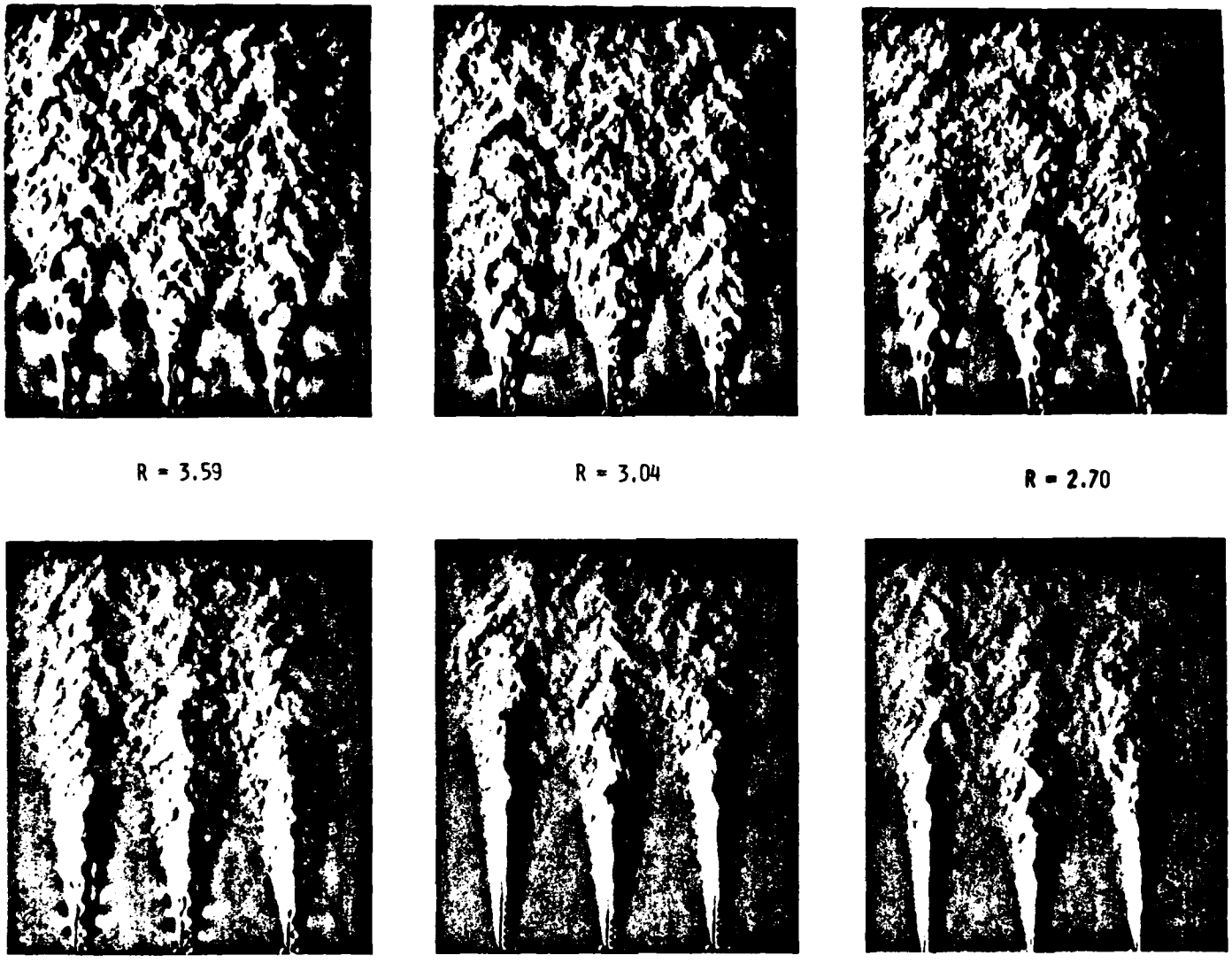

Figure 4a. **Single exposure schlieren photogrpahs of a multiple free jet at different pressure ratios.**

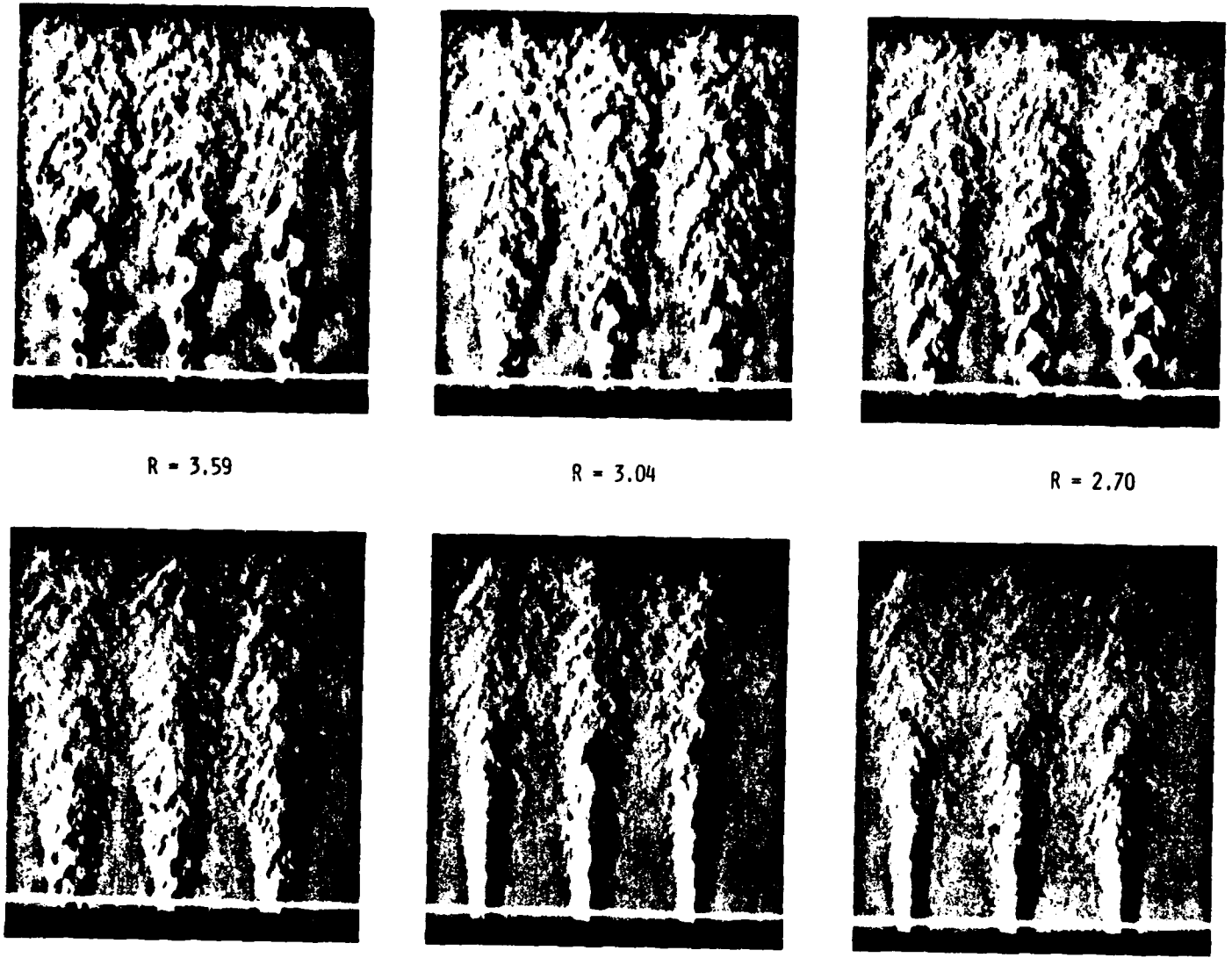

Figure 4b. **Single exposure schlieren photographs of a 3 jet ejector at different pressure ratios; A.R. = 20:1.**

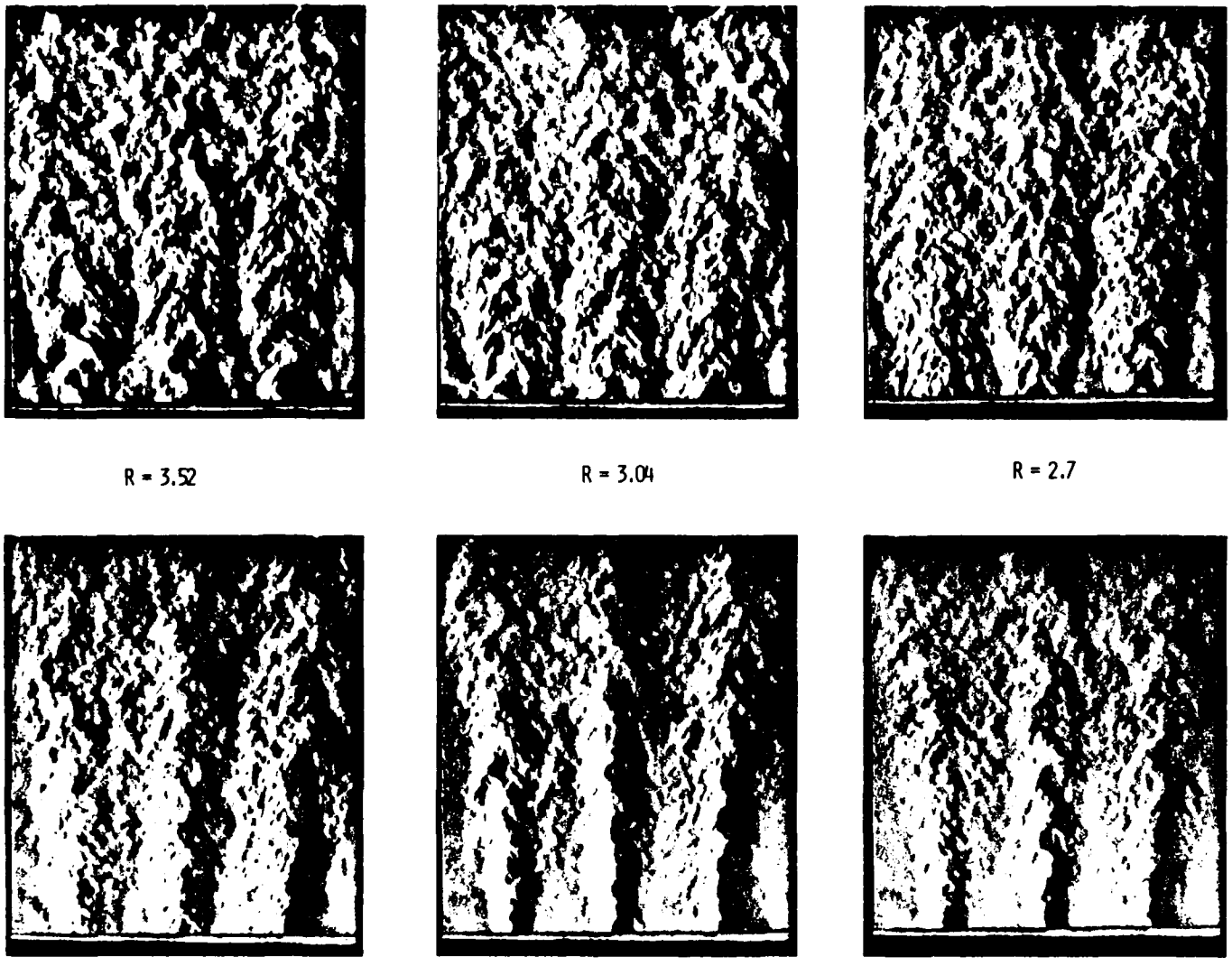

Figure 4c. **Single exposure schliren photographs of a 3 jet ejector at different pressure ratios; A.R. = 14:1.**

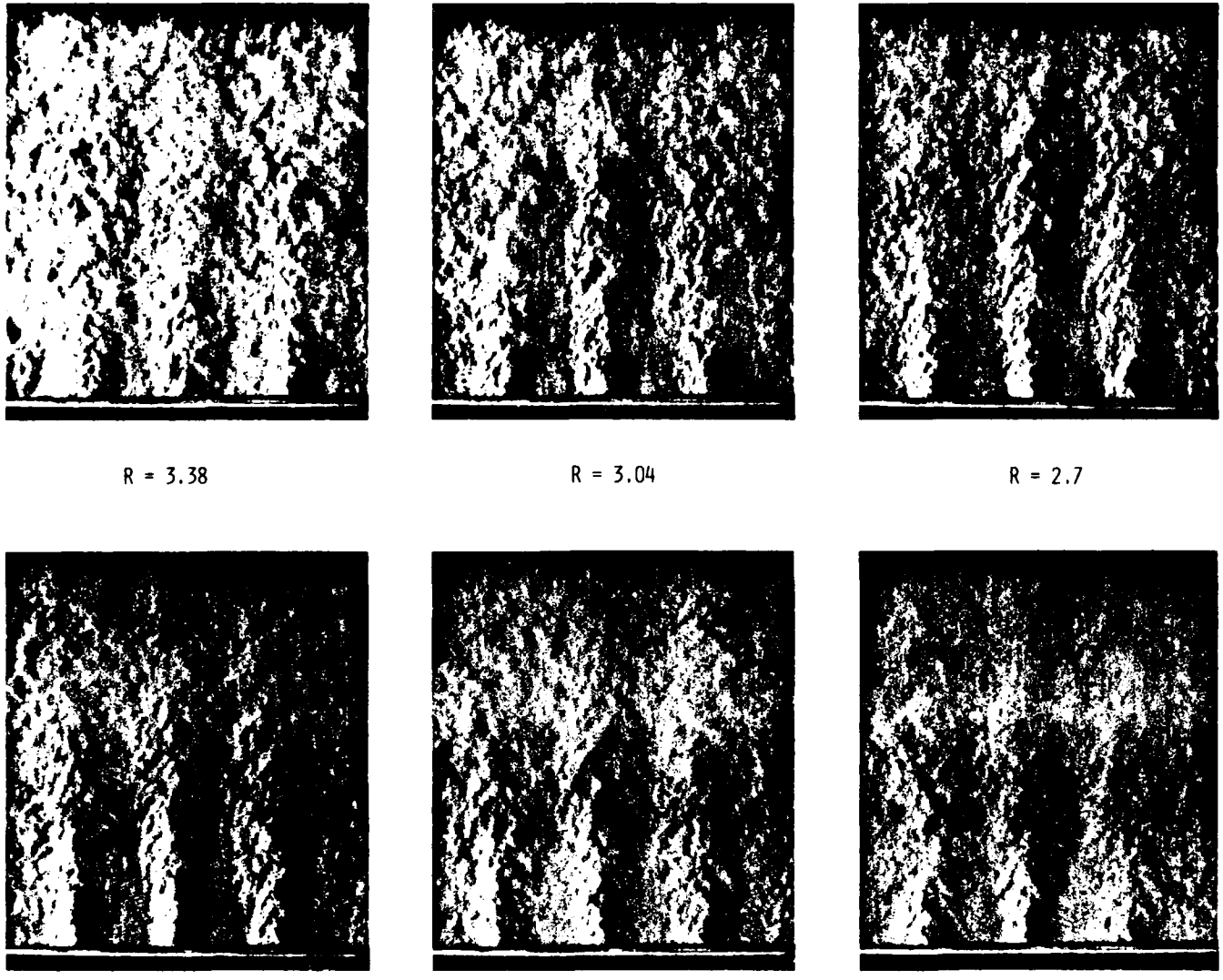

Figure 4d. Single exposure schlieren photographs of a 5 jet ejector at different pressure ratios; A.R.=20:1.

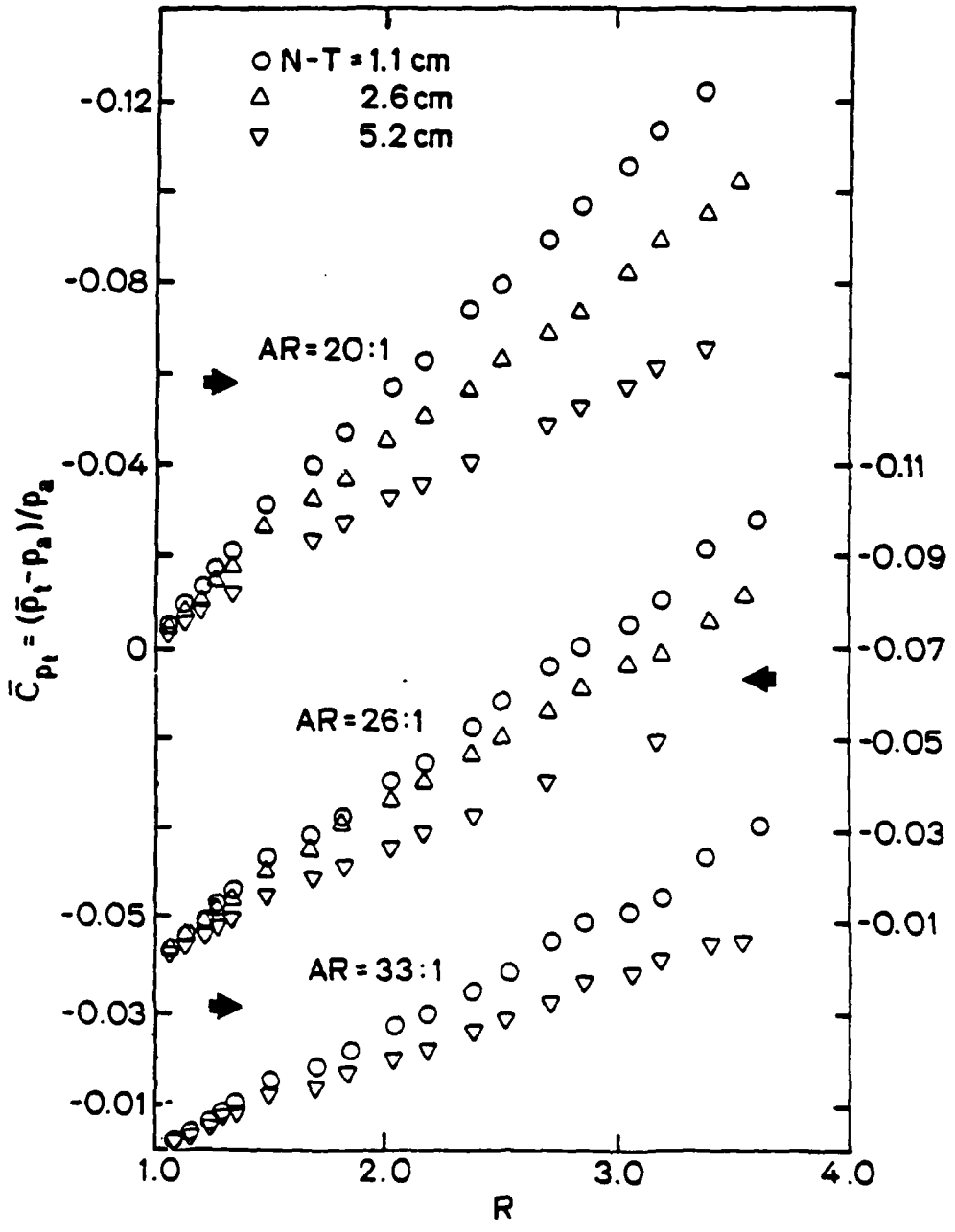

Figure 5a. Effect of nozzle-throat distance on throat static pressure coefficient for different area ratios; 3 jet ejector.

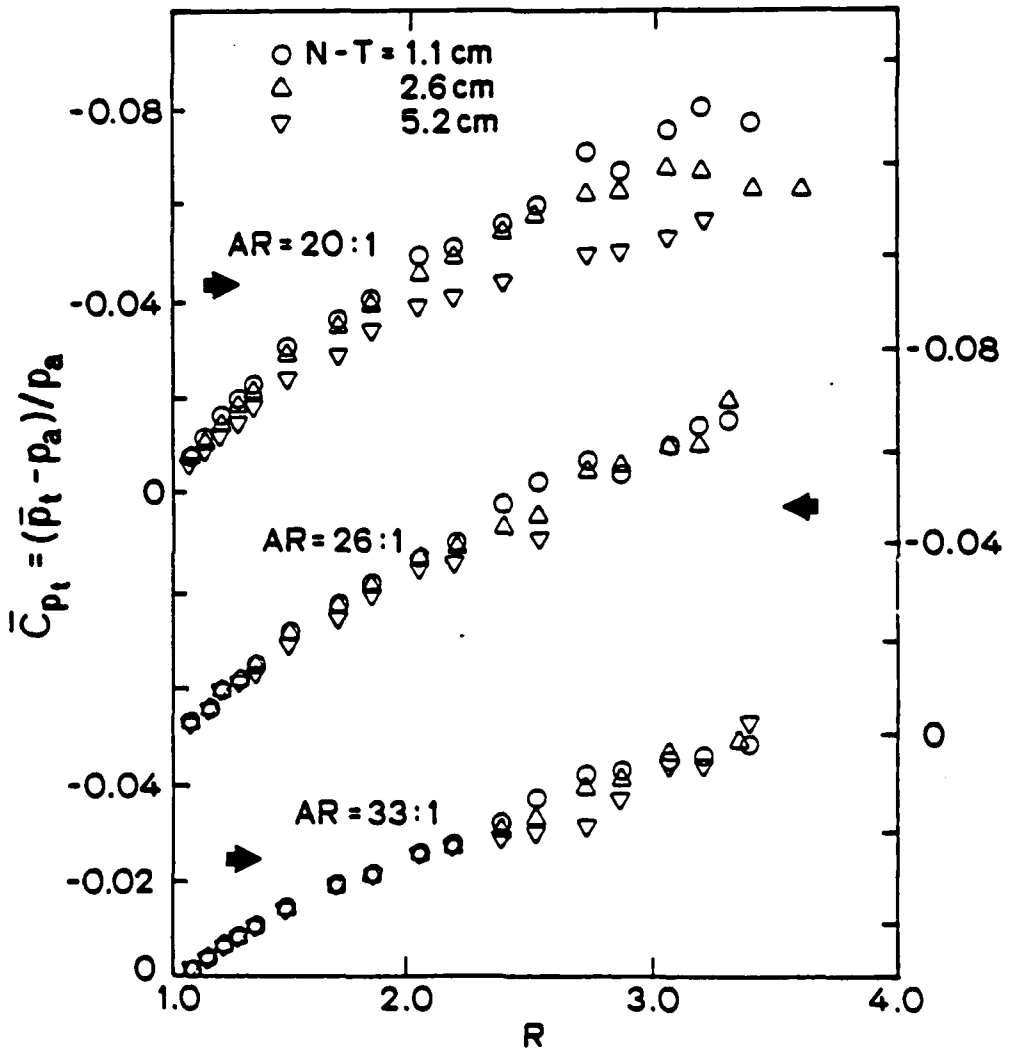

Figure 5b. Effect of nozzle-throat distance on throat static pressure coefficient for different area ratios; equivalent single jet ejector.

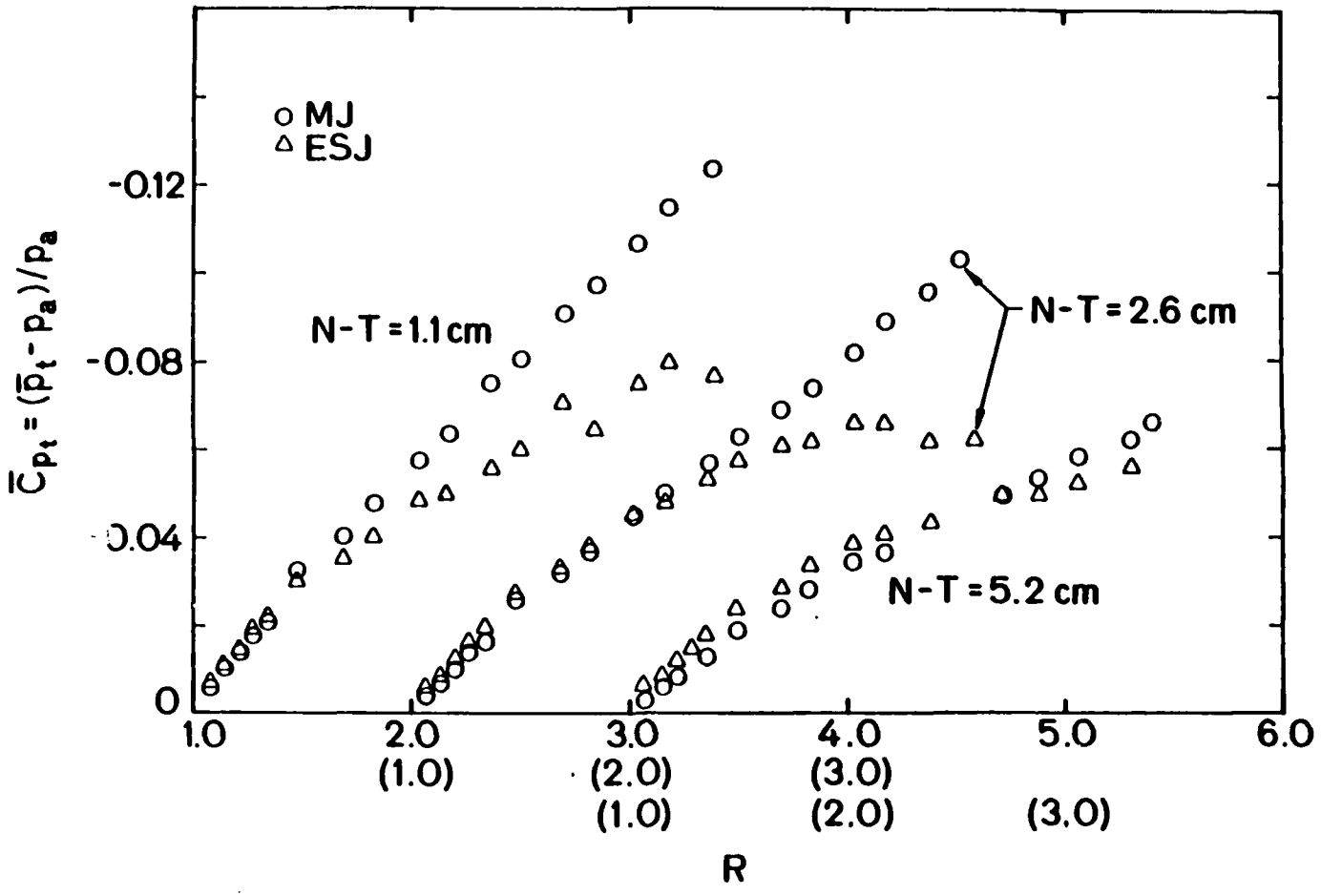

Figure 6a. Comparison of throat static pressure coefficients in equivalent single jet and multiple jet ejectors; AR=20:1.

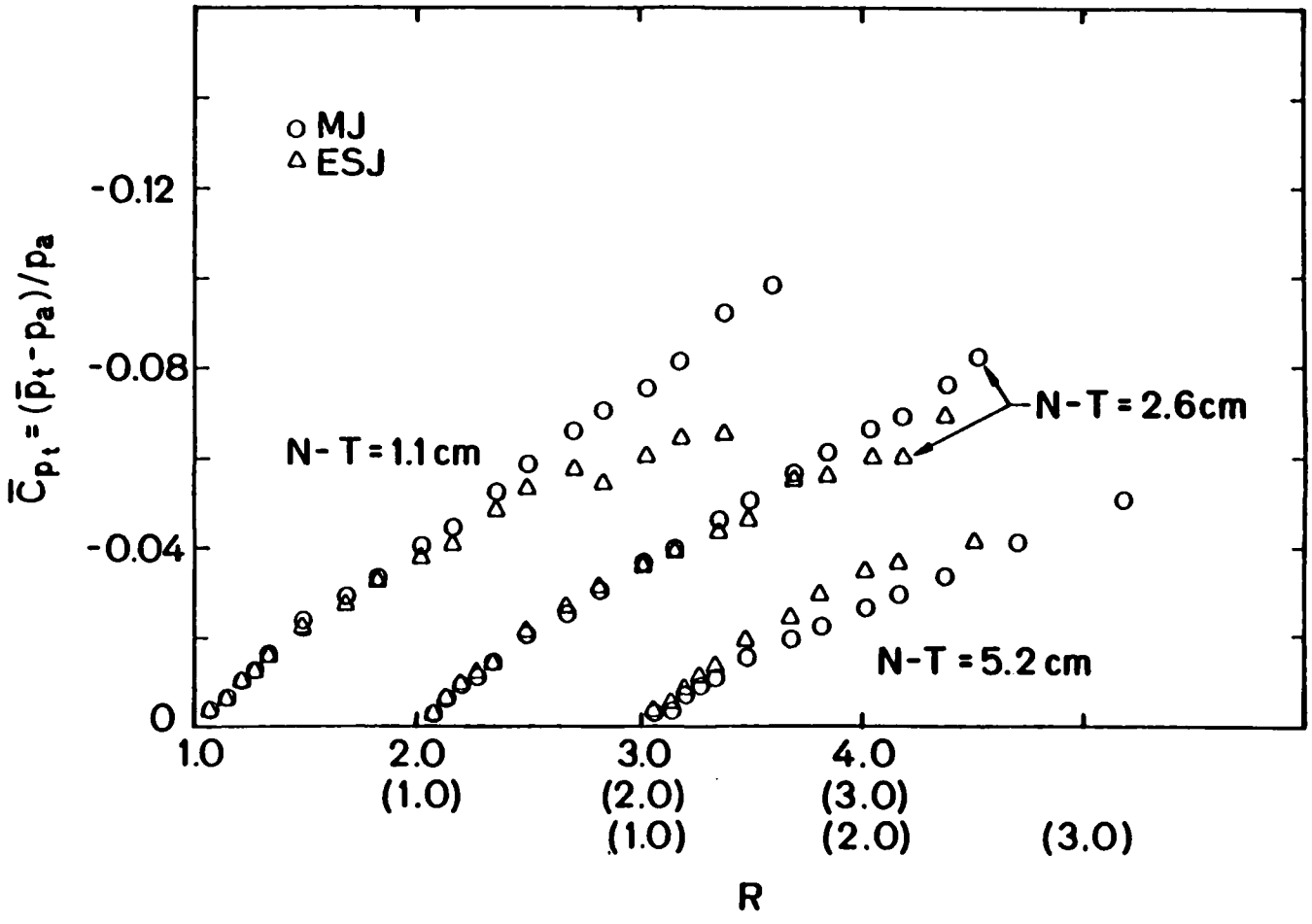

Figure 6b. Comparison of throat static pressure coefficients in equivalent single jet and multiple jet ejectors; A.R.=26:1.

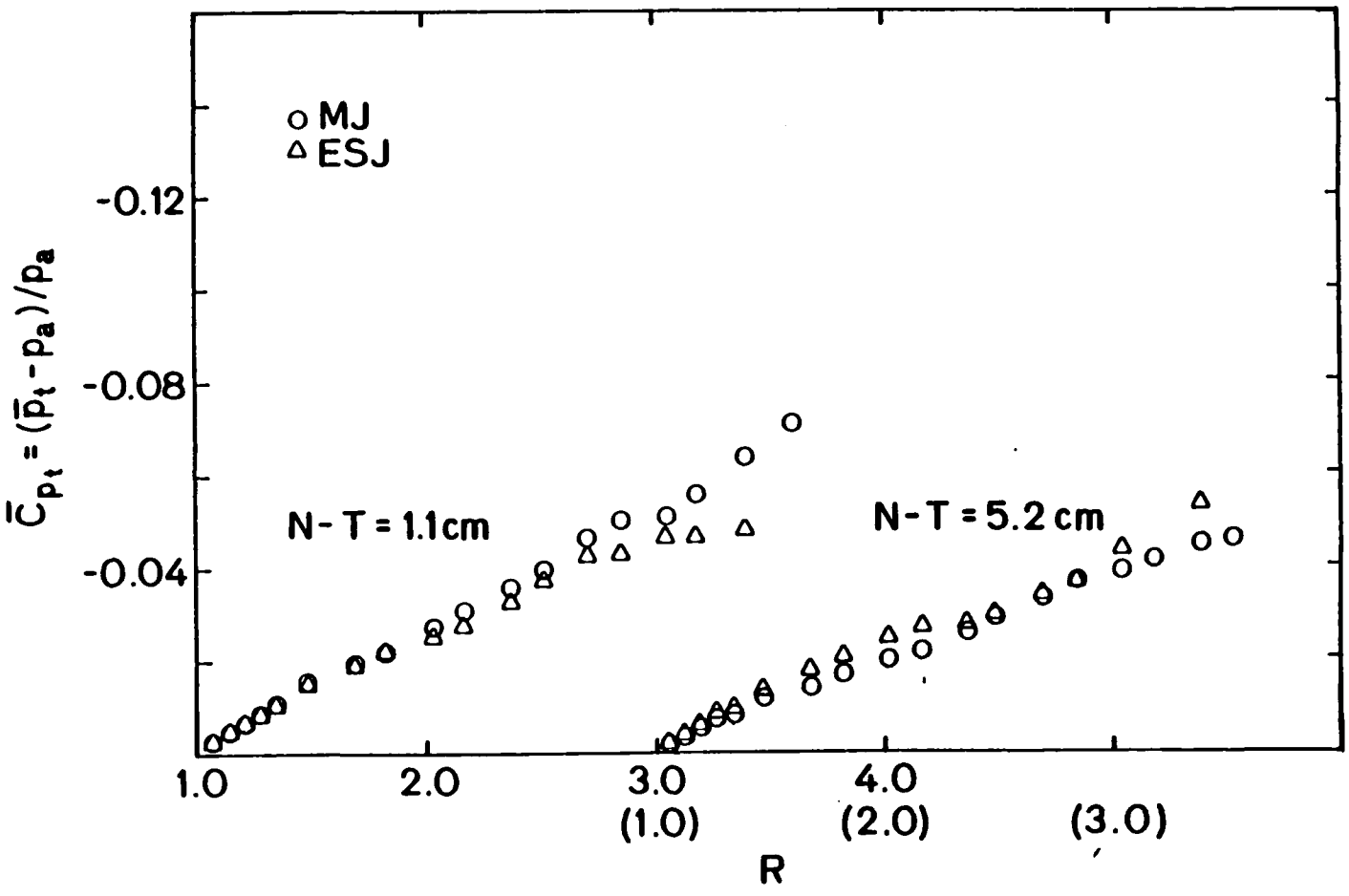

Figure 6c. Comparison of throat static pressure coefficients in equivalent single jet and multiple jet ejectors; A.R.=33:1.

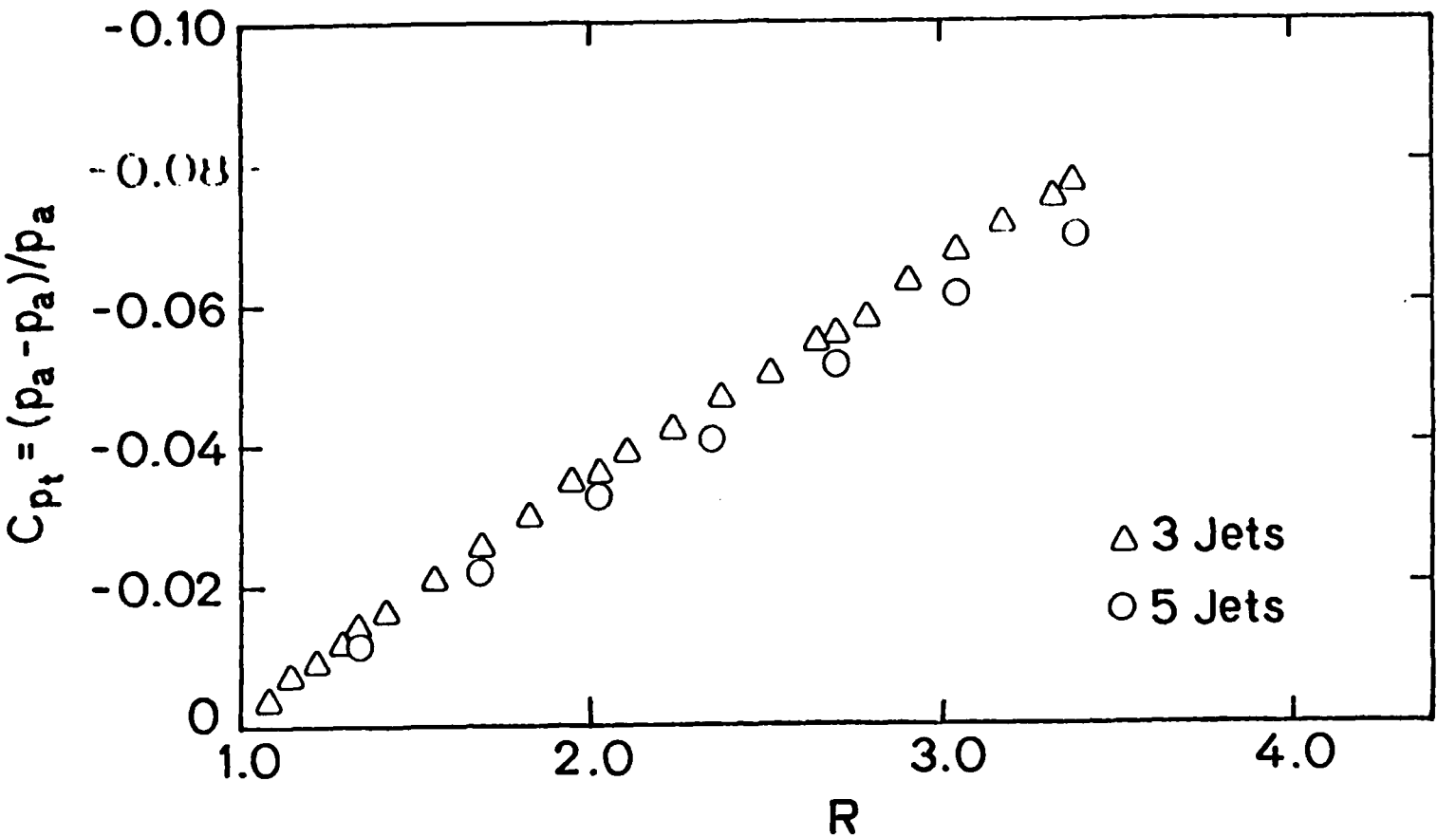

Figure 7. **Comparison of throat static pressure coefficients in 3 and 5 jet ejectors.**

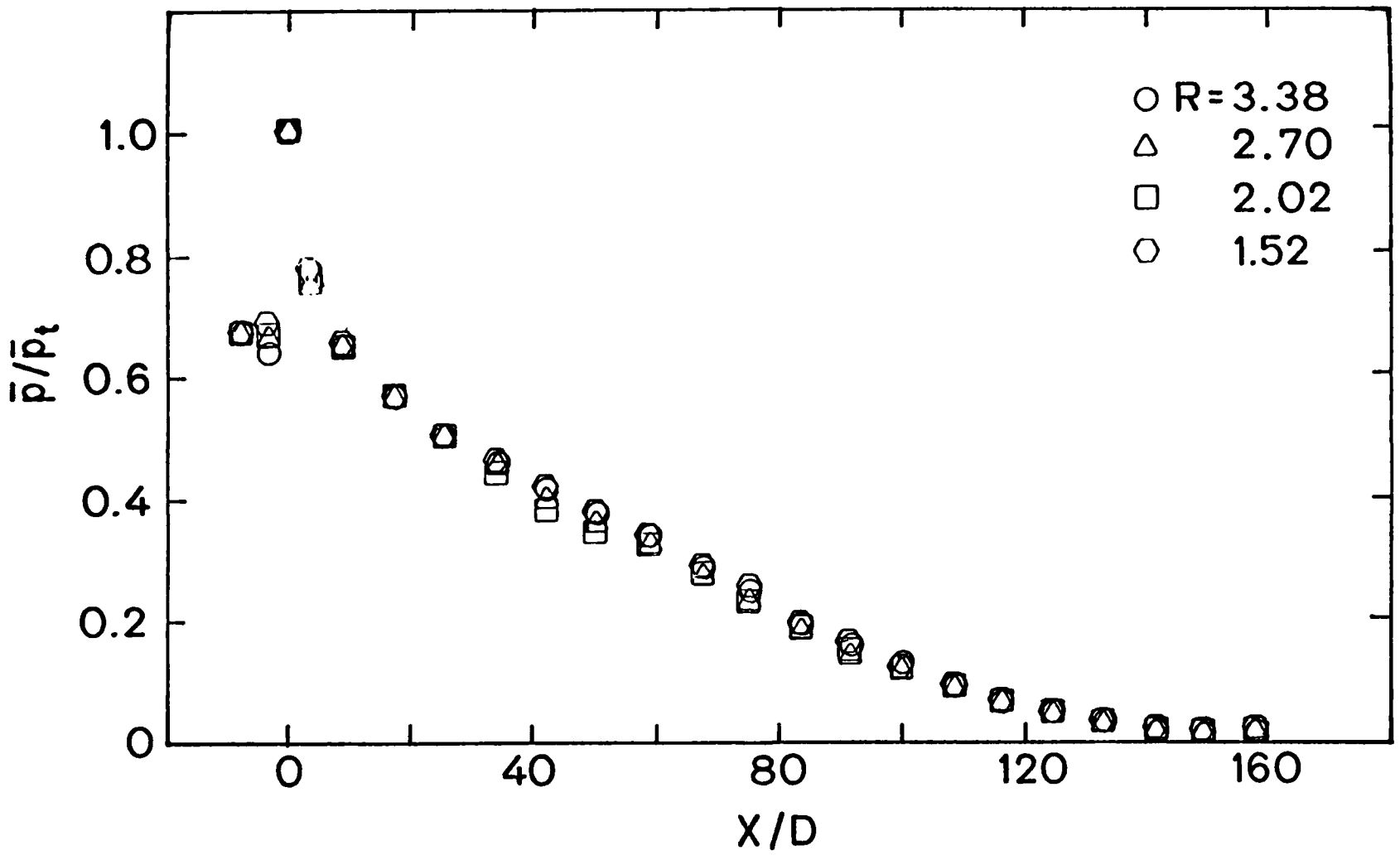

Figure 8a. Wall static pressure distributions in the 20:1, 3 jet ejector; N-T=1.1 cm.

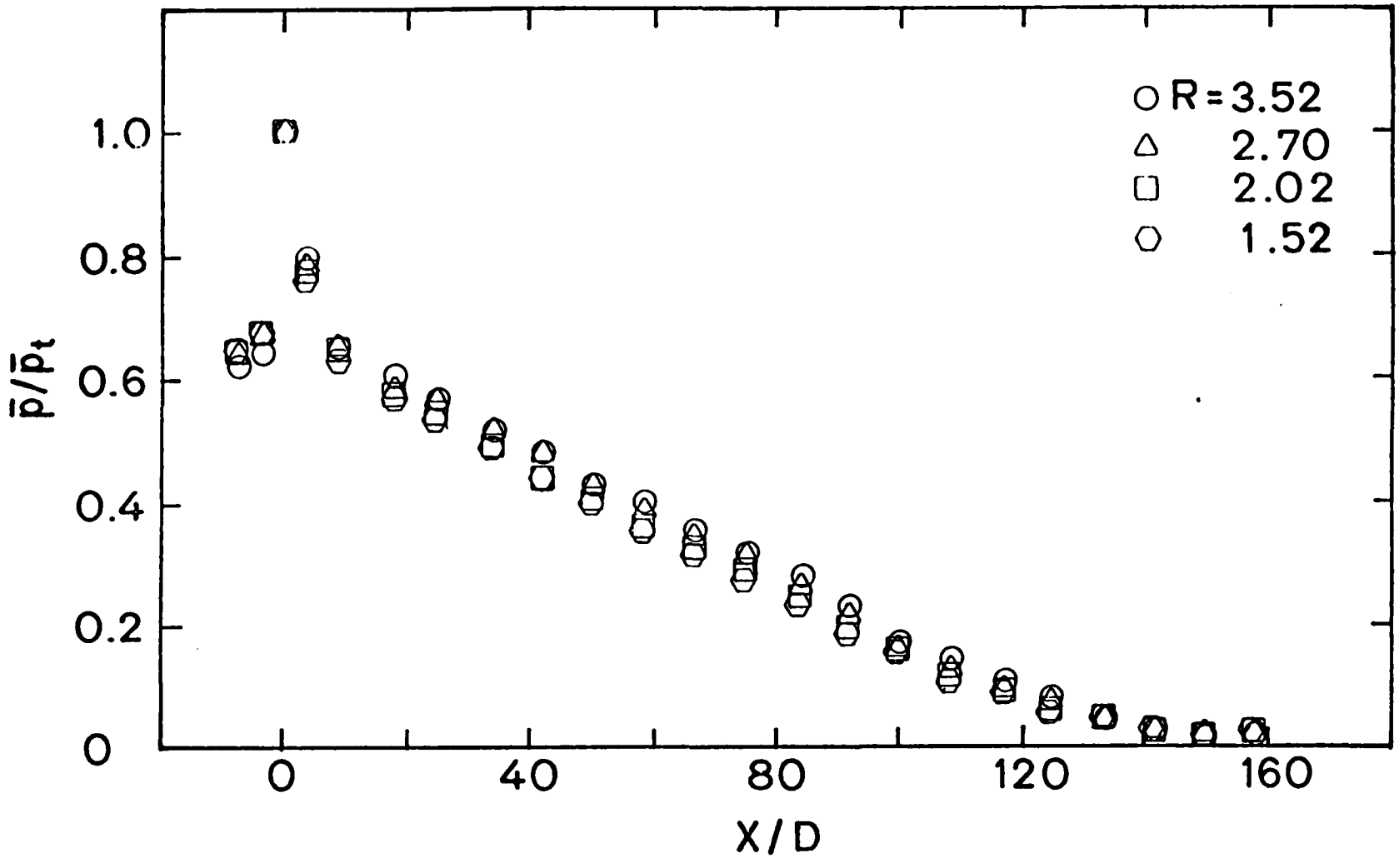

Figure 8b. Wall static pressure distributions in the 20:1, 3 jet ejector; N-T=2.6 cm.

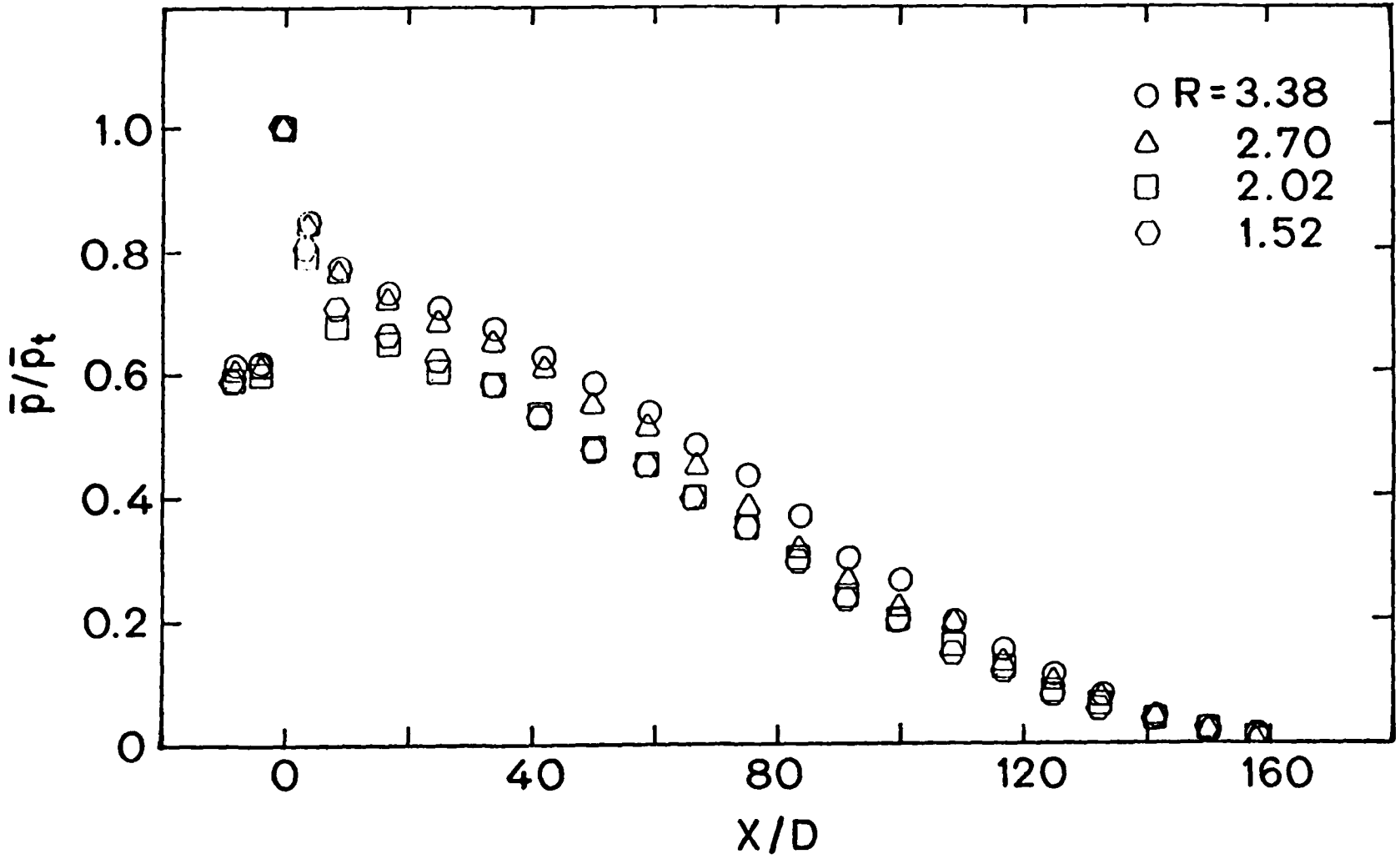

Figure 8c. Wall static pressure distributions in the 20:1, 3 jet ejector; N-T=5.2 cm.

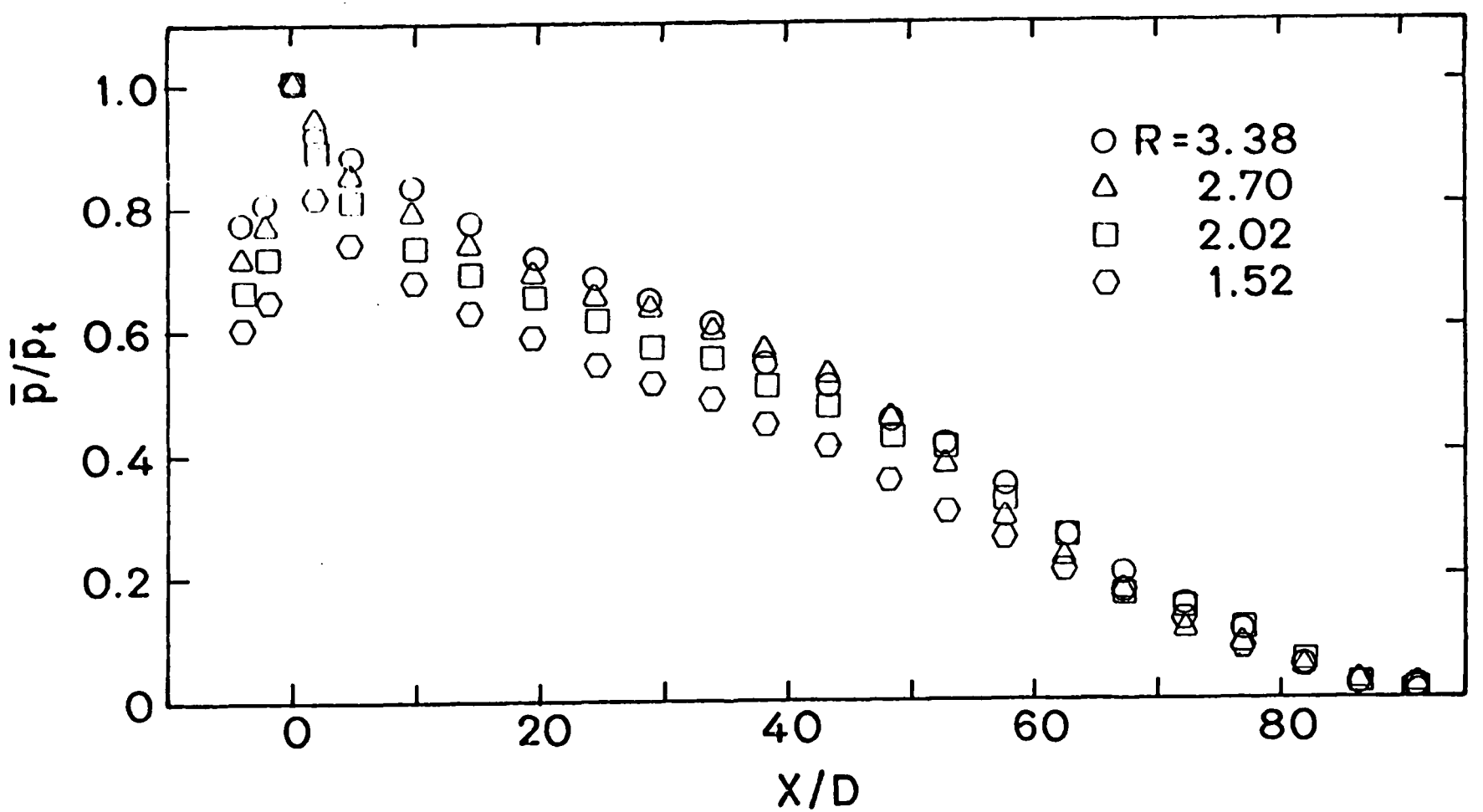

Figure 9a. Wall static pressure distributions in the 20:1, equivalent single jet ejector; N-T=1.1 cm.

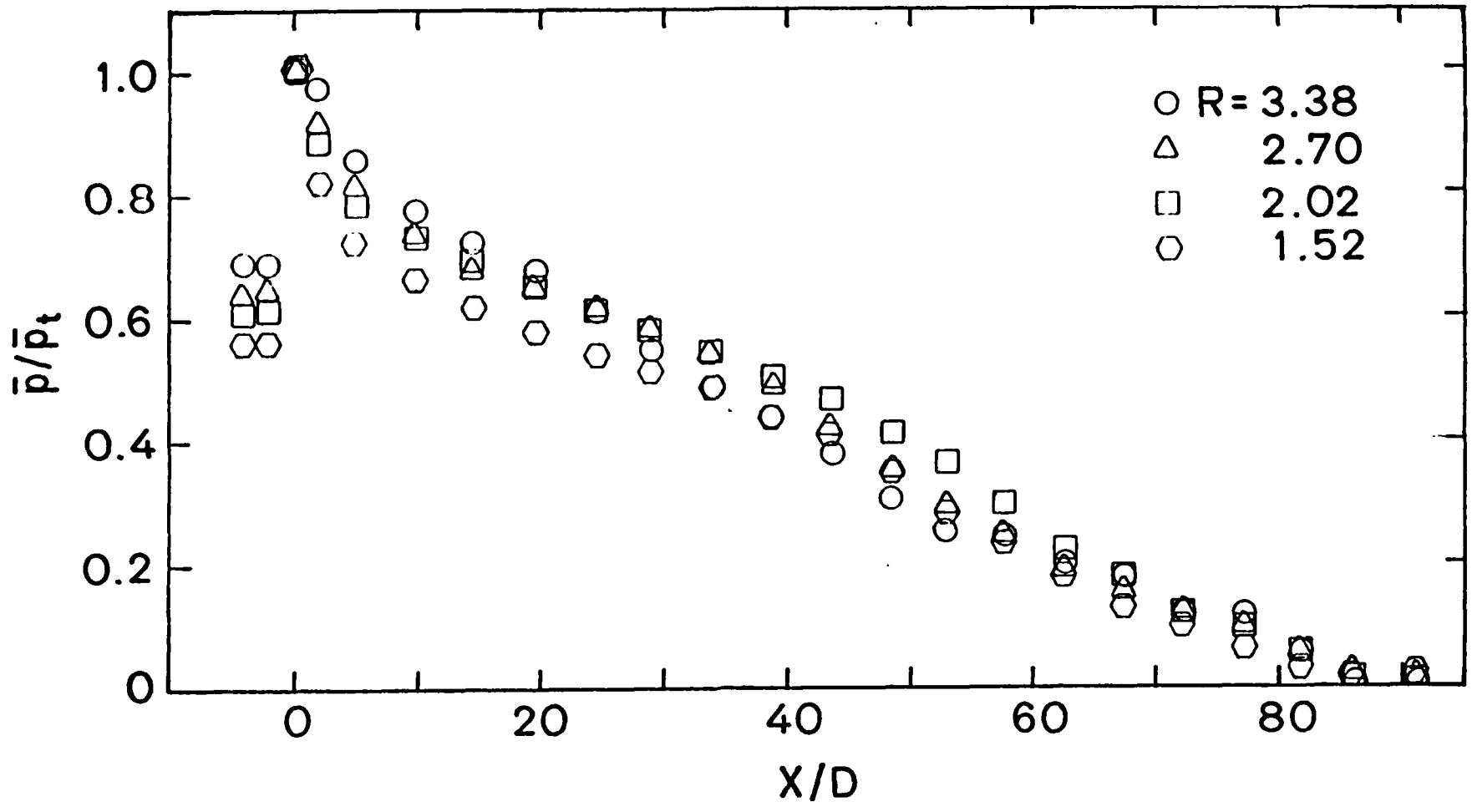

Figure 9b. Wall static pressure distributions in the 20:1, equivalent single jet ejector; N-T=2.6 cm

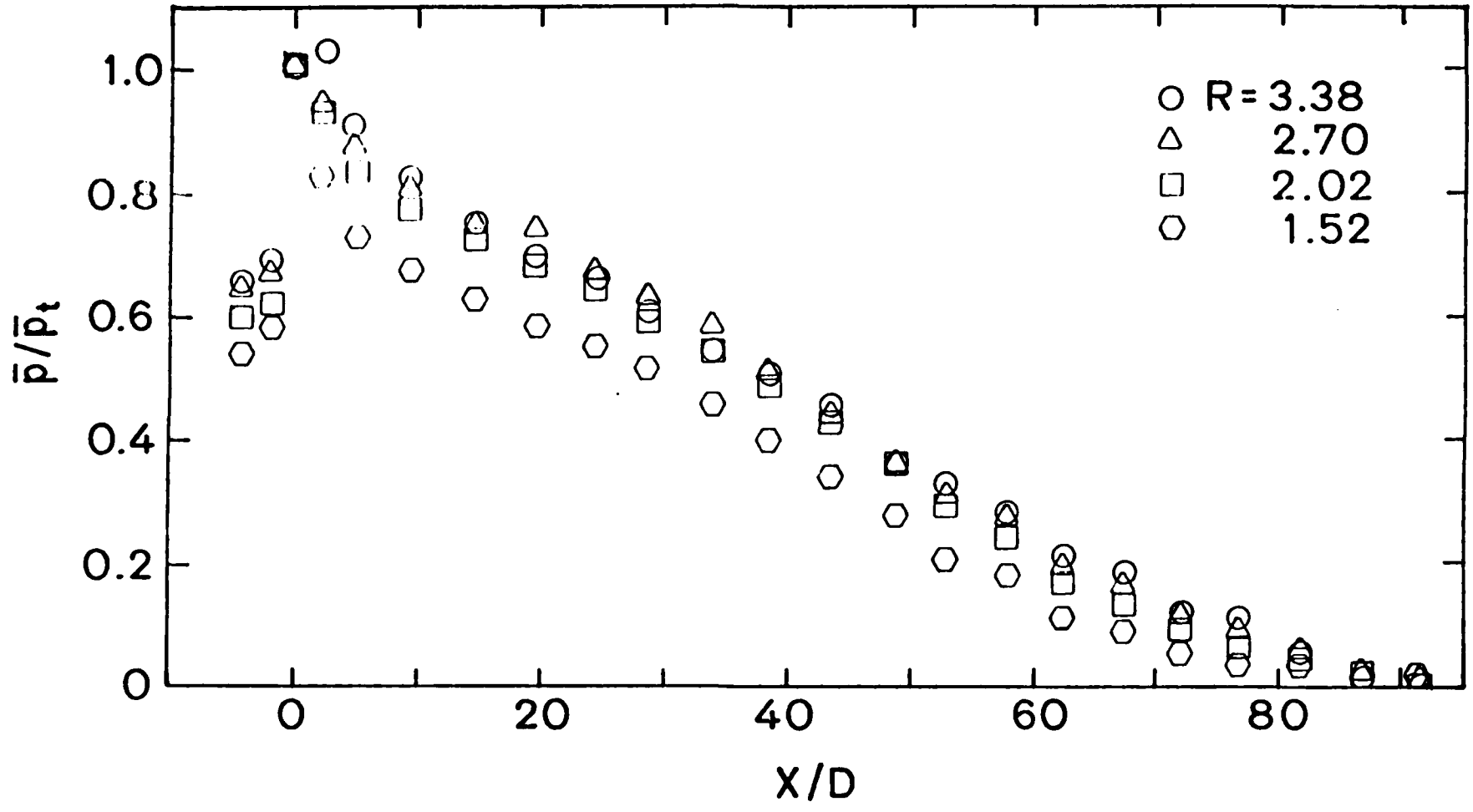

Figure 9c. **Wall static pressure distributions in the 20:1, equivalent single jet ejector; N-T=5.2cm**

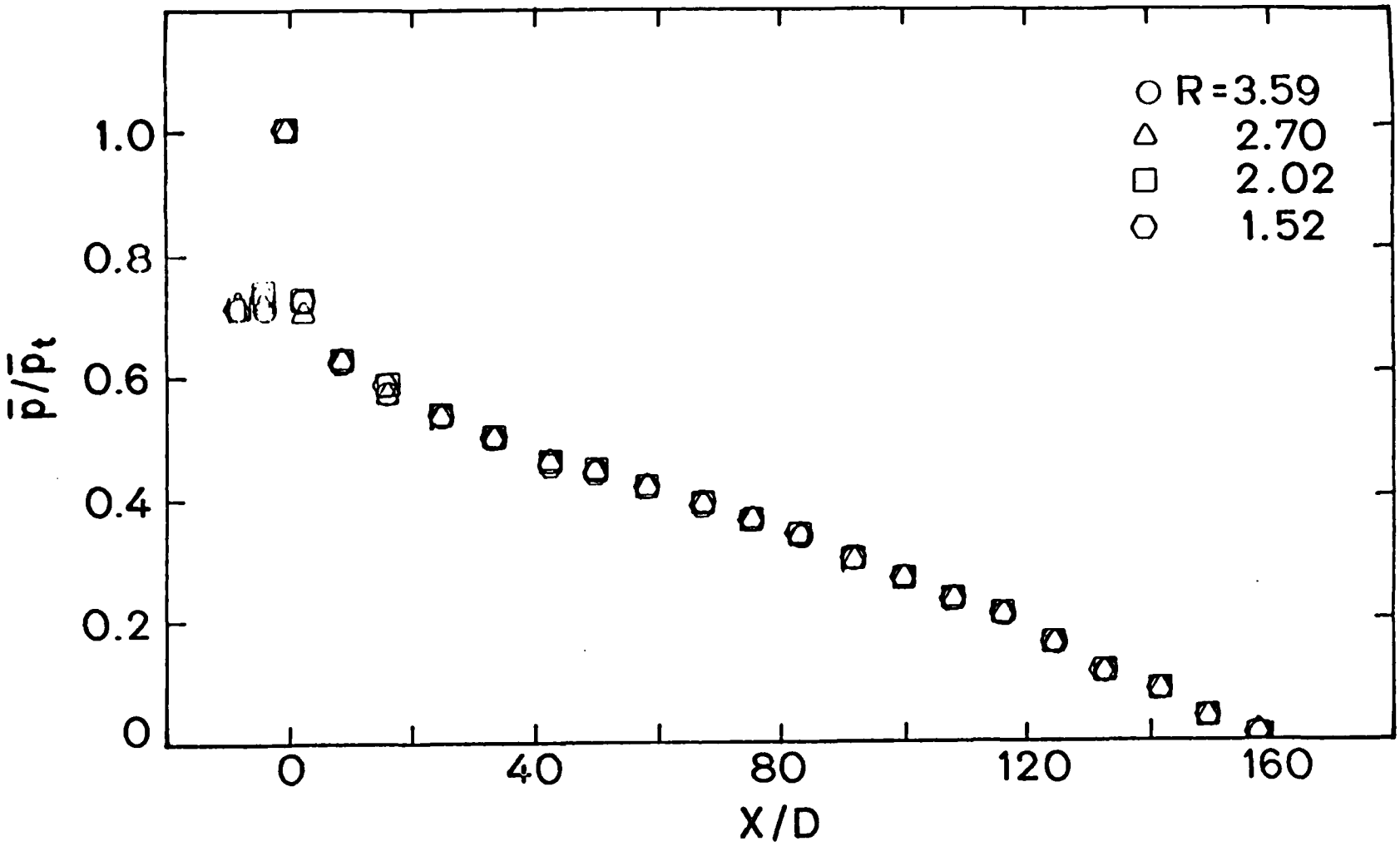

Figure 10a. Wall static pressure distributions in the 26:1, 3 jet ejector; N-T=1.1cm

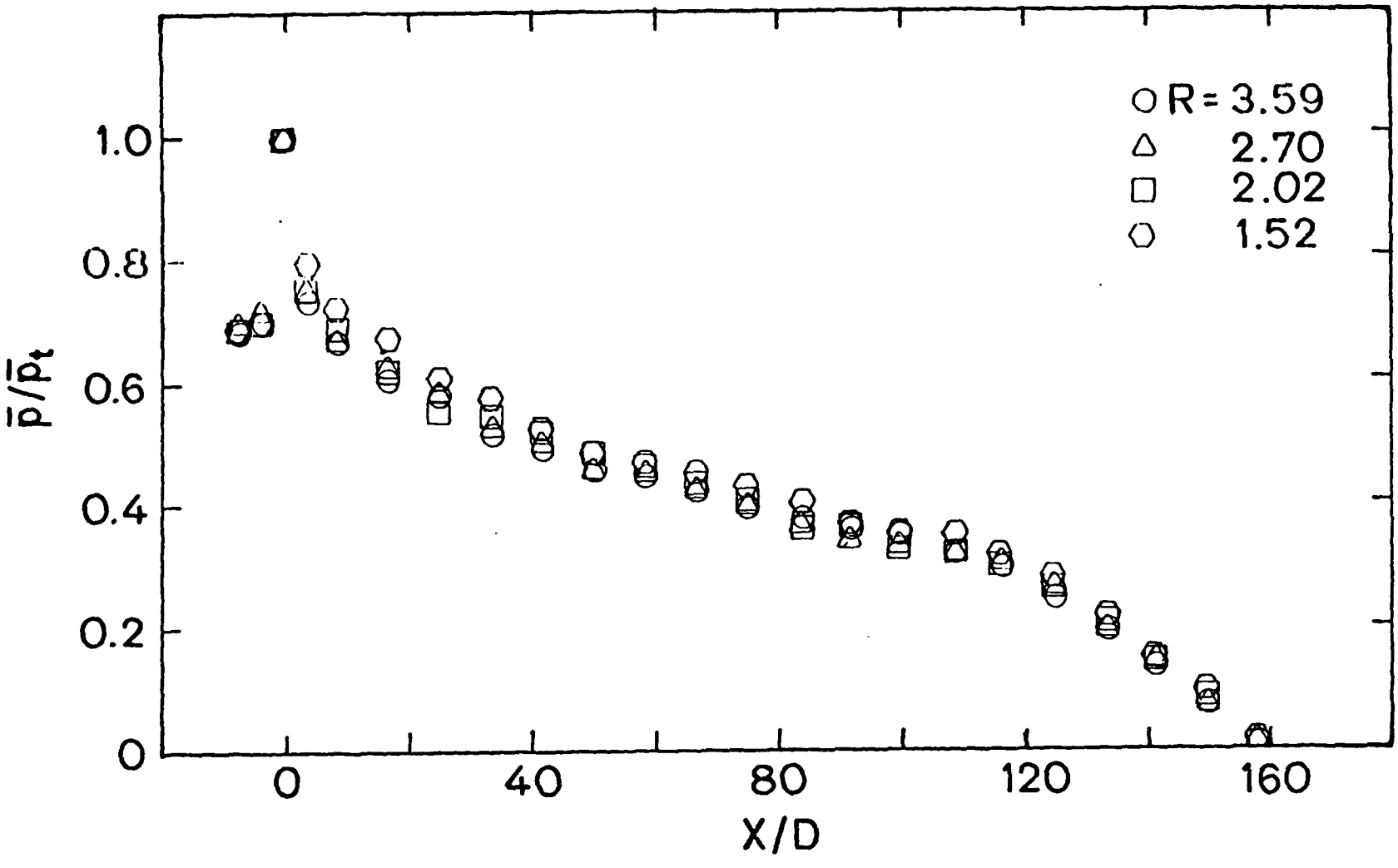

Figure 10 b. Wall static pressure distributions in the 33:1, 3 jet ejector; N-T=1.1cm

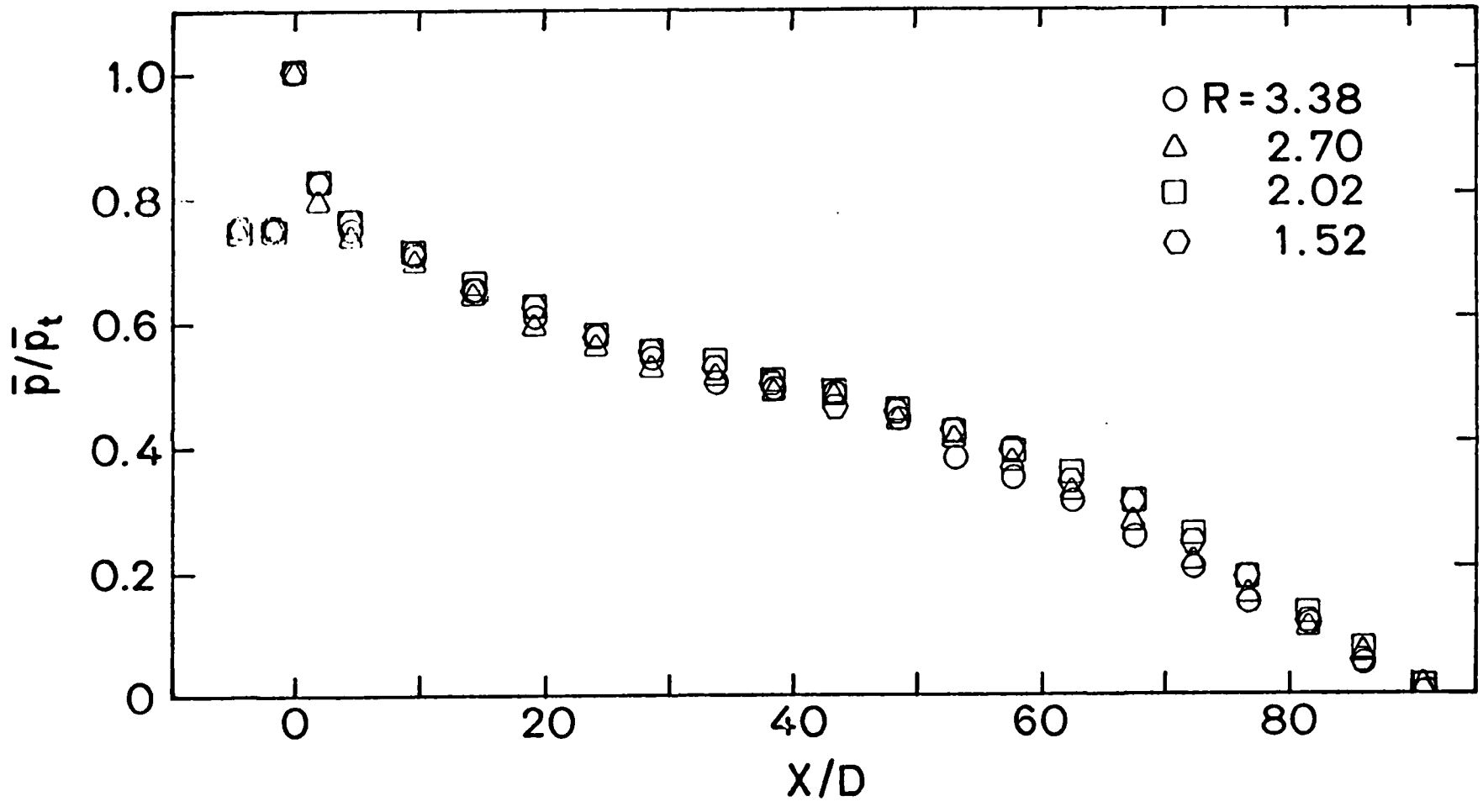

Figure 11a. Wall static pressure distributions in the 26:1, equivalent single jet ejector; N-T=1.1 cm

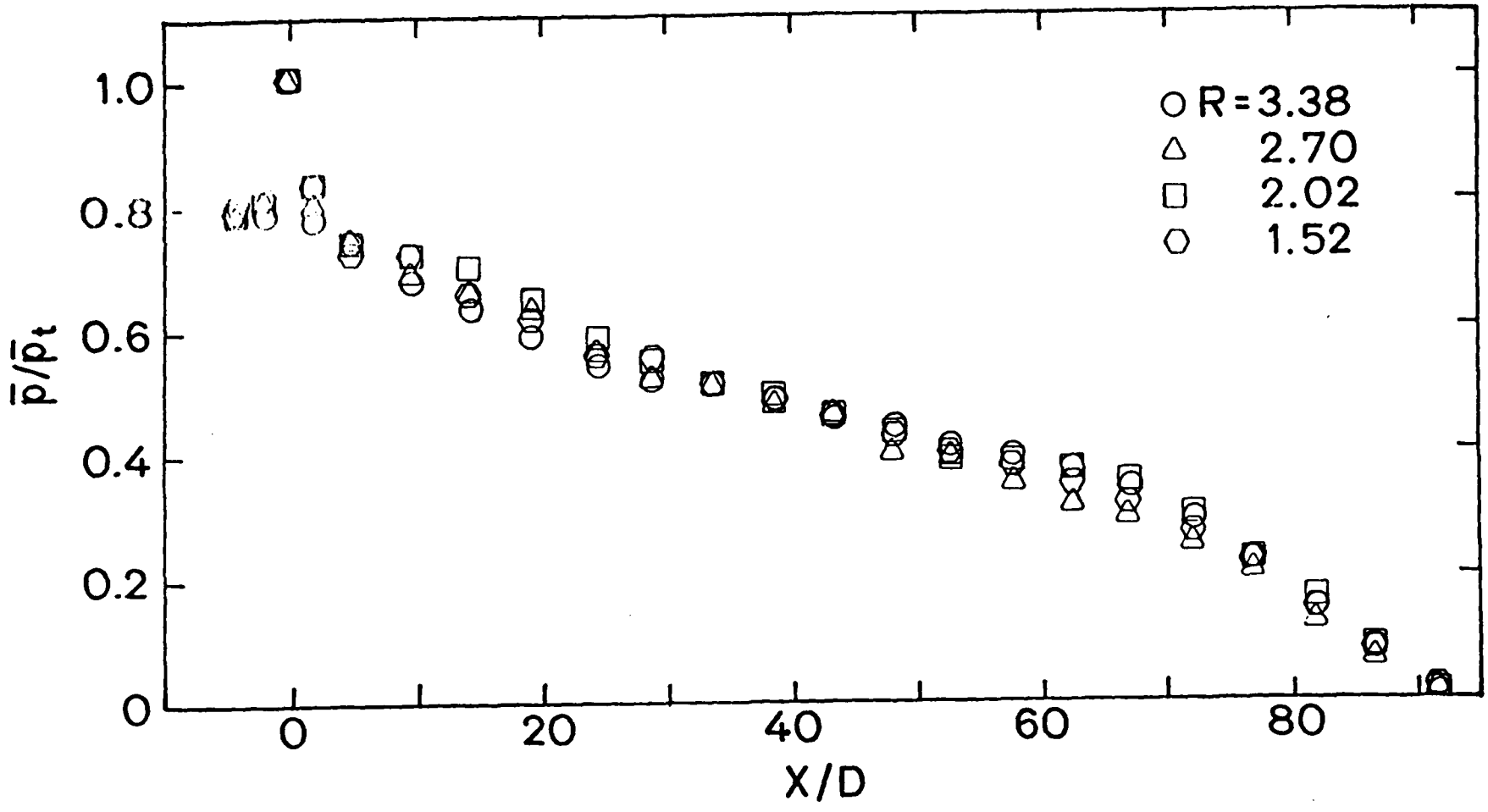

Figure 11 b. Wall static pressure distribution in the 33:1, equivalent single jet ejector; N-T=1.1cm.

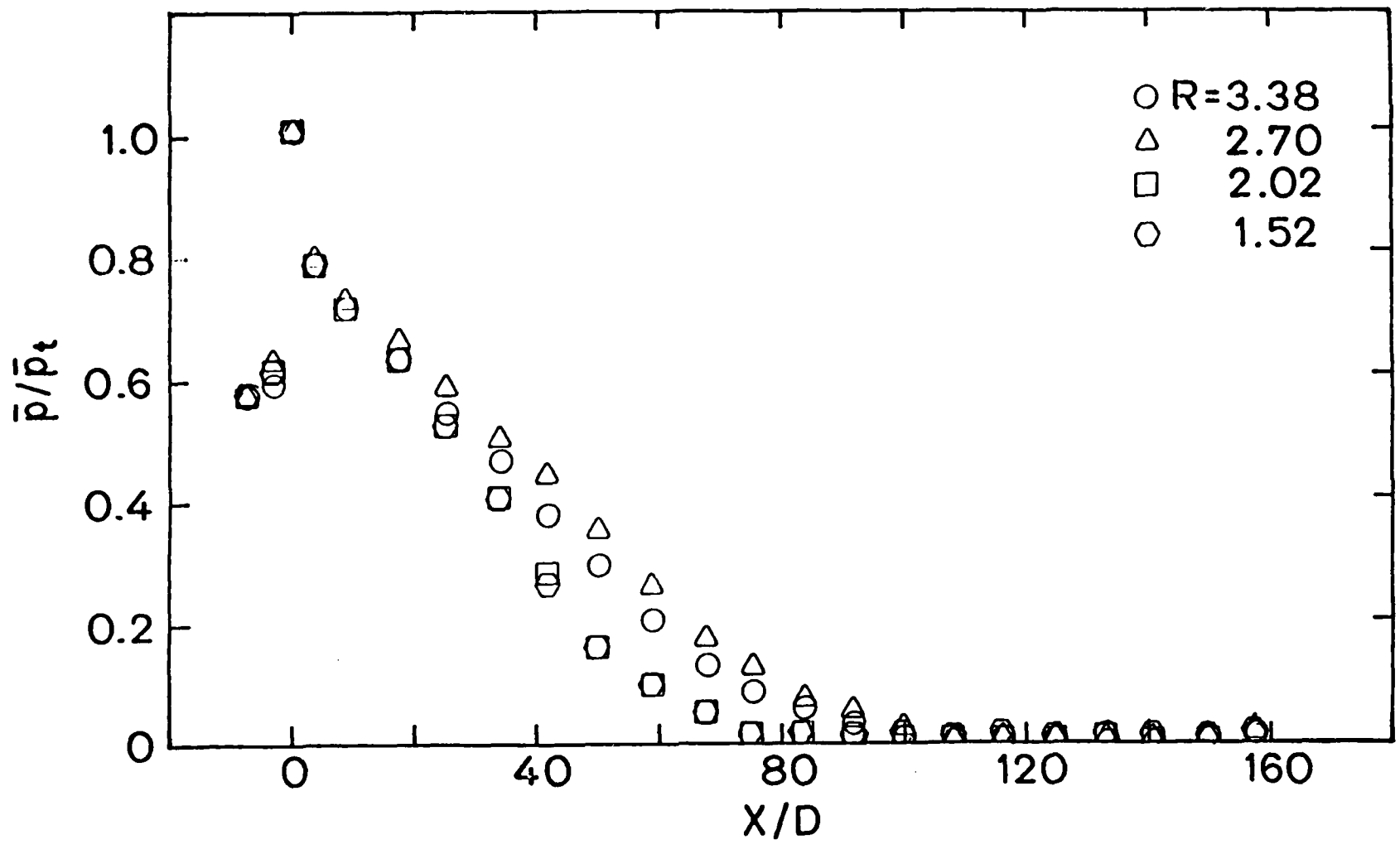

Figure 12a. Wall static pressure distributions in the 14:1, 3 jet ejector; N-T=2.5cm.

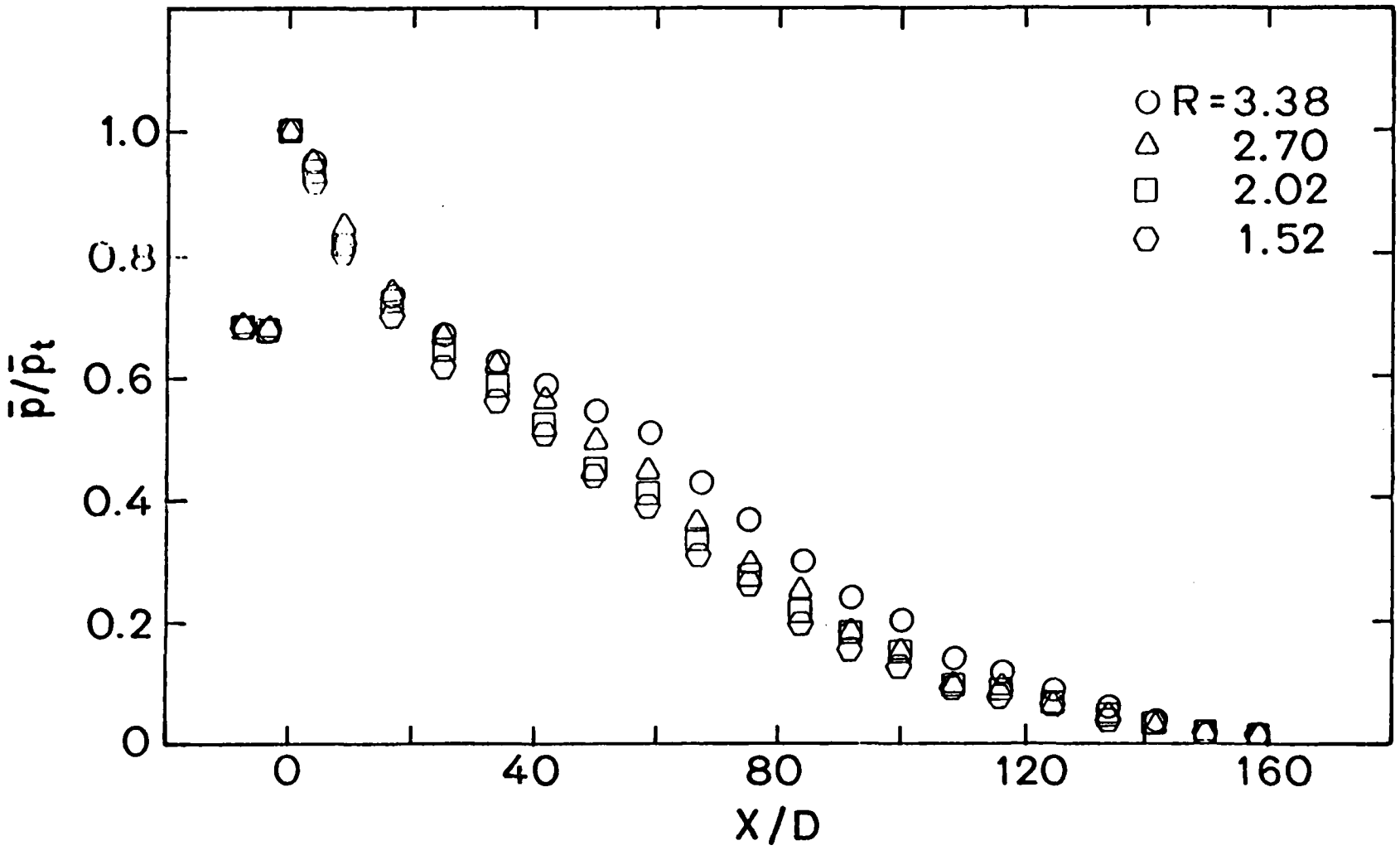

Figure 12b. Wall static pressure distributions in the 14:1, 3 jet ejector; N-T=5.2cm.

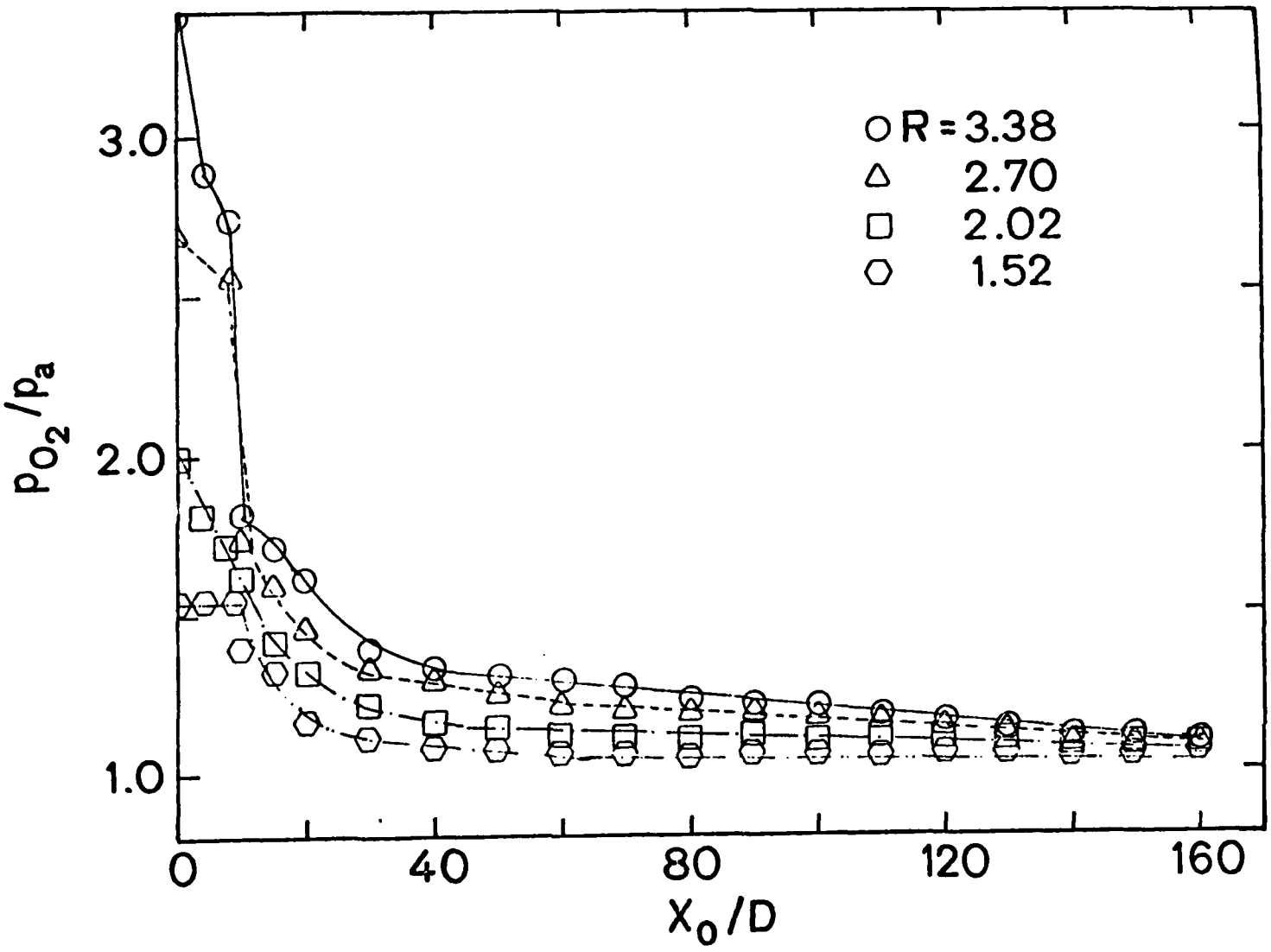

Figure 13a. **Distributions of axial total pressures in the 20:1, 3 jet ejector.**

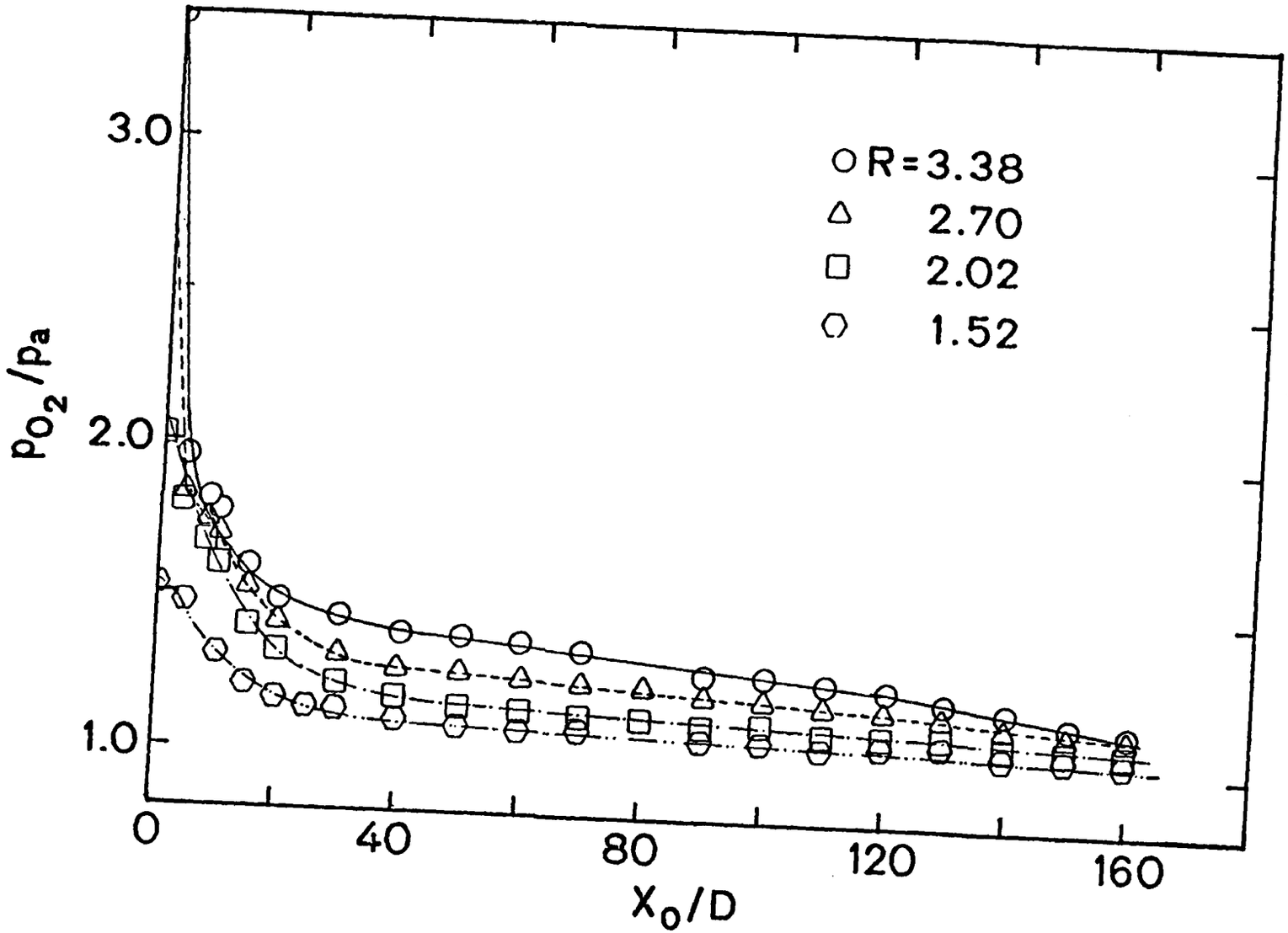

Figure 13b. Distributions of axial total pressures in the 26:1, 3 jet ejector.

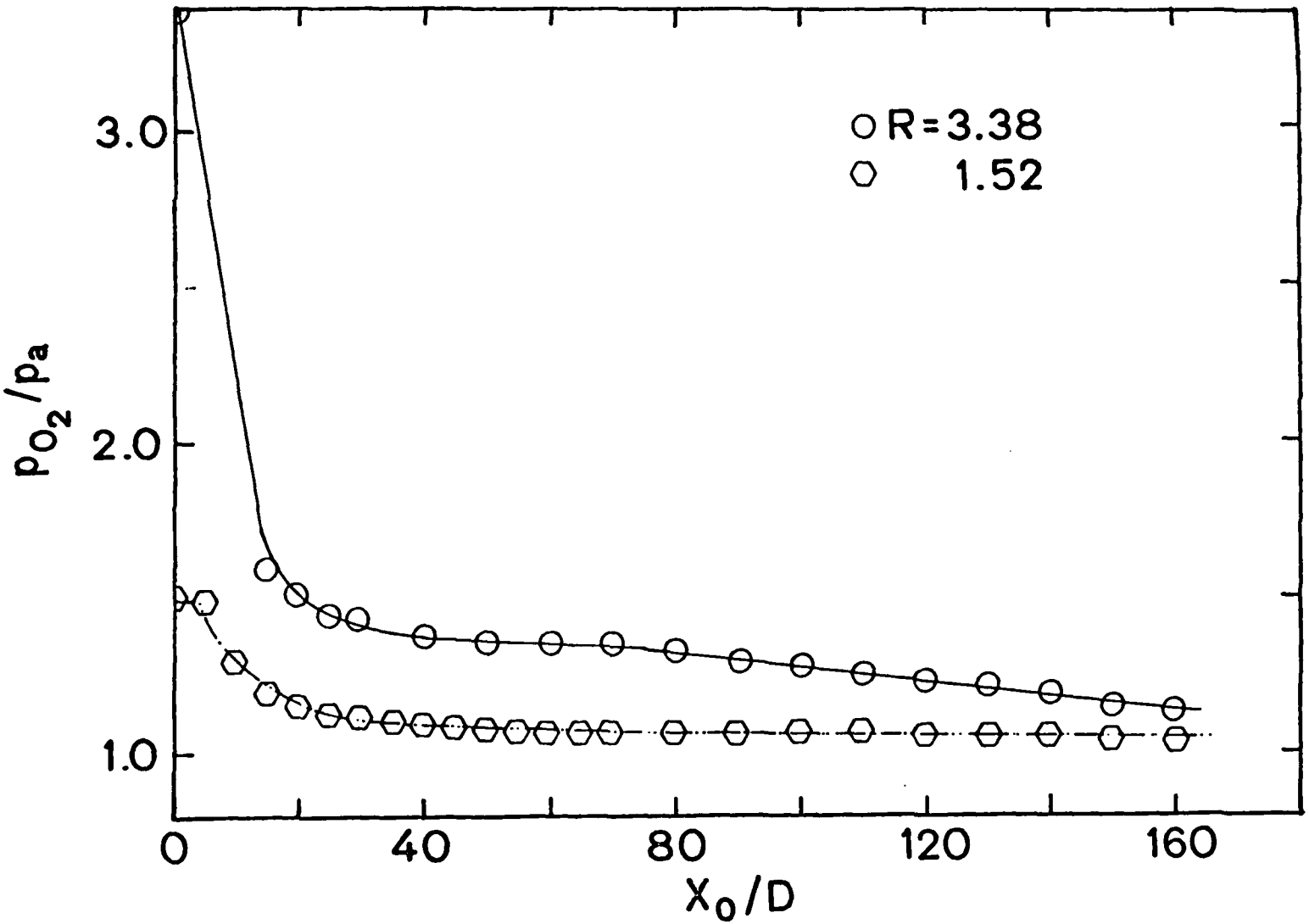

Figure 13c. Distributions of axial total pressures in the 33:1, 3 jet ejector.

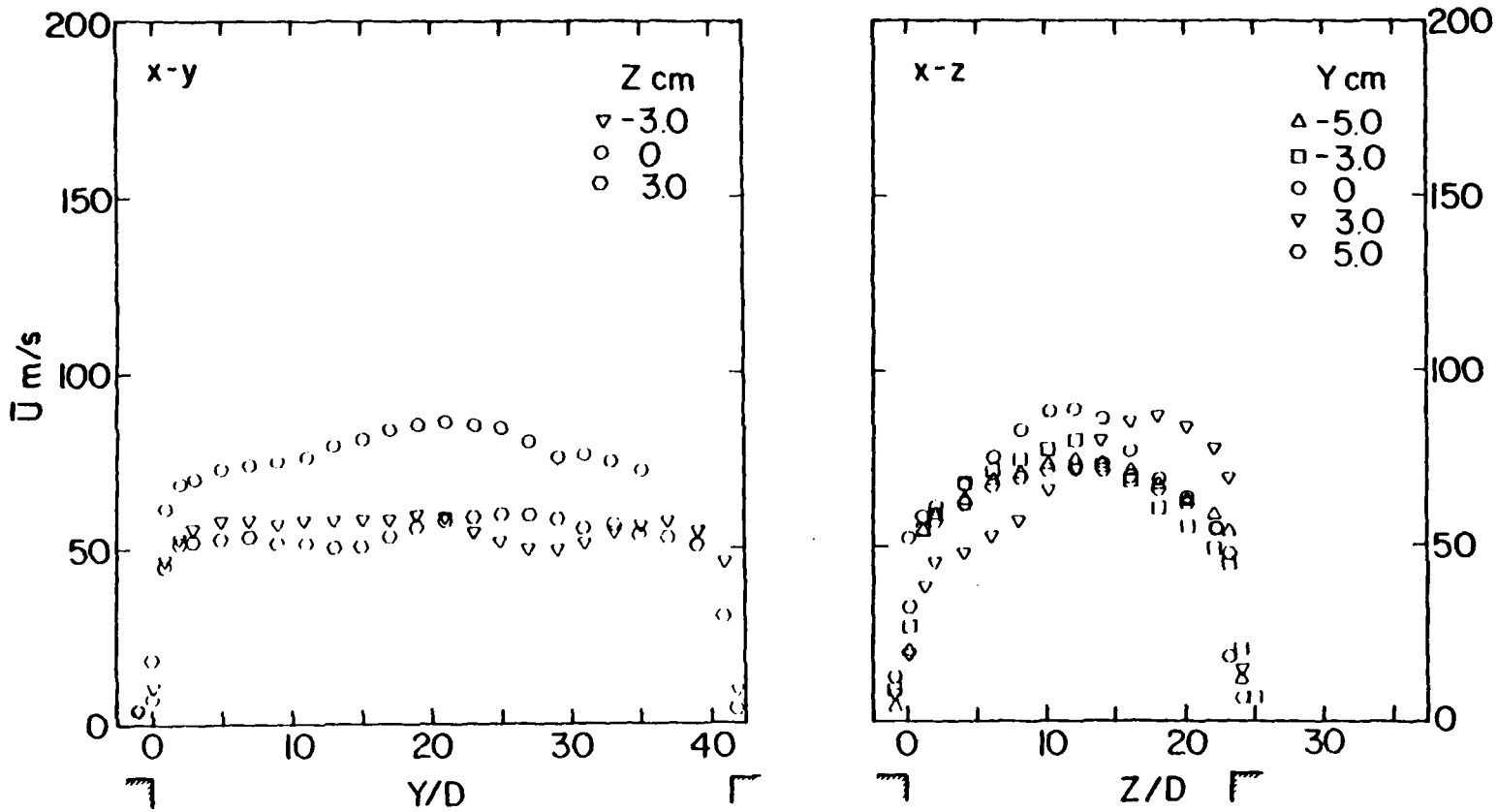

Figure 14a. **Mean velocity profiles at duct exit; 3 jet ejector, AR=20:1, R=1.52.**

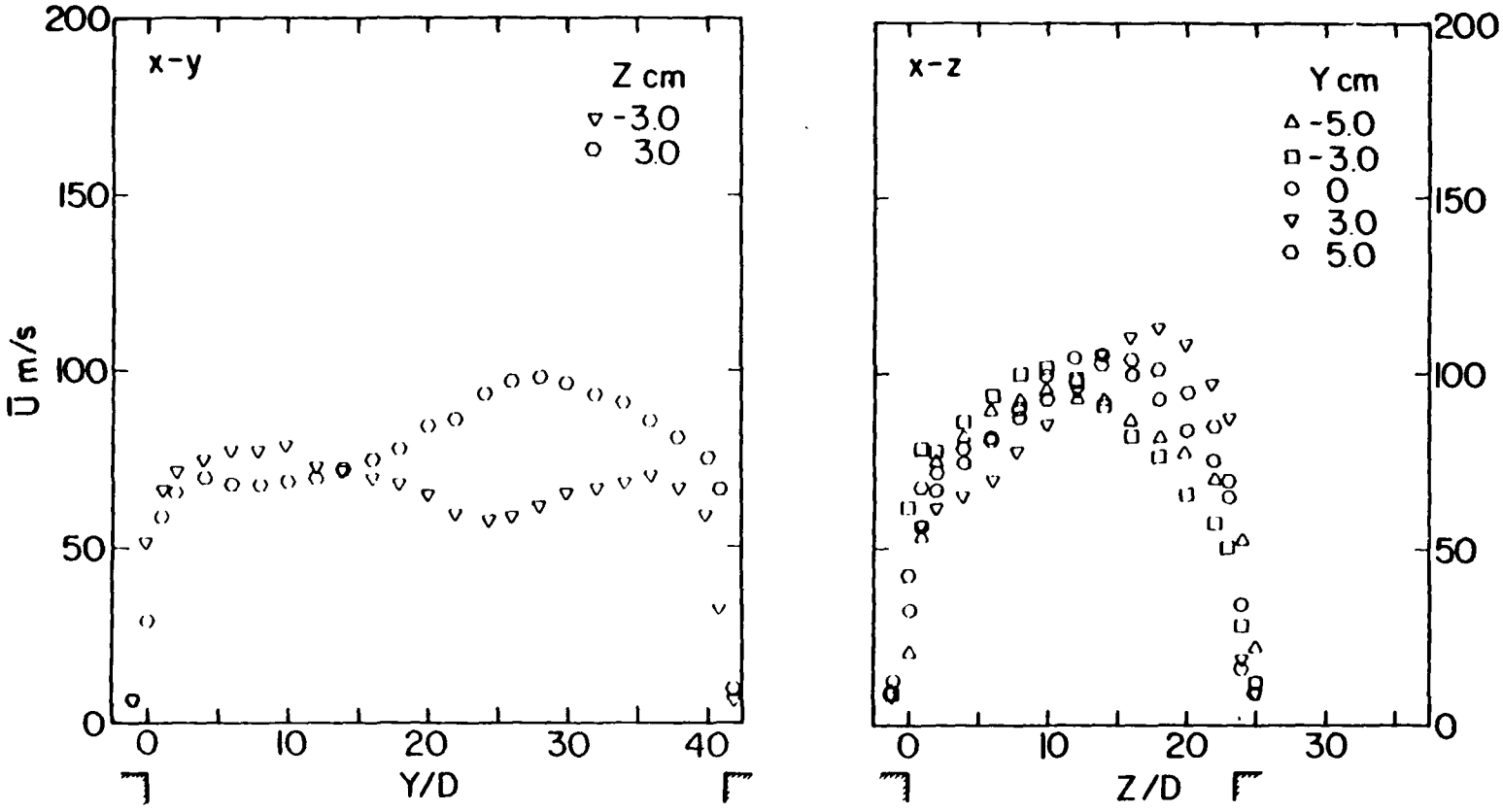

Figure 14b. Mean velocity profiles at duct exit; 3 jet ejector; AR = 20:1, R = 2.02.

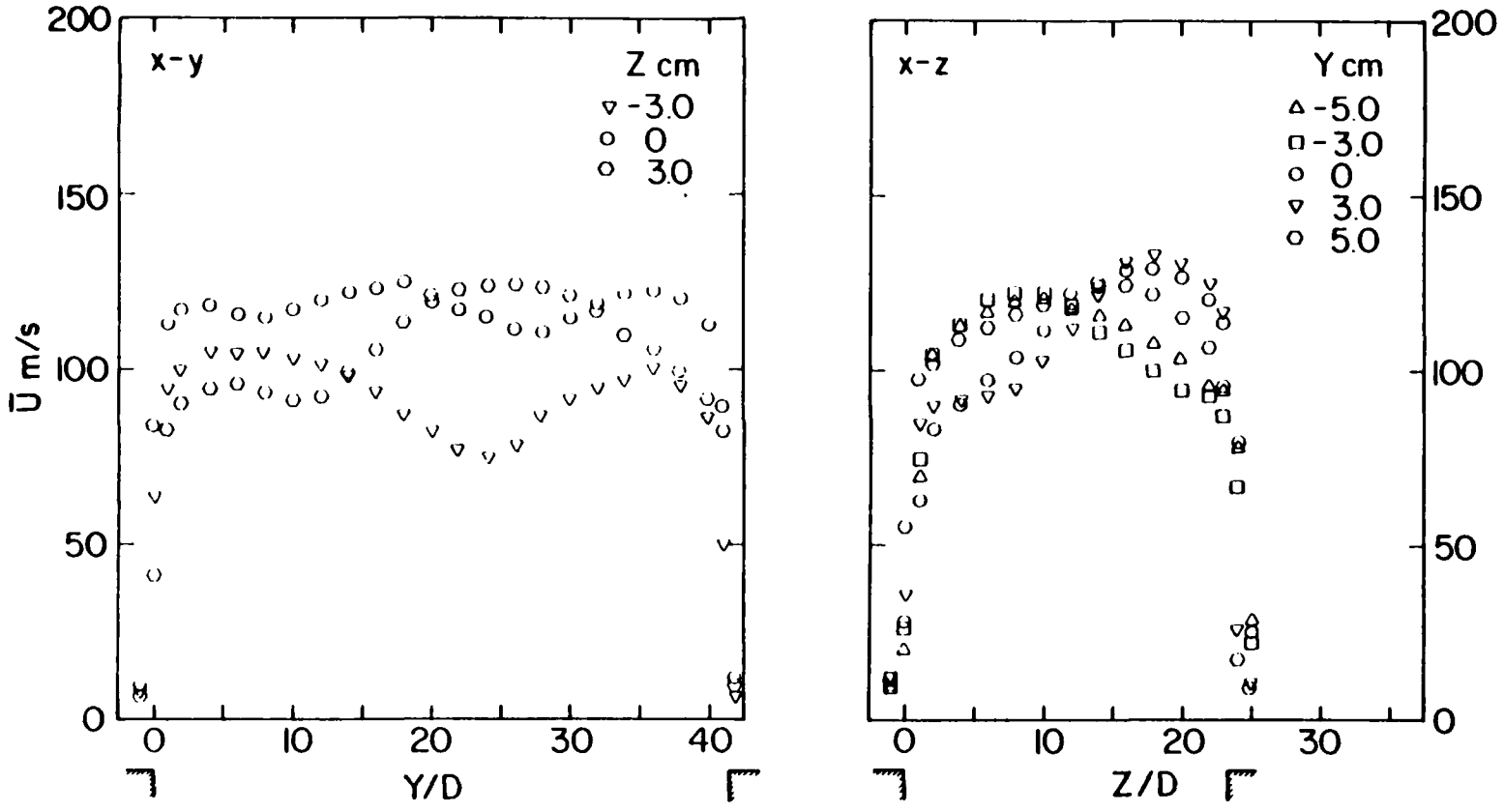

Figure 14c. Mean velocity profiles at duct exit; 3 jet ejector; AR = 20:1, R=2.7.

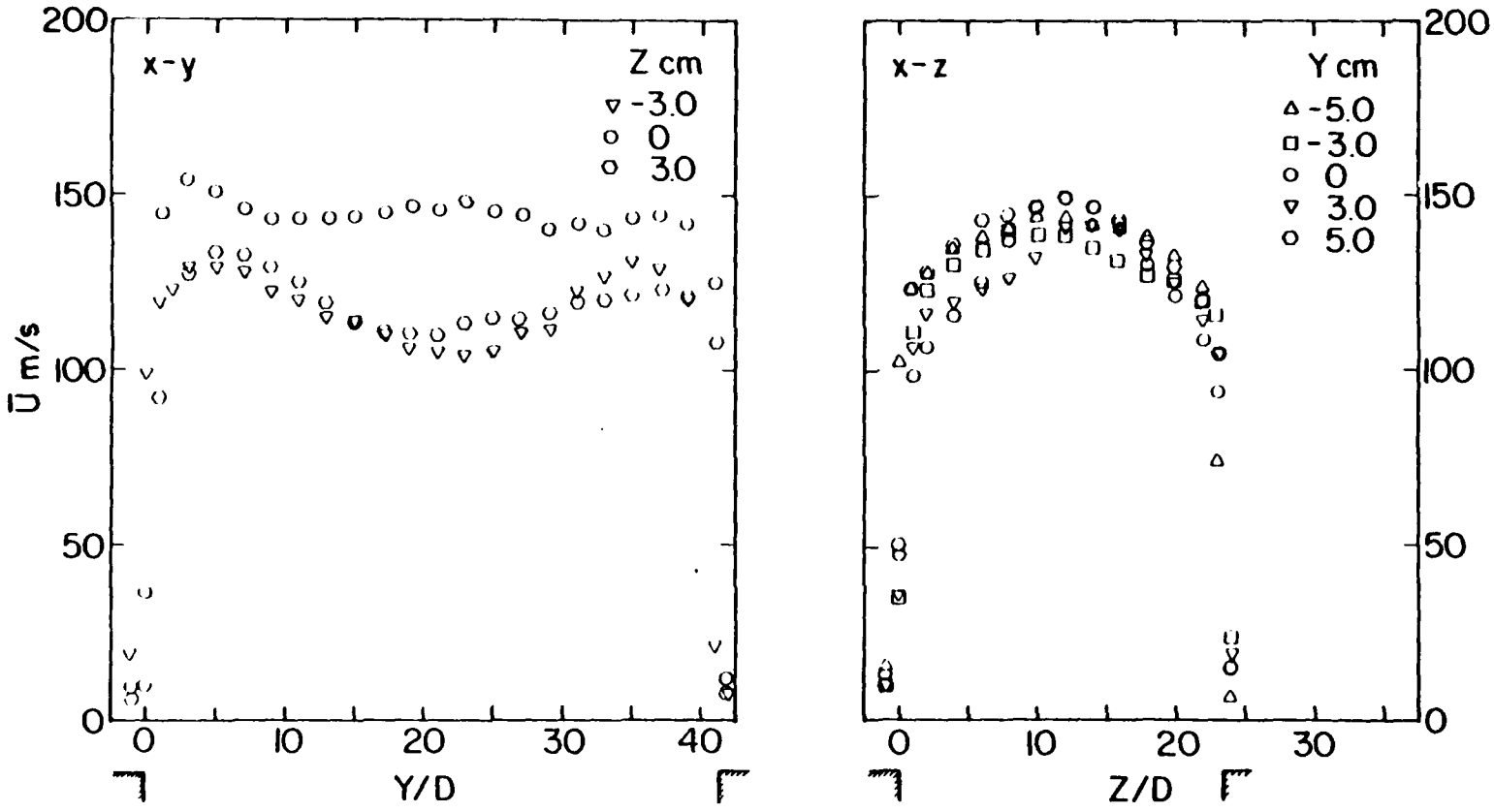

Figure 14d. Mean velocity profiles at duct exit; 3 jet ejector; AR = 20:1, R = 3.38.

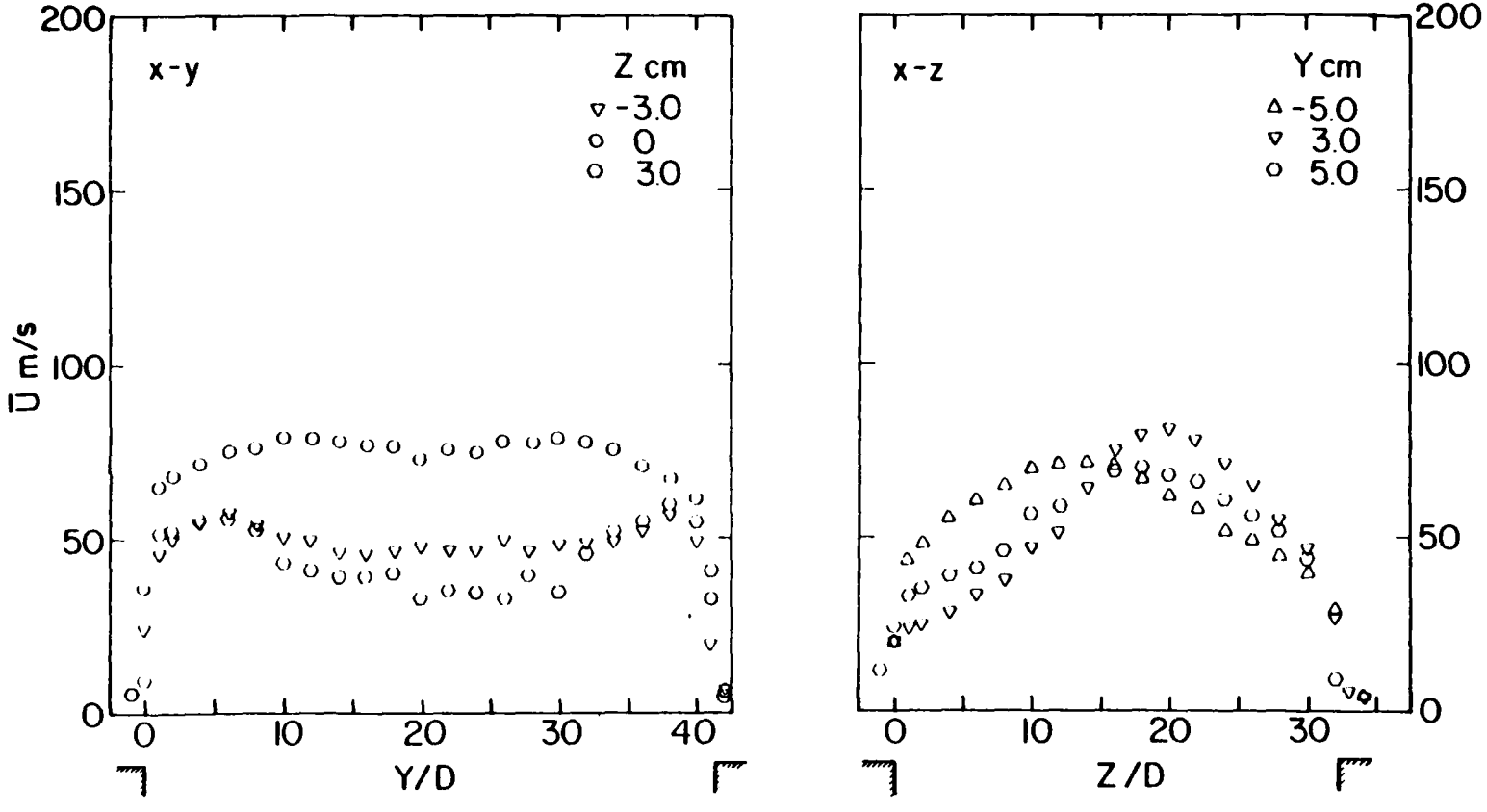

Figure 15a. **Mean velocity profiles at duct exit; 3 jet ejector; AR=26:1, $\bar{R}$=1.52.**

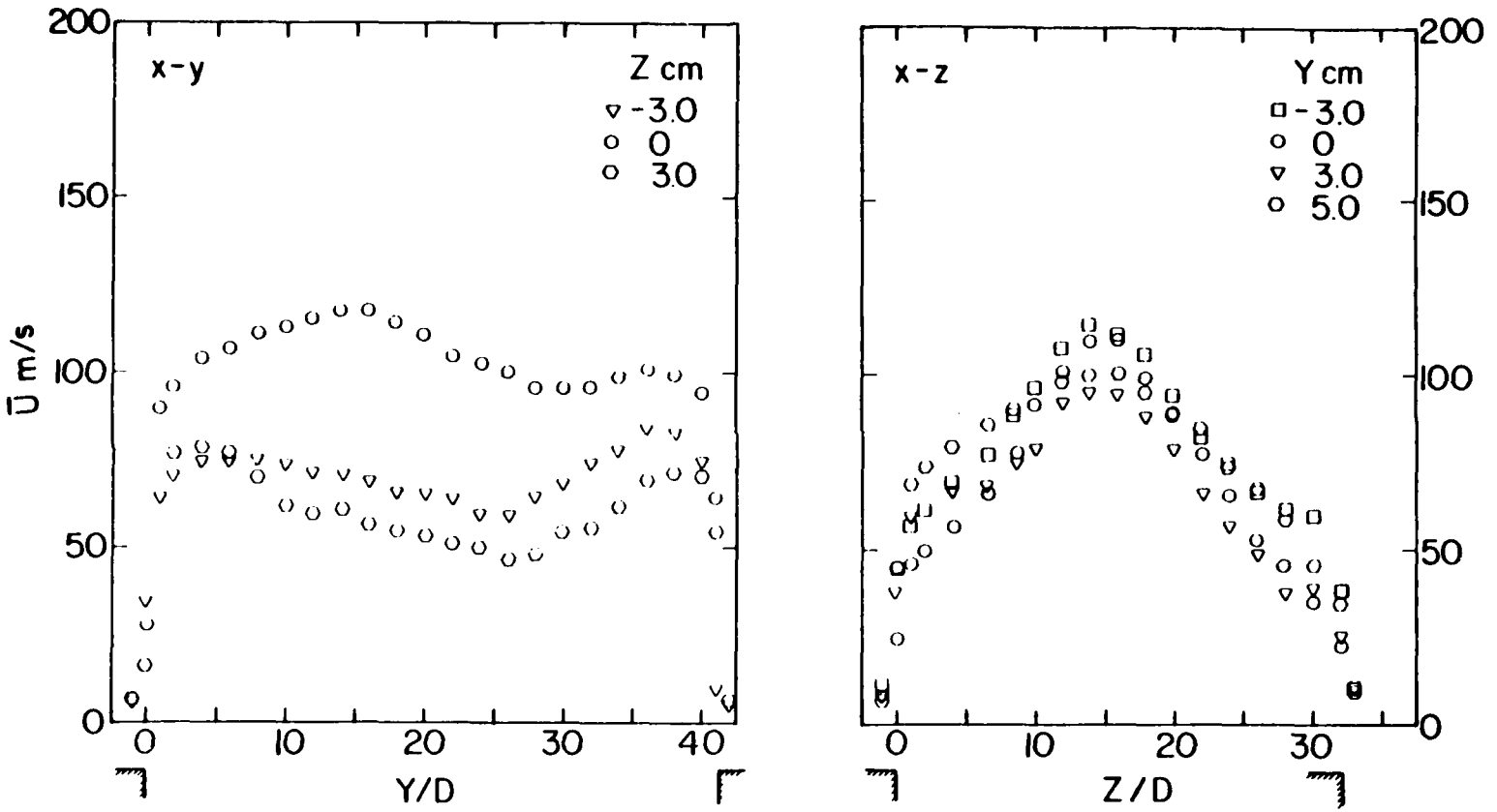

Figure 15b. Mean velocity profiles at duct exit; 3 jet ejector; AR= 26:1, R= 2.02.

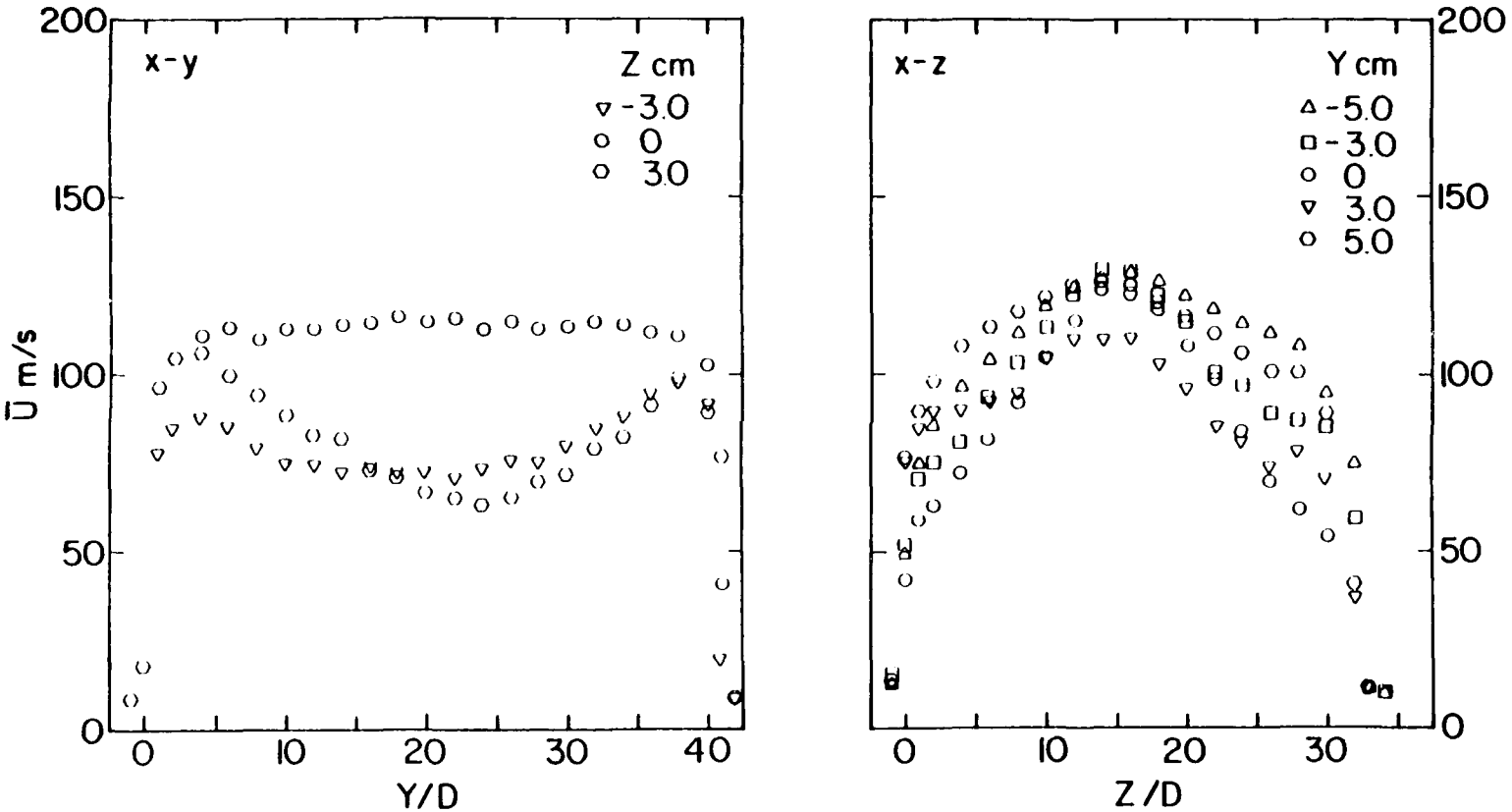

Figure 15c. Mean velocity profiles at duct exit; 3 jet ejector; AR=26:1, R=2.7.

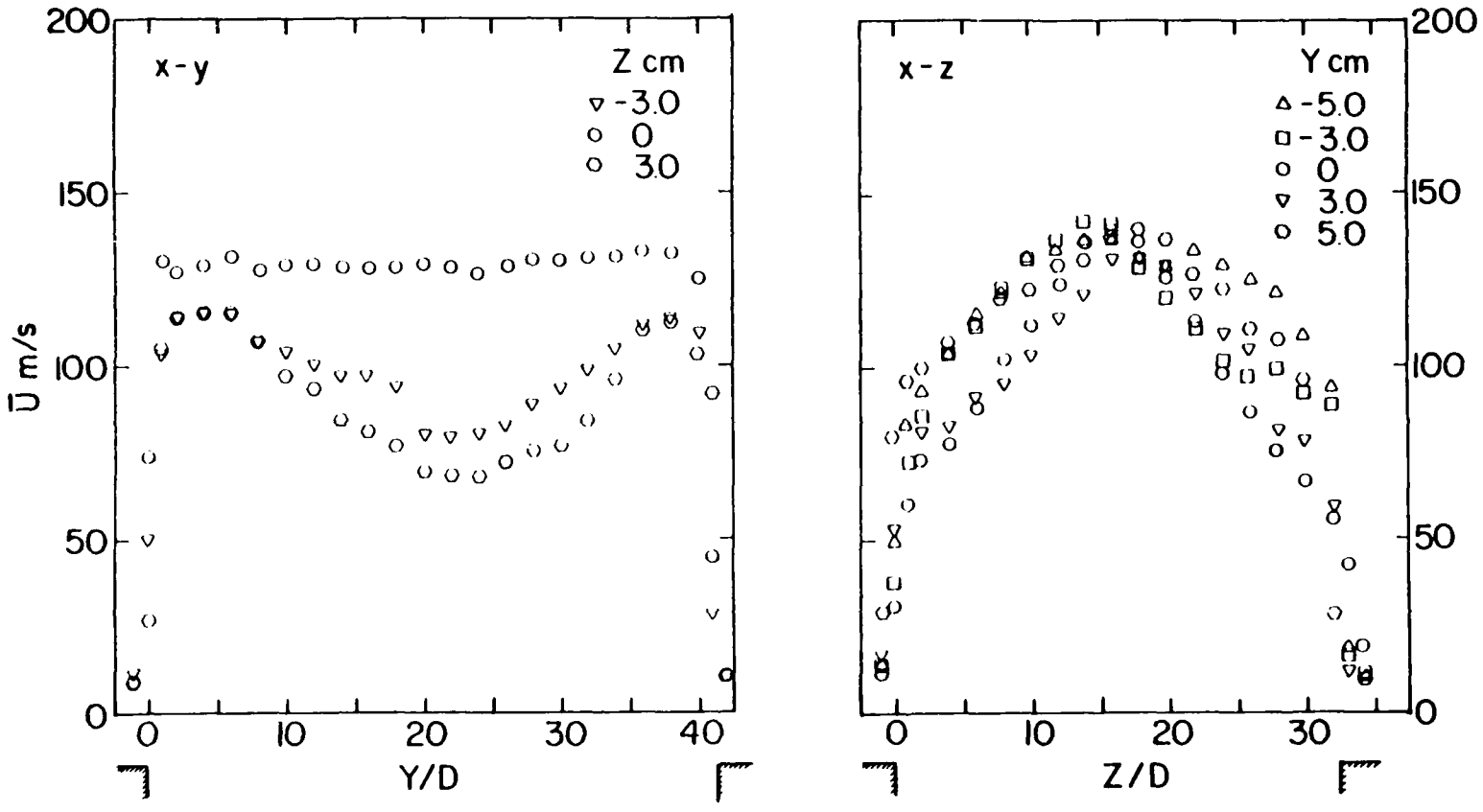

Figure 15d. Mean velocity profiles at duct exit; 3 jet ejector; AR=26:1, R=3.38

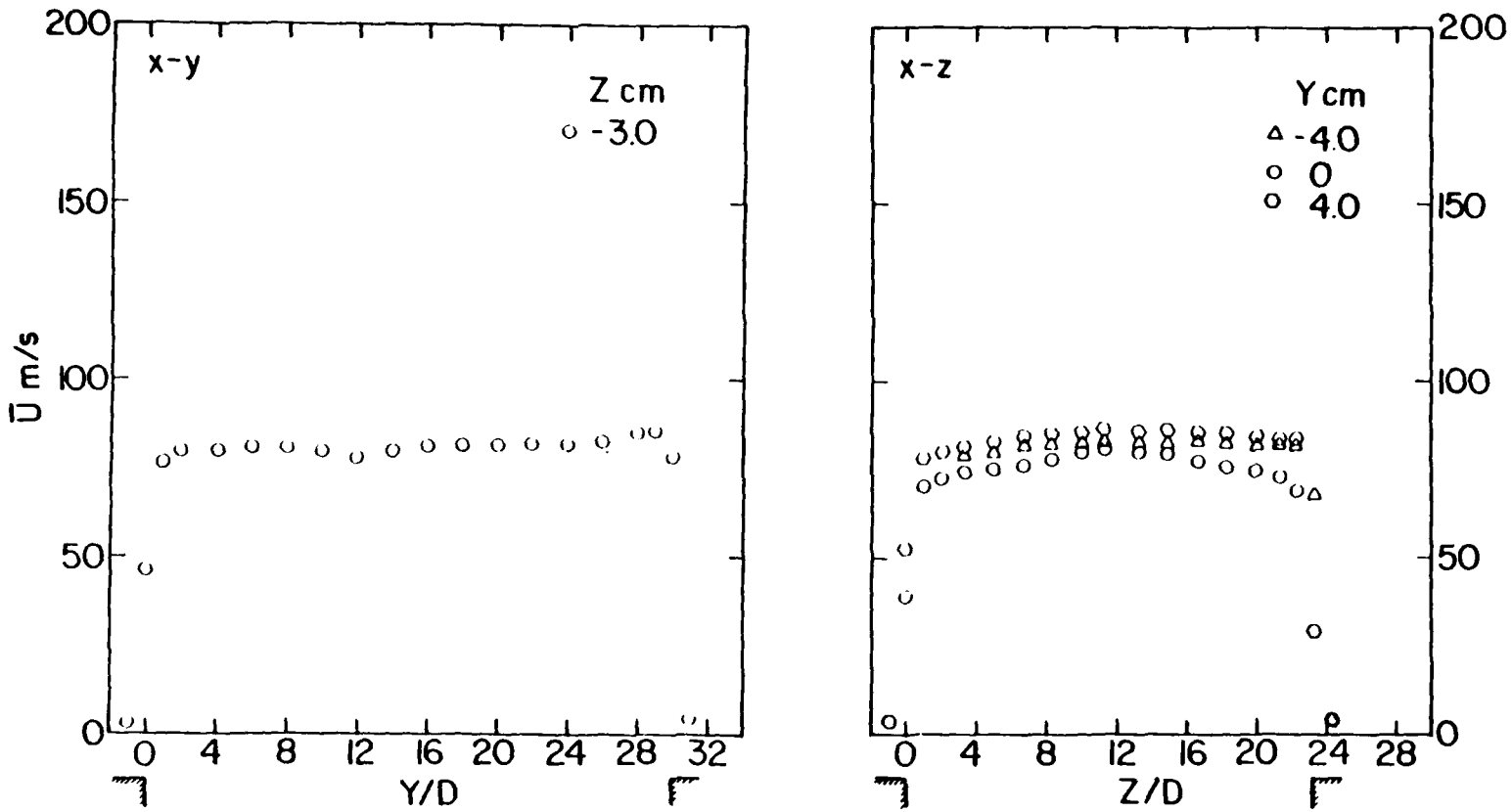

Figure 16a. **Mean velocity profiles at duct exit; 3 jet ejector; AR = 14:1, R = 1.52.**

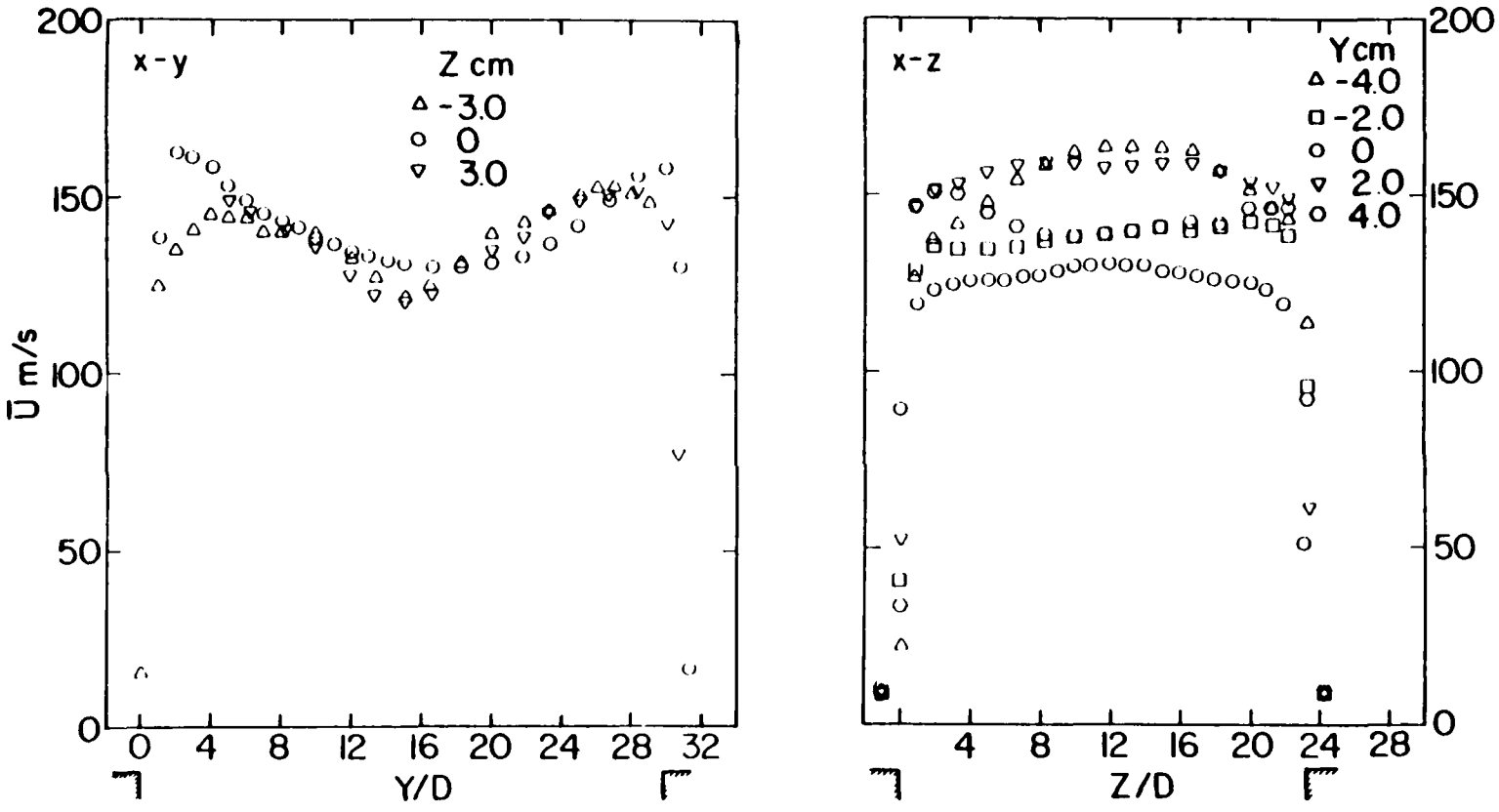

Figure 16b. Mean velocity profiles at duct exit; 3 jet ejector; AR=14:1, R=3.04.

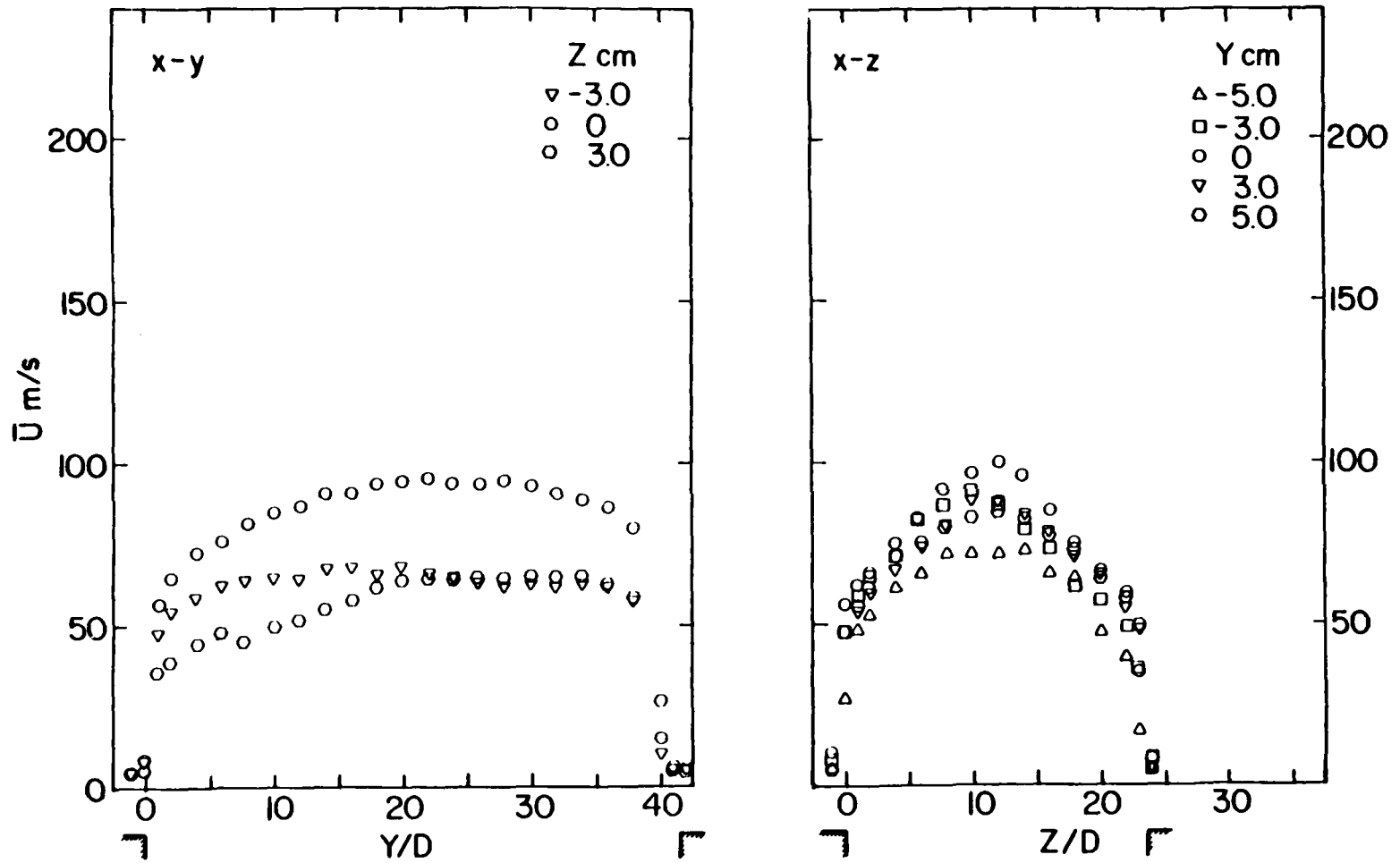

Figure 17a. Mean velocity profiles at duct exit; equivalent single jet ejector; AR=20:1, R=1.52.

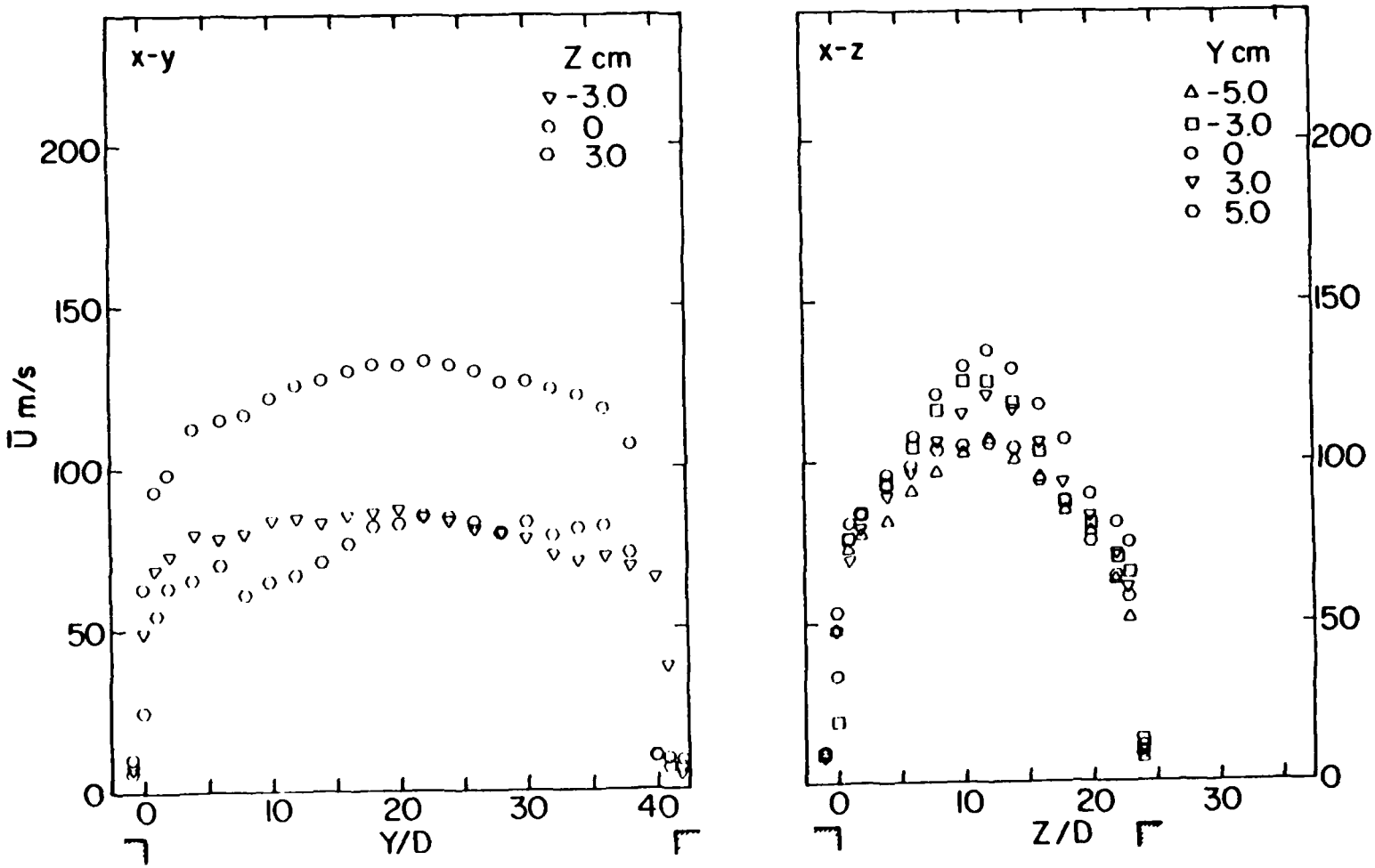

Figure 17b. **Mean velocity profiles at duct exit; equivalent single jet ejector; AR=20:1, R=2.02.**

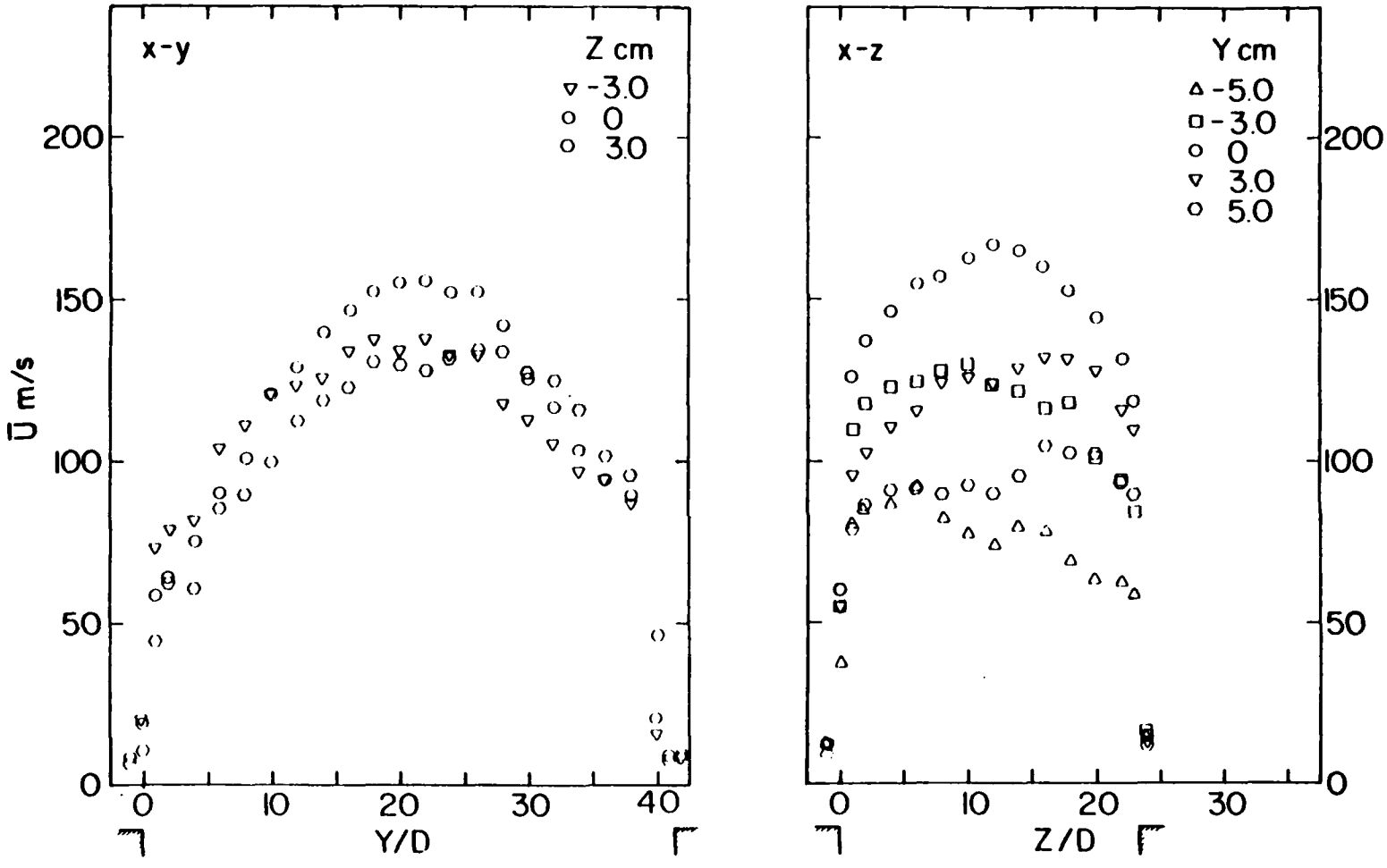

Figure 17c. **Mean velocity profiles at duct exit; equivalent single jet ejector; AR=20:1, R=2.7.**

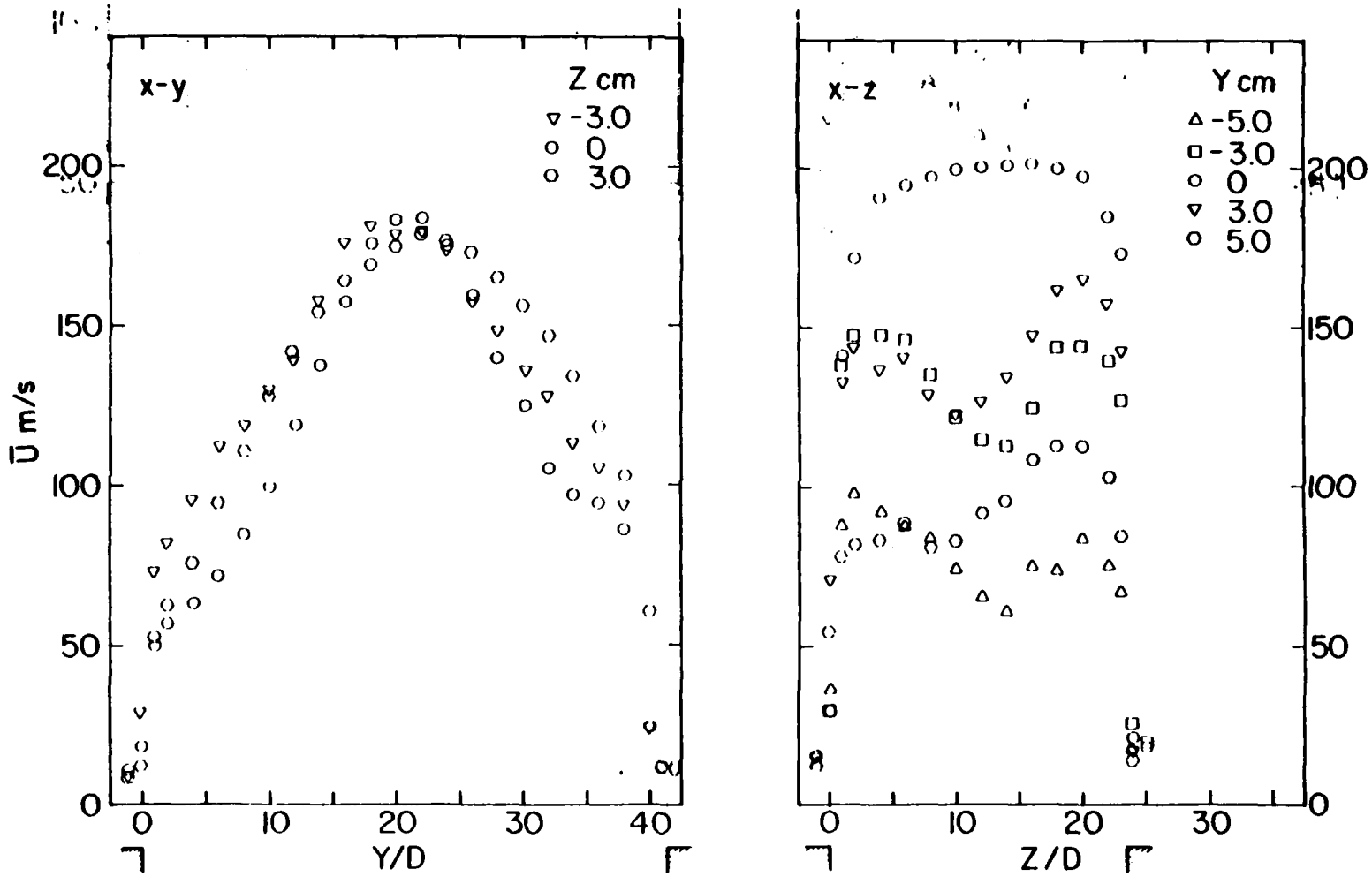

Figure 17d. Mean velocity profiles at duct exit; equivalent single jet ejector; AR = 20:1, R = 3.38.

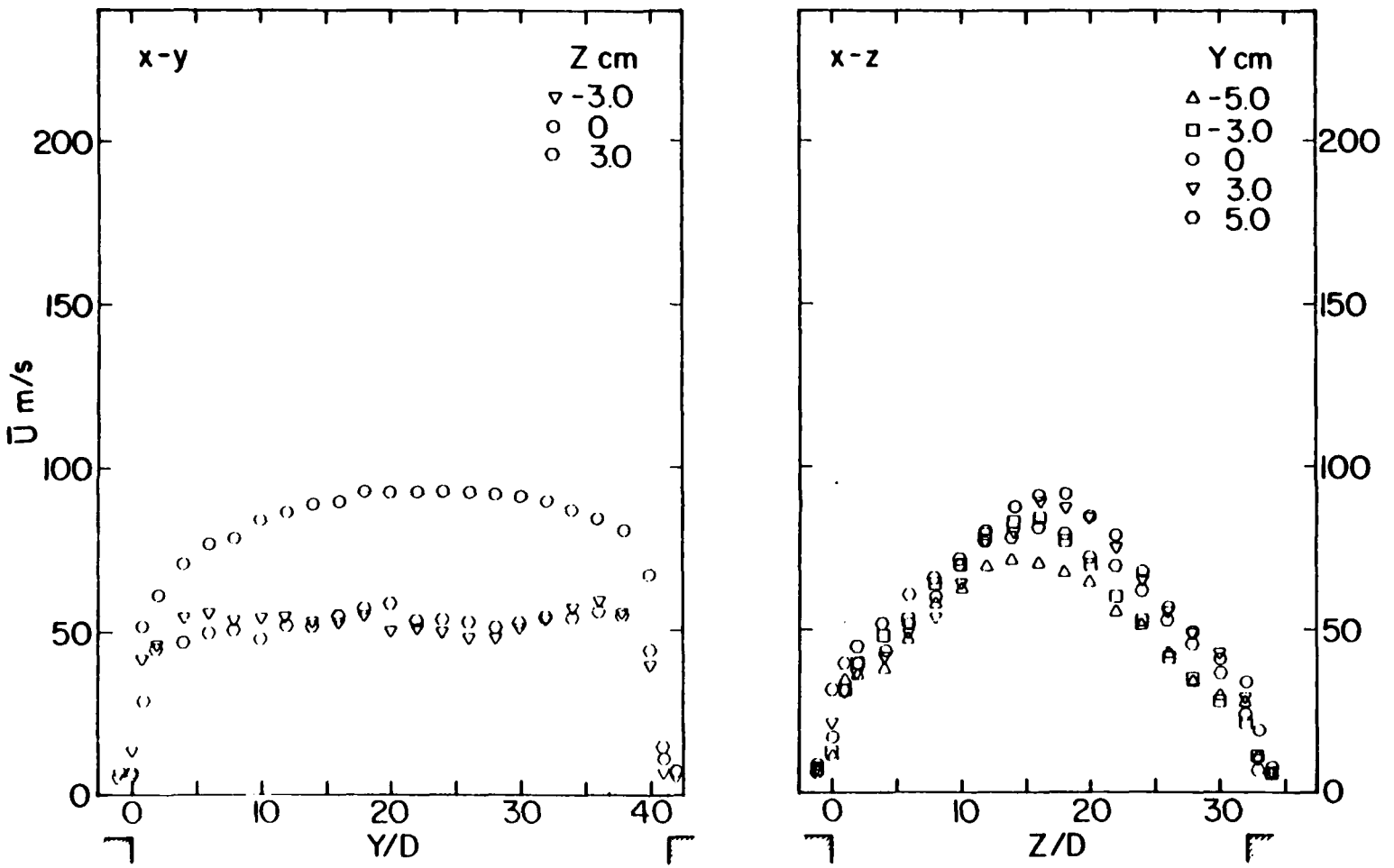

Figure 18a. Mean velocity profiles at duct exit; equivalent single jet ejector; AR=26:1, R=1.52.

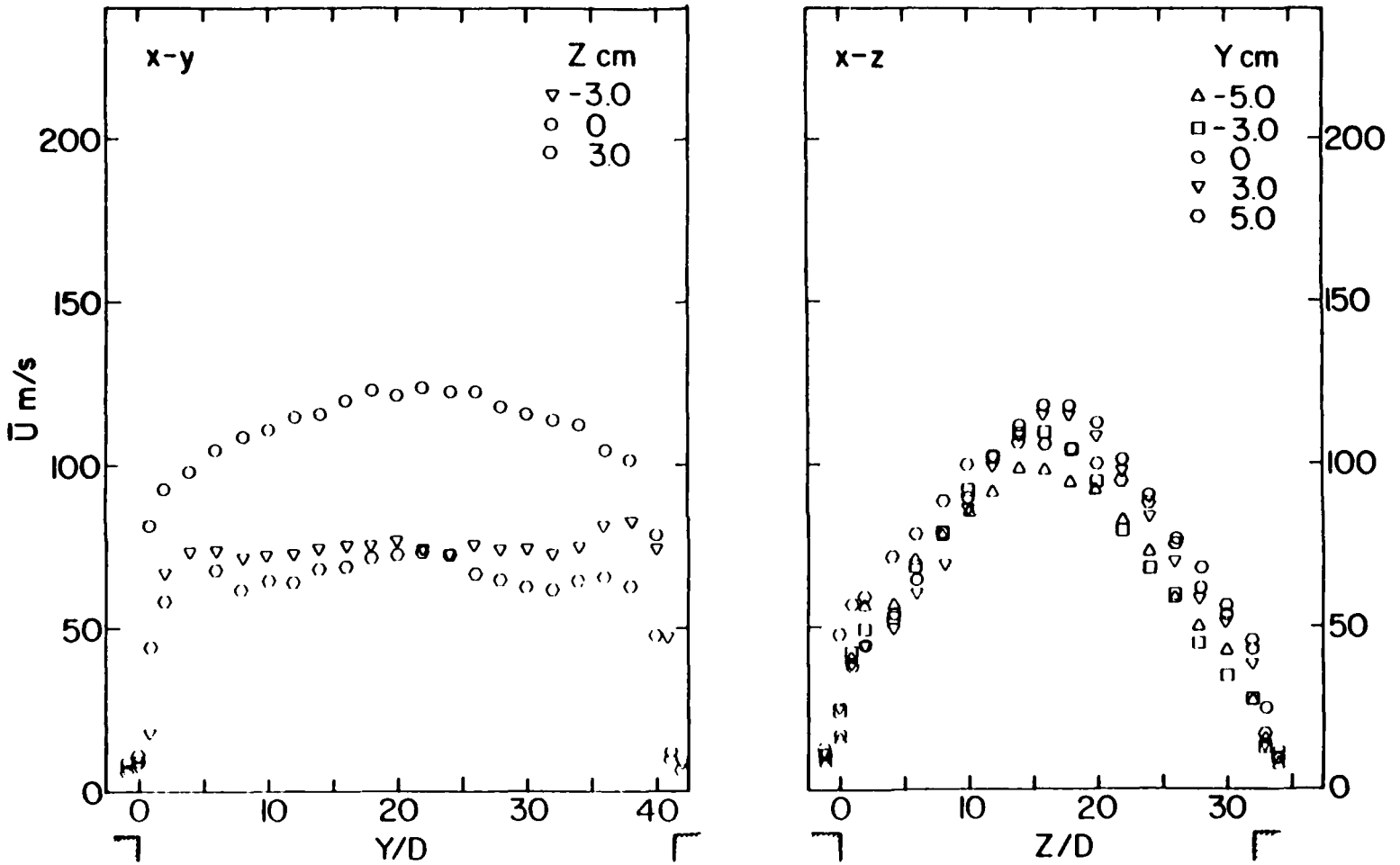

Figure 18b. Mean velocity profiles at duct exit; equivalent single jet ejector; AR= 26:1, R= 2.02.

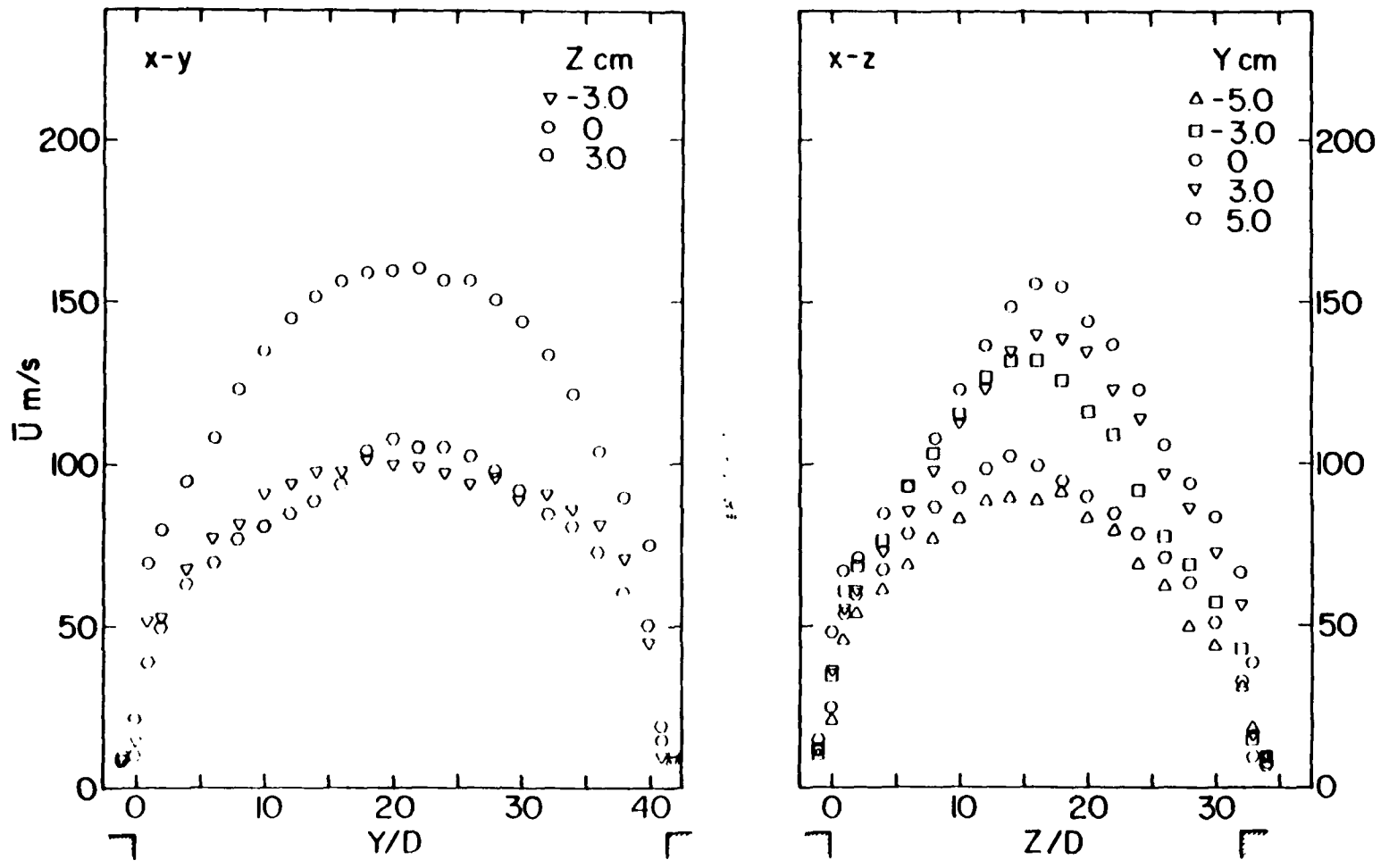

Figure 18c. Mean velocity profiles at duct exit; equivalent single jet ejector; AR=26:1, R=2.7.

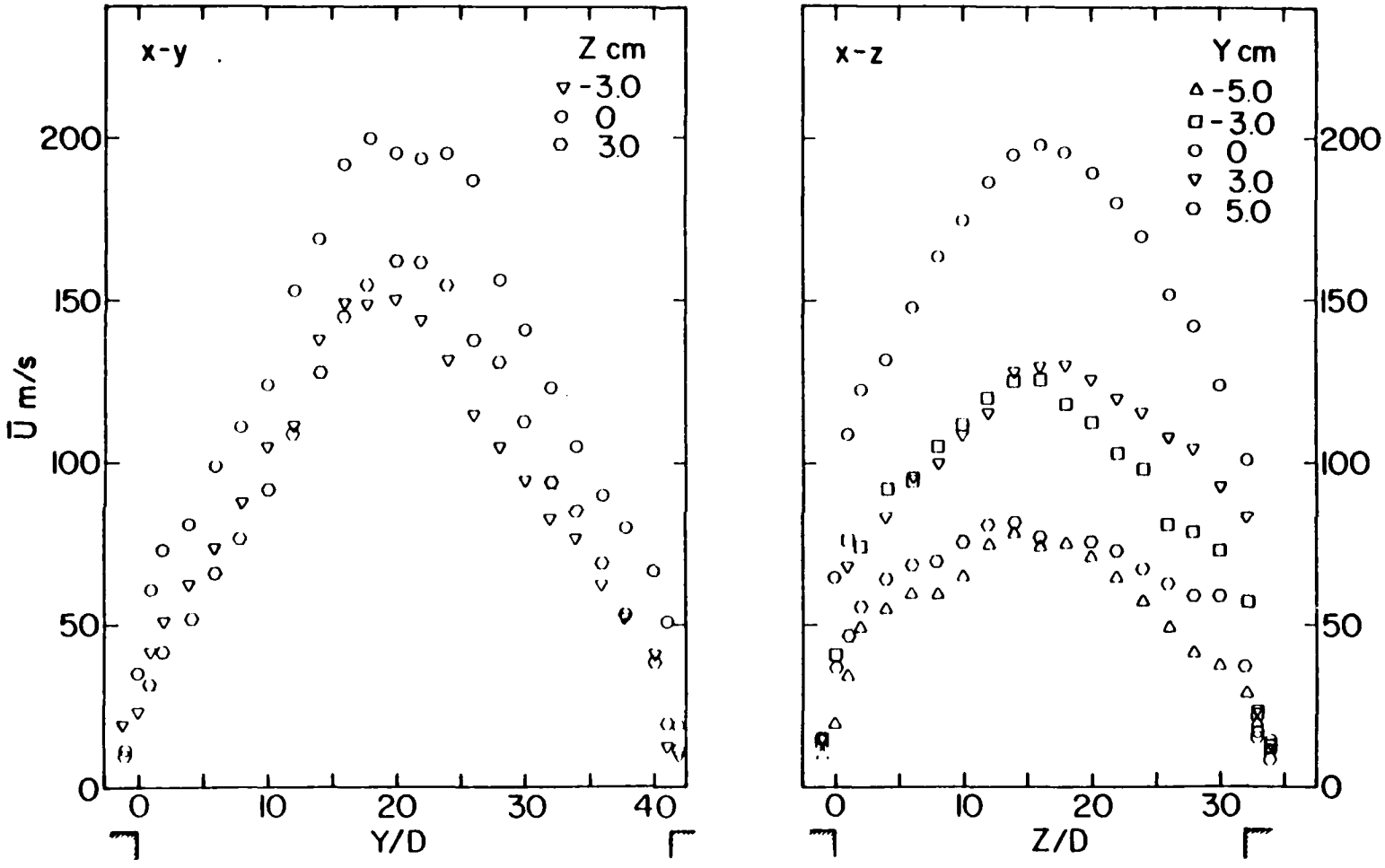

Figure 18d. Mean velocity profiles at duct exit; equivalent single jet ejector; AR=26:1, R=3.38

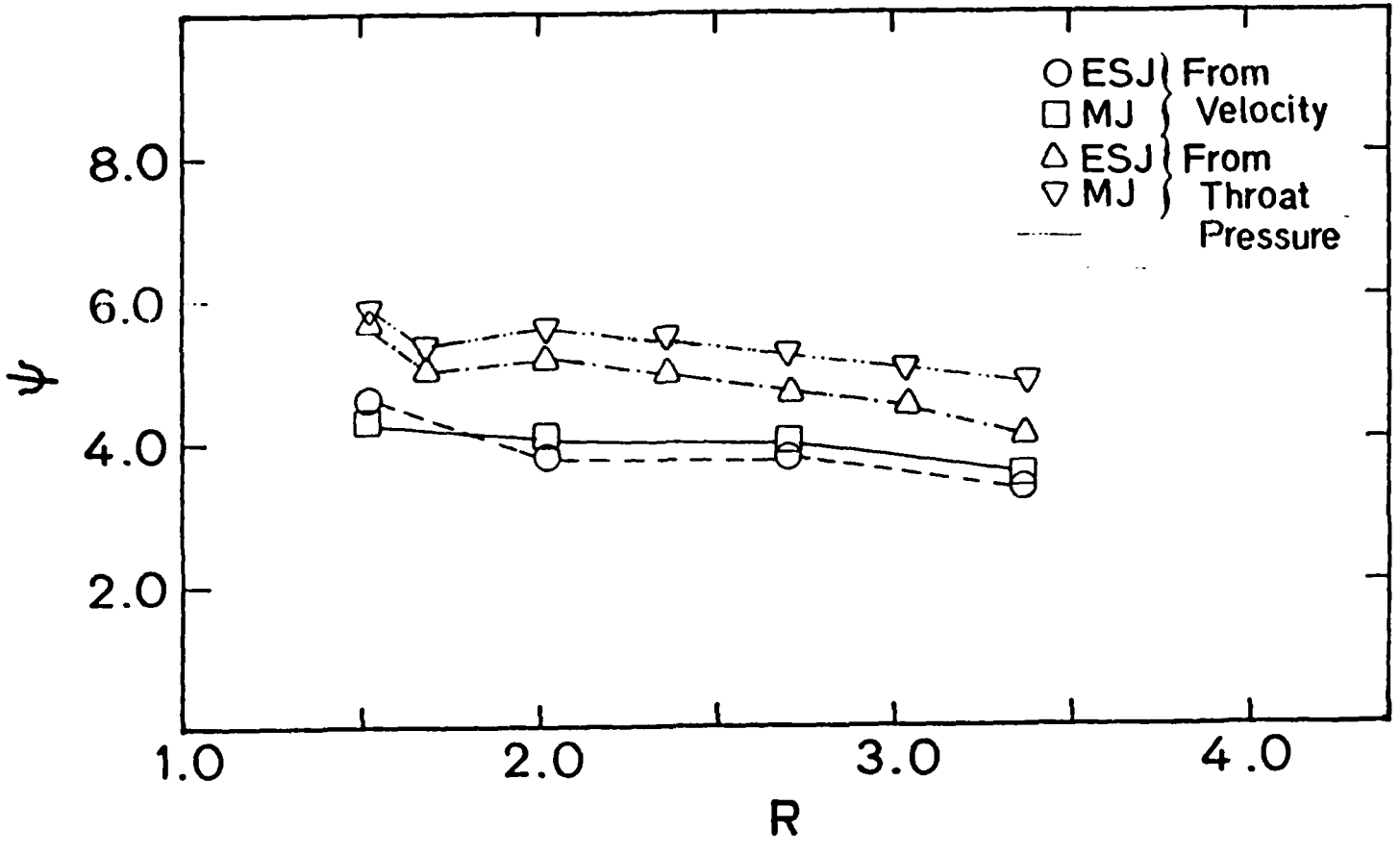

Figure 19a. Mass augmentation characteristics of 3 jet and equivalent single jet ejectors; AR=20:1.

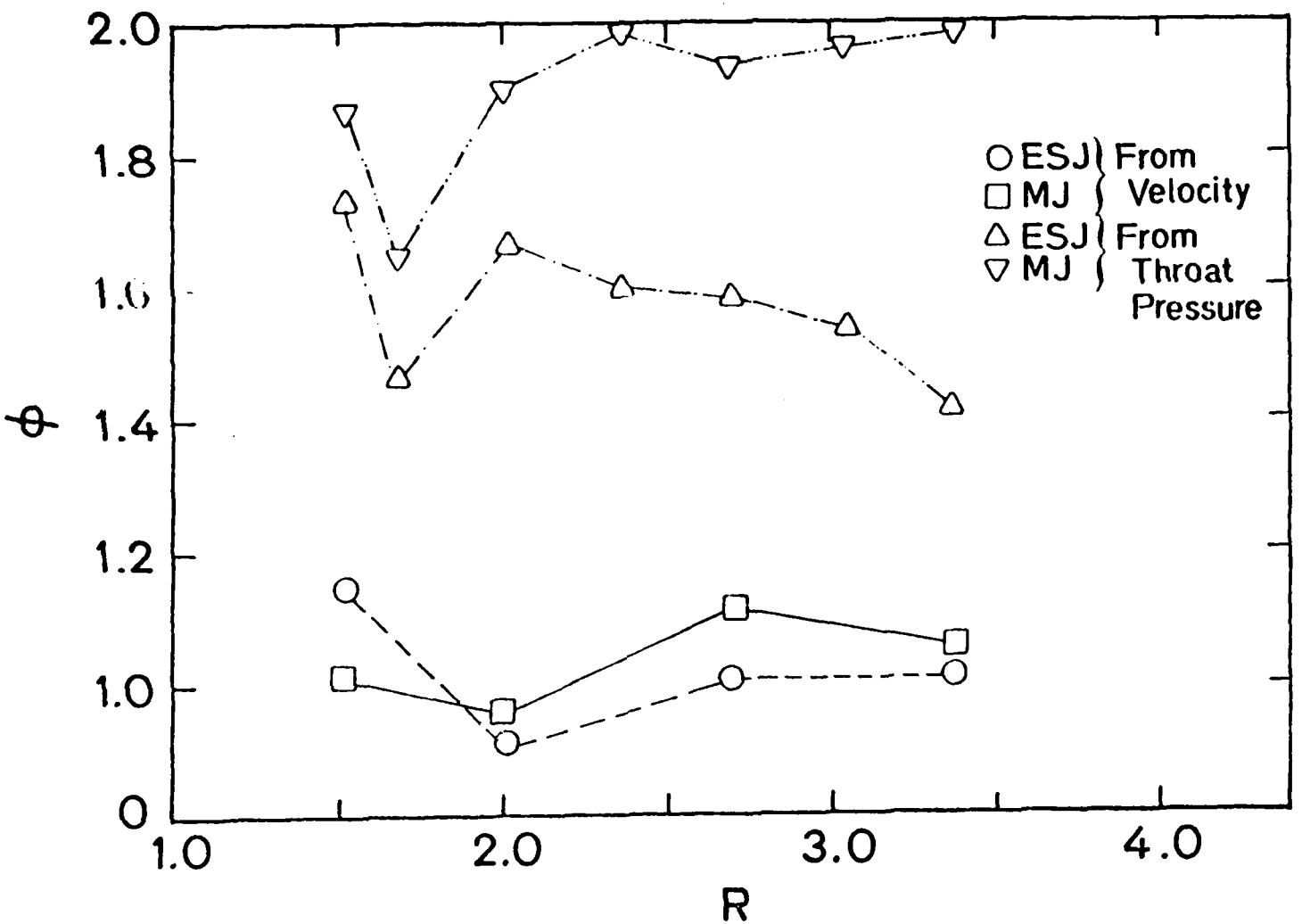

Figure 19b. Thrust augmentation characteristics of 3 jet and equivalent single jet ejectors; AR=20:1.

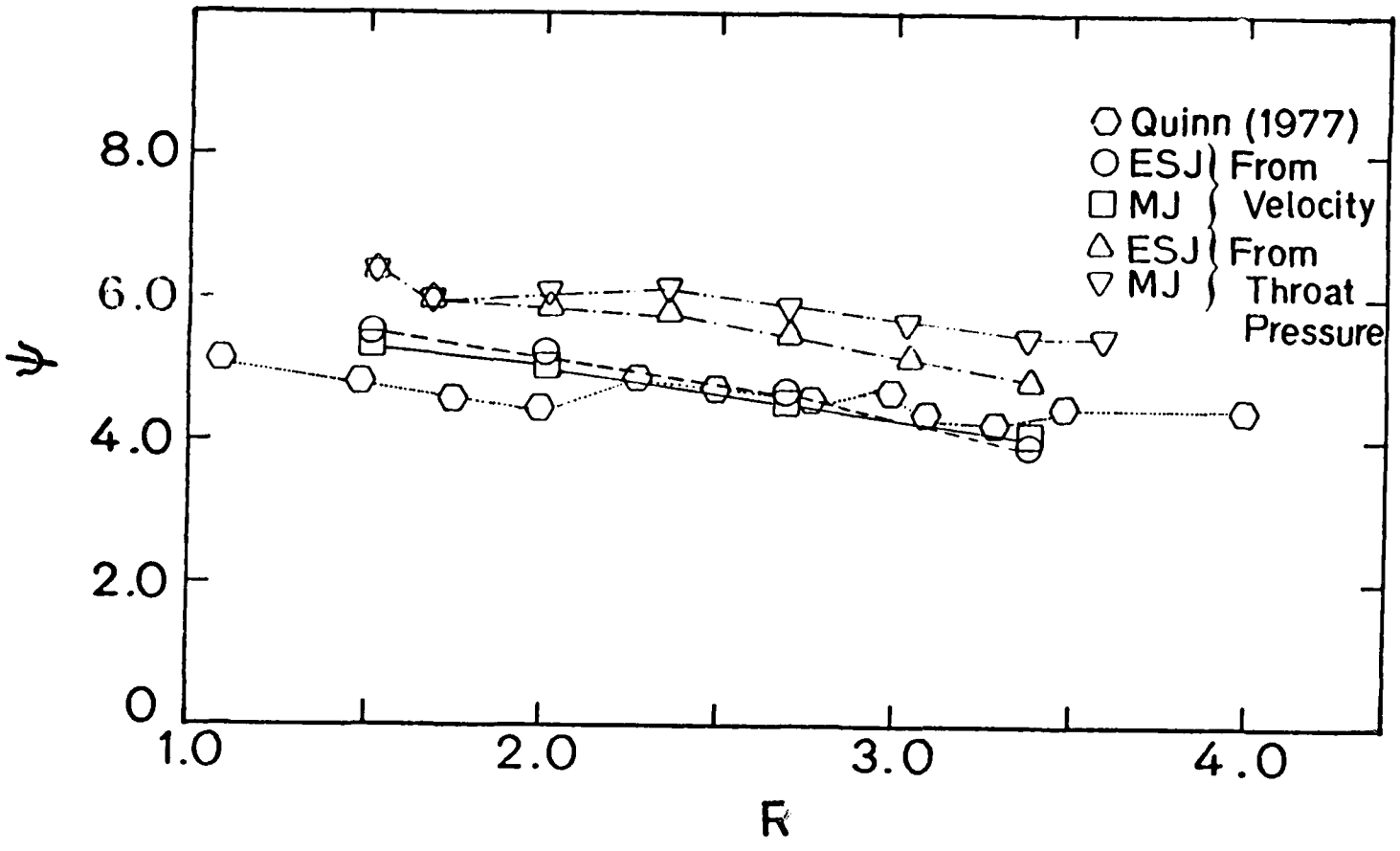

Figure 20a. Mass augmentation characteristics of 3 jet and equivalent single jet ejectors; AR=26:1.

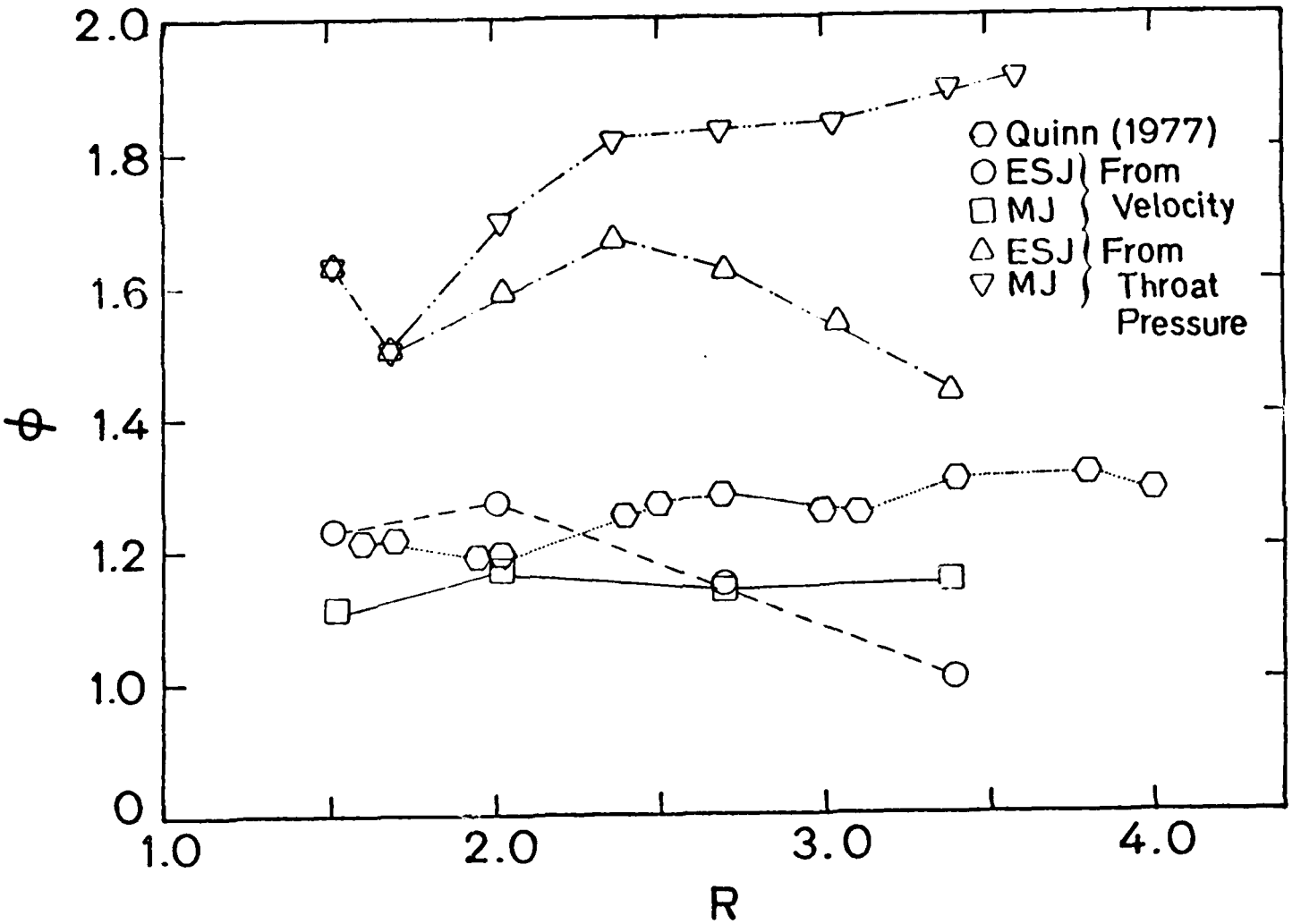

Figure 20b. Thurst augmentation characteristics of 3 jet and equivalent single jet ejectors; AR=26:1.

END

FILMED

2-85

DTIC